NEW MEXICO BUREAU OF GEOLOGY AND MINERAL RESOURCES

Geology of the Eastern Plains of San Agustin and Upper Alamosa Creek

Daniel J. Koning and Alex Rinehart

Open File Report 611
June 2021

New Mexico Bureau of Geology and Mineral Resources

A Research Division of New Mexico Institute of Mining and Technology

Socorro, NM 87801
(575) 835 5490
Fax (575) 835 6333
www.geoinfo.nmt.edu

Geology of the Eastern Plains of San Agustin and Upper Alamosa Creek

Daniel J. Koning and Alex Rinehart

Open File Report 611
June 2021

New Mexico Bureau of Geology and Mineral Resources

PROJECT FUNDING

Funding for this project has been collaborative, with support from the New Mexico Bureau of Geology and Mineral Resources, Aquifer Mapping Program of the NM Bureau of Geology and Mineral Resources, Healy Foundation, Office of the State Engineer, and USGS National Cooperative Geologic Mapping Program (STATEMAP).

CONVERSION FACTORS

Multiply	By	To obtain
miles	1.609	kilometers
feet	0.3048	meters
inches	2.54	centimeters
(Fahrenheit -32)	0.556	Celsius

ABBREVIATIONS

ft	foot, feet
km	kilometer, kilometers
m	meter, meters
mi	mile, miles
Ma	Millions of years in age, mega anum
VLA	Very Large Array radio telescope observatory
SA	San Agustin

DISCLAIMER

The reports and data provided here are intended to aid in the understanding of the geologic and hydrologic resources of New Mexico. However, there are limitations for all data, particularly when subsurface interpretation is performed, or when data are aggregated that may have been collected at different times, by different agencies or people, and for different purposes. The information and results provided are also dynamic and may change over time. Users of these data and interpretations should exercise caution, and site-specific conditions should always be verified. These materials are not to be used for legally binding decisions. Any opinions expressed do not necessarily reflect the official position of the New Mexico Bureau of Geology and Mineral Resources, New Mexico Tech, or the State of New Mexico.

Although every effort is made to present current and accurate information, data is provided without guarantee of any kind. The data are provided "as is," and the New Mexico Bureau of Geology and Mineral Resources assumes no responsibility for errors or omissions. No warranty, expressed or implied, is made regarding the accuracy or utility of the data for general or scientific purposes. The user assumes the entire risk associated with the use of these data. The New Mexico Bureau of Geology and Mineral Resources shall not be held liable for any use or misuse of the data described and/or contained herein. The user bears all responsibility in determining whether these data are fit for the user's intended use. The views and conclusions are those of the authors, and should not be interpreted as necessarily representing the official policies, either expressed or implied, of the State of New Mexico.

Cover: Photograph of a dish-shaped antenna of the Very Large Array radio telescope observatory, situated in the eastern Plains of San Agustin. View is to the southeast; the forested, western part of Mount Withington lies in the background. The shaded slope in the grasslands, just beyond and right of the antenna, is an eroded fault scarp created by repeated earthquake events along a north-south, west-down fault—Photo by Daniel Koning.

CONTENTS

Figures

Tables

Appendices

(Available in digital format, https://geoinfo.nmt.edu/publications/openfile/details.cfml?Volume=611)

Plates

EXECUTIVE SUMMARY

This report gives a detailed treatment of the geology of the eastern Plains of San Agustin and the upper (northern) reaches of Alamosa Creek (aka Alamosa basin). We synthesize previous studies of geology and provide new detail on basin fill stratigraphy and sedimentology. This report is a complement to a hydrogeologic study (due to be released 2021; summarized in OFR-615) regarding groundwater movement, age, and storage under the Plains of San Agustin and the upper Alamosa Creek watershed.

The Plains of San Agustin is a 55 mi long, 10–20 mile wide geographic feature located about 120–150 miles southwest of Albuquerque. It is comprised of a series of hydraulically closed basins that collectively form a northeast-southwest topographic depression. A set of low hills south of Datil divide the topographic depression into the West and East San Agustin basins. This report focuses on the East San Agustin basin, which hosts the Very Large Array (VLA) radio telescope observatory. It is also where the Augustin Plains Ranch, LLC, has proposed a contentious, large-scale groundwater extraction and artificial recharge project. Three grabens have been identified in the East San Agustin basin, where the Earth's crust has subsided along fault lines and the sedimentary basin fill is relatively thick. The Augustin Plains Ranch project is located in the north-south trending North graben, which has a bedrock floor and overlying strata that are tilted westwards towards faults at the base of the eastern Datil Mountains. Basin fill thickens westwards towards these faults, where it is at least 3,500 ft thick.

The upper reaches of Alamosa Creek flows 15 miles south in a ~9 mi wide, north-south trending topographic low that we call the upper Alamosa basin. This basin coincides with the northern Winston graben. This geologic structure is tilted westwards towards faults at the eastern foot of the Black Range. Basin fill thus thickens westward, as it does for the North graben, and is estimated to be as thick as 4,600 ft.

The geology of the study area has four main components: older sedimentary bedrock, volcanic bedrock, basin fill, and valley-fill alluvium The bedrock consists of volcanic and volcaniclastic rocks of the Mogollon-Datil volcanic field that overlie 750–1,900 ft of sandstones and mudstones of the Eocene-age Baca Formation. The lower Spears Group, composed mainly of tuffaceous debris flows and mud flows, comprises the lower 1,500–2,000 ft of the Mogollon-Datil field volcanic package and is interpreted to be an aquitard. Above the lower Spears Group lies 1,300–5,900 ft-thick sequence of interbedded ash-flow tuffs (ignimbrites), lava flows, volcaniclastic sediment (assigned to the middle-upper Spears Group) and minor tongues of non-volcanic, windblown sand (eolianites). The volcaniclastic sediments of the middle to upper Spears Group probably are poor aquifers. Eolianites are inferred to have both intergranular and fracture flow, and likely have higher permeability than the volcaniclastic sediments.

In addition, fracture networks may be sufficiently open and connected in the lava flows and tuffs, particularly the regionally extensive and thick ignimbrites, to allow appreciable groundwater movement.

Basin fill strata of the Santa Fe Group can be subdivided into the following facies: proximal to medial piedmont, distal piedmont, basin floor (or alluvial flat), and playa. In the southern part of the North graben, we recognize piedmont versus basin floor facies using geophysical-well-log and cuttings criteria from three wells with detailed wireline logs and/or cuttings records. Here, we interpret a western piedmont facies interfingering eastward with a finer-grained basin floor facies, which in turn interfingers eastward with an eastern piedmont facies. Two to three, "layer-cake" stratigraphic intervals can be locally recognized using inferred disconformities in wireline data or abrupt lithologic changes, but mapping their lateral extent away from wells awaits further study.

Overall, the texture of the basin fill in the southern North graben, the location of the proposed well field by Augustin Plains Ranch, is sand and clayey-silty sand that is capped by a 300–350 ft-thick, upper gravel-bearing interval with a notably high proportion of clay. This upper gravel-bearing interval experienced a dramatic eastward progradation in the Pleistocene that could be related to a slow down of faulting or paleoclimatic changes. Analyses of sonic and density-porosity well-log data from the 3,500 ft-deep SA-221 well indicates a general range in sand porosity of 5–25%, decreasing with depth. The notable clay content of subsurface sediment here—and also inferred for the northern part of the North graben and most of the C-N embayment—makes these areas susceptible to groundwater-related subsidence if there is large-scale pumping. In addition, the high clay content in the coarse, uppermost western piedmont unit of the southern North graben may impede infiltration from the surface to the water table. In the North graben, piedmont deposits of the lower part of the upper Santa Fe Group appear to have the highest proportion of high-porosity sands.

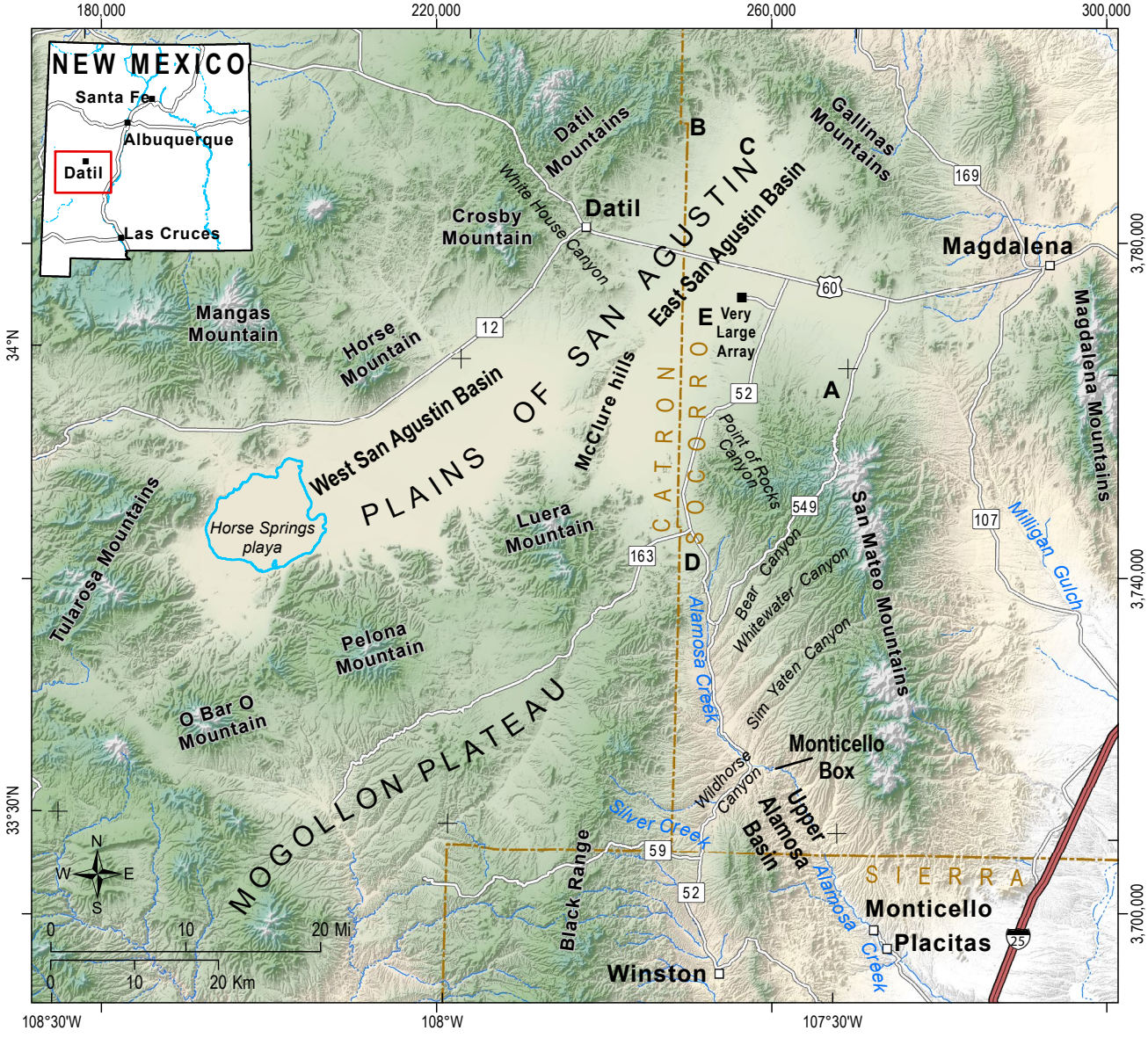

Figure 1. Geographic and topographic features of the Plains of San Agustin and Alamosa Creek. Note that the informally named McClure hills divides the Plains into a western and eastern topographic basin. A large playa exists at the southwest end of the West San Agustin Basin; note that this basin was called the "Horse Springs basin" by Weber (1994) and we informally apply that name to the playa. Capital letters A through E are the locations of photographs depicted in Figure 2.

I. INTRODUCTION

This report is a complement to a hydrogeologic study (due to be released 2021; summarized in OFR-615) regarding groundwater movement, age, and storage under the Plains of San Agustin and the upper Alamosa Creek watershed. The report presented here gives a detailed treatment of the geologic aspects of these areas. In addition, this report presents a background summary of the region's topography, geography, vegetation, and climate.

Previous Work

Much of this report involves compilation from previous work. Cepeda and Allison (1994) provided vegetation details. Information regarding the geology of mountain ranges surrounding the eastern Plains of San Agustin was obtained from Lopez and Bornhorst (1979) and various master's theses produced under the supervision of Charles E. Chapin: Brouillard (1984); Chamberlin (1974); Coffin (1981); Harrison (1980); and Wilkinson (1976). We used the volcanic stratigraphic nomenclature and correlations of Osburn and Chapin (1983), Cather et al. (1994), and Ferguson et al. (2012). Various mapping efforts by Charles A. Ferguson and G.R. Osburn were essential for understanding the volcanic geology in the C-N embayment and upper Alamosa Creek watershed: Ferguson (1986a, 1991); Ferguson and Osburn (1994, 2007, 2011, 2012, 2014); Osburn and Ferguson (2007, 2010, 2011, 2014). For the eastern Plains of San Agustin, we utilized electric resistivity soundings and related interpretations by Myers et al. (1994).

Geographic and Topographic Setting

About 120–150 miles southwest of Albuquerque and 50–60 miles west of Socorro lies the Plains of San Agustin (Figs. 1, 2), where the Augustin Plains Ranch, LLC, proposes to conduct large-scale pumping of groundwater to sell to potential users in the Rio Grande valley. The Plains of San Agustin occupy a 55 mile long, 10–20 mile wide, northeast-trending topographic low that extends across Catron and Socorro counties. These grasslands lie at 6,775–7,500 ft elevation; the general elevation of the surrounding, forested mountains is 8,000–10,000 ft. The one town in the area is Datil (population of ~50–60). Elsewhere, only widely scattered ranches populate this lonely, picturesque landscape. Note that the spelling of San Agustin has varied with time, with San Augustin and San Augustine variants used in past literature.

Other than the aforementioned water project, the Plains of San Agustin may be best known for hosting the Karl G. Jansky Very Large Array (VLA) radio telescope observatory, where twenty-seven large (82 ft wide), dish-shaped antennas are arranged in a three-armed pattern. This extremely sensitive system detects naturally emitted radio signals from objects in space. This observatory also provided the ideal backdrop for *Contact*, the 1997 film starring Jodie Foster.

The Plains of San Agustin is comprised of a series of topographically closed hydrologic basins, where all surface drainage ends in playa lakes (Figs. 1, 3). In its entirety, the Plains of San Agustin has a drainage catchment area of approximately 2,000 square miles (Phillips et al., 1992). A topographic high that we informally call the McLure hills extends southward between the town of Datil and the Luera Mountains. Rising 65–330 ft above the flat-floored plains, it divides the Plains of San Agustin into two geographic features that we call the West and East San Agustin basins (Figs. 1, 3), the latter being of interest for this report.

The designation of basins within the Plains of San Agustin has varied with past workers. For example, the groundwater study of Myers et al. (1994) consider the Plains of San Agustin as one basin (the San Agustin Basin), but another study focusing on surface drainage and paleolakes (Weber, 1994) differentiated four topographic (or hydrologic) basins in the Plains of San Agustin containing four respective playas: Horse Spring, C-N, White Lake, and North Lake basins. The Horse Spring playa in the West San Agustin basin lies at an elevation of 6,775 ft, while the other three playas in the East San Agustin Basin are 119–177 ft higher in elevation. Note that the

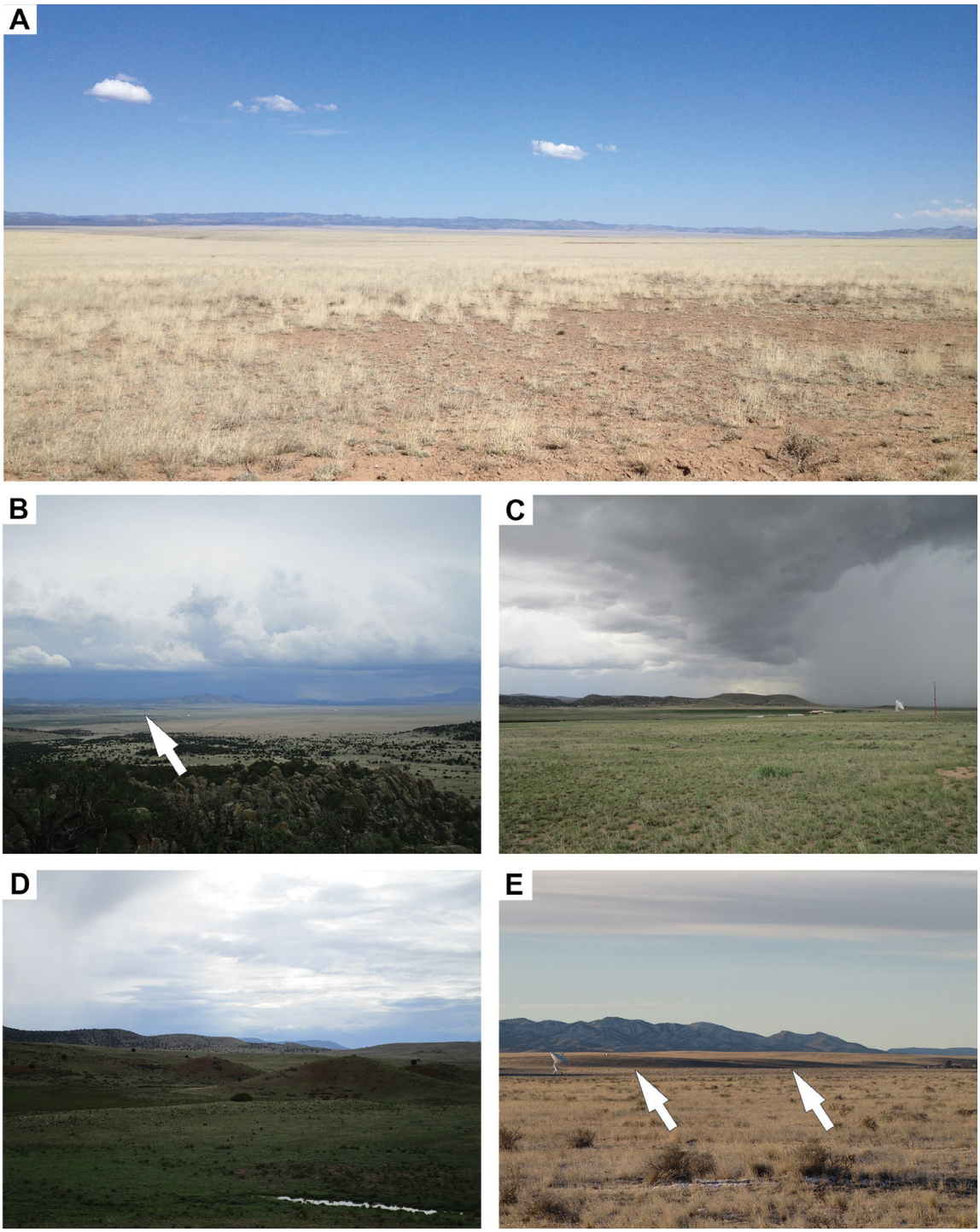

Figure 2. Photographs of the San Agustin Plains. A) Photograph looking towards the north end of the East San Agustin basin, where the northern Datil Mountains (left) and the northern Gallinas Mountains (right) converge. B) Photograph looking southeast across the northern East San Agustin basin. The white arrow points to a topographic depression, called North Lake, likely created by tectonic subsidence between two normal faults (Coffin, 1981). C) Close-up of ranch buildings and a VLA radio telescope antenna located just south of the topographic depression in Photo B (near head of left black arrow in Photo B). D) Low hills in the topographic saddle between the upper Alamosa basin and the C-N embayment. View is to the west. E) Photograph looking southeastward at a north-trending fault scarp southwest of the VLA headquarters. Shading by early morning sunlight accentuates the steep slopes of this particular scarp (at head of white arrows). One of the VLA telescope radio antennas can be observed on the left. Fault scarps are created by vertical displacement across faults during earthquake events. Geologists estimate it has been about 100,000 years since the last surface rupture occurred along faults near the VLA (McFadden et al., 1994).

topographic highs separating the three playas in the East San Agustin basin are relatively low (≤ 35 ft). As discussed below, our study differentiates the East San Agustin topographic basin into smaller structural basins using geologic criteria, particularly faults and the elevation of the base of Oligocene-Quaternary basin fill (i.e., the Santa Fe Group).

South of the East San Agustin Basin lies a south-flowing, ephemeral drainage called Alamosa Creek (Fig. 1). It drains relatively high topography of the adjoining Black Range (to the west) and the San Mateo Mountains (to the east). Alamosa Creek flows ~15 miles south before bending east and cutting a gorge in volcanic bedrock; this gorge is called the Monticello Box (Fig. 1). From there, the creek turns southeast and goes past the town of Monticello, eventually joining the Rio Grande at Elephant Butte Reservoir (18 miles downstream of Monticello).

Plains of San Agustin

The West San Agustin basin is orientated northeast-southwest, and is 30–35 miles long and ~9 miles wide (Fig. 1). High topography that surrounds this basin includes the northern escarpment of the Mogollon Plateau and the Luera, Pelona, and O-Bar-O mountains to the southeast, the Tularosa Mountains on the southwest, and the Mangas, Horse, and Crosby mountains to the northwest. An extensive 35 mi^2 playa lies on the southwest side of the West San Agustin basin, (Fig. 1). On the north side of this playa, the 2,000 ft-long Oberlin core was obtained from two boreholes spaced 3–4 ft apart (Foreman et al., 1959).

The East San Agustin basin is more equant than the West San Agustin basin (Figs. 1, 3), with maximum dimensions of 24 mi (NE-SW) by 23 mi (NW-SE). The 9 mi-wide C-N embayment on the southwest side of the basin, holding the C-N playa, extends 10 mi to the south between the Luera Mountains and northern San Mateo Mountains (Fig. 3). An area of low topographic relief is present on the southeast side of the East San Agustin basin, east of which is the head of Milligan Gulch. The north end of the East San Agustin basin narrows to the north between the Datil and Gallinas mountains (Figs. 2A, 3).

Both the West and East San Agustin basins are internally drained and exhibit low slopes. Ephemeral drainages in the West San Agustin basin flow towards the 35 mi^2 playa on its southwest side (Horse Springs playa, Fig. 1). The East San Agustin basin drains centrally towards the White Lake playa in its north part (north of the VLA Visitor Center), which has an elevation of 6,952 ft, and towards the C-N Lake playa in the C-N embayment (elev. of 6,894 ft) (Fig. 3). A topographic rise of 6,980 ft-elevation separates the White Lake and C-N playas. The lowest elevation in the McClure hills west of C-N Lake is 6925 ft, which is 31 ft above the floor of C-N Lake playa (Fig. 3). The playa corresponding to North Lake occupies a 0.4 mi^2 depression at the far north end of the East San Agustin basin (Figs. 2c, 3). Only ephemeral streams flow into the East and West San Agustin basins. Associated stream channels are ill-defined to non-existent in the interior of the basins, but are more apparent on the flanking alluvial fans. The aforementioned playas are wet intermittently, typically during the summer monsoon season. The playa on the southwest side of the West San Agustin basin may be wet for several months if there is above-normal precipitation during the summer monsoon season.

Alamosa Creek

Alamosa Creek flows 15 mi south in a ~9 mi-wide, north-south trending topographic low that we call the upper Alamosa basin (Figs. 1, 3). Ranging in altitude from ~6,200 to 7,000 ft, the upper Alamosa basin receives runoff from two opposing topographic highs: the Black Range to the west (maximum elevation of 8,500 ft) and the San Mateo Mountains to the east (maximum elevation of 10,000 ft). The northern end of Alamosa Creek is separated from the southern edge of the C-N embayment by a low topographic divide (7,190 ft elevation), which lies ~300 ft above C-N playa (Figs. 2d, 3). Alamosa Creek is ephemeral until it swings east and exits the upper Alamosa basin via the Monticello Box bedrock gorge (Fig. 1). Here, several springs discharge sufficient water to form a perennial stream for 11 mi downstream of the head of the gorge (with an average annual discharge rate of 8.3 ft^3 per second, per Myers et al., 1994). Water diverted from this stream is delivered to farms, ranches, and residences in Alamosa Canyon between the Monticello Box and the downstream communities of Placitas and Monticello.

Vegetation

Four plant associations are found in the region of the Plains of San Agustin and upper Alamosa basin that are strongly (but not wholly) dependent on elevation (listed from lower elevation to higher elevations): Plains-Mesa Grassland, Juniper Savanna, Coniferous and Mixed Woodland, and Montane and Subalpine Coniferous Forest (Cepeda and Allison, 1994). Plains-Mesa grassland cover the Plains of San Agustin and at ~7000 ft elevation merges upwards into Juniper Savanna or woodlands (Fig. 2a,b). The dominant plant type is blue grama grass. Other typical grass species are sideoats and black grama. Typical forbs include red globemallow, curly cup gumweed, and zinnia (Cepeda and Allison, 1994).

Grassland also covers the southern and western floor of upper Alamosa basin, extending onto high geomorphic surfaces in its eastern part. Juniper woodlands occupy the north-facing slopes of drainages in this basin. In the northeast part of Upper Alamosa basin, junipers grow on both northwest- and southeast-facing, relatively steep slopes of canyons.

Various woodlands dominate steeper slopes surrounding the Plains of San Agustin, as well as the eastern flanks of the Black Range and the western slopes of the San Mateo Mountains. Juniper Savana in this region consists mostly of one-seed juniper and Rocky Mountain juniper; locally, piñon pine is abundant. Blue grama and sideoats grama comprise the dominant grasses. Coniferous and Mixed Woodland consists of a mixture of junipers (with alligator juniper locally abundant), oaks, and piñon pine. In the Montane and Subalpine Coniferous Forest zone, ponderosa pine and gamble oak dominate the lower elevations; higher elevations in the zone contain Douglas fir, blue spruce, Engelmann spruce, and limber pine (Cepeda and Allison, 1994).

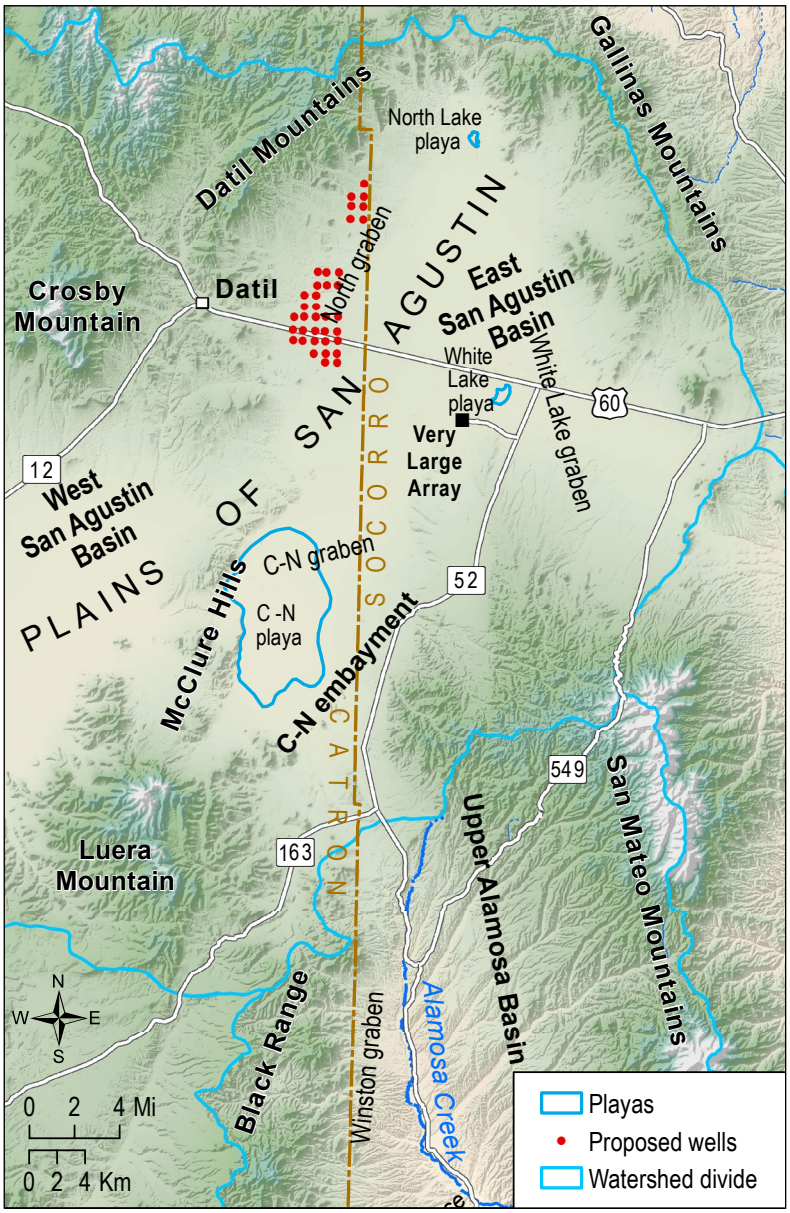

Figure 3. Geographic and topographic features of the eastern Plains of Agustin and upper Alamosa basin, which comprises the study area. Surface watershed divides are shown as thick, light blue lines. Also shown are locations of four grabens, which are geologic features. Note that the names C-N emabyment, C-N playa, an C-N graben are respectively unique geographic, topographic, and geologic features.

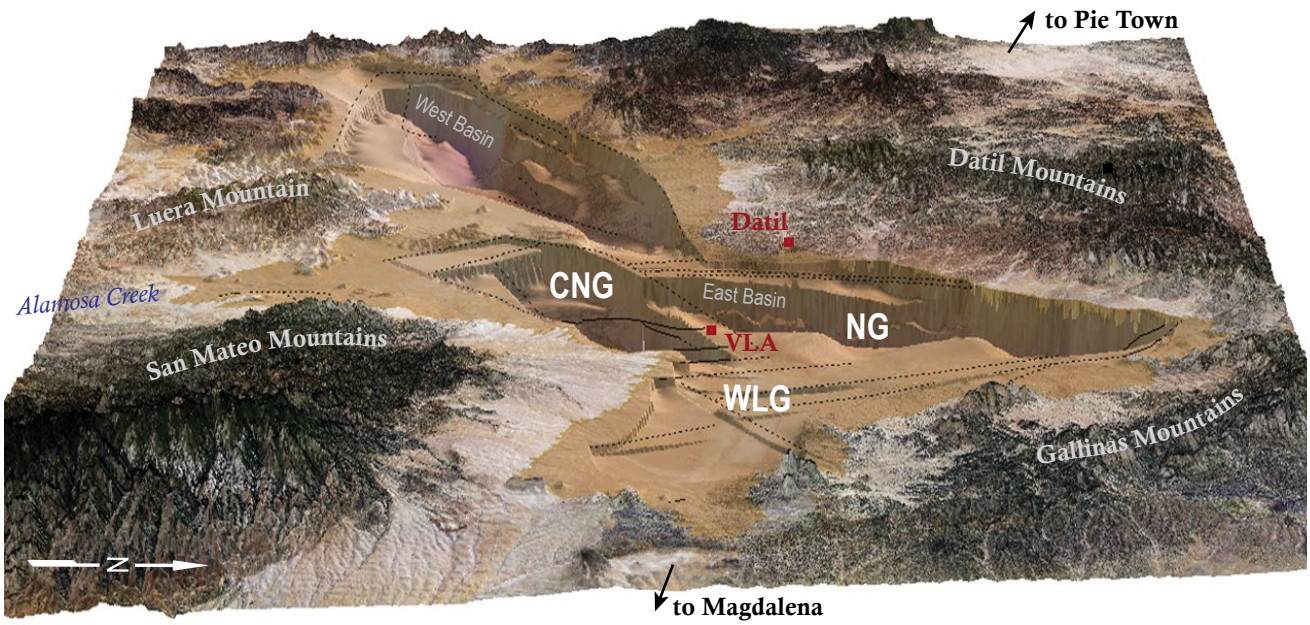

Figure 4. Three-dimensional model of the geologic structure under the Plains of San Agustin, constructed using our subsurface contouring (see Fig. 11) and Arc Scene. Dark-shaded, deep areas are where basin fill has been digitally removed to illustrate the geologic structure. The locations of the town of Datil and the VLA headquarters are shown in red. The three grabens of the East San Agustin basin are abbreviated as: CNG = C-N graben, NG = North graben, and WLG = White Lake graben. Faults are shown as dotted lines. View is to the west.

Climate

The region's climate is semiarid. Lower elevations receive about 10–15 inches of annual precipitation and higher topography receives as much as 30 inches (Phillips et al., 1992). Climate records for the eastern Plains of San Agustin are obtained by a weather station near the VLA (Augustine 2 E). For the years 1926 through 2016, this station recorded an average precipitation of 11 inches, a little over half of it received during the summer monsoonal months of July through September (Western Regional Climate Center, 2014). Myers et al. (1994) notes an average annual precipitation of 13 inches. Annual maximum temperatures average 66.3°, with average winter (December through February) maximum temperatures of 49°F and average summer (June through August) maximum temperatures of 83.5°F (Western Regional Climate Center, 2014). Annual minimum temperatures average 30.9°F, with average winter and summer minimum temperatures of 15.2°F and 49.3°F, respectively (Western Regional Climate Center, 2014). The upper Alamosa basin receives an average of 14 inches of annual precipitation; within the basin, annual precipitation ranges from less than 12 inches in lower Alamosa Creek to more than 20 inches in the surrounding mountains (Meyers et al., 1994). Similar to the Plains of San Agustin, the upper Alamosa basin receives most of its precipitation in July, August, and September from monsoonal thunderstorms.

II. GEOLOGY

The geology of the study area has four main components: older sedimentary rocks, volcanic bedrock, basin fill, and valley-fill alluvium. The older sedimentary rock includes a ~5,800 ft-thick package of sedimentary strata representing the Paleozoic, Mesozoic, and middle Cenozoic Eras. Overlying volcanic bedrock is 3,000–5,000 ft thick and about 38–24 million years old. This bedrock includes lava flows, ash-flow tuffs, and sediment eroded from past volcanoes during or shortly after they erupted. "Basin fill" refers to younger sediment (less than 26 million years old) filling geologic depressions called structural basins, which have bedrock floors that have been dropped down by faults over millions of years. Compared to the volcanic bedrock, the basin fill in the study area is much less cemented. Basins underlying the Plains of San Agustin are illustrated in Figure 4, which conceptually depicts how the landscape would look if basin fill was removed. We present two maps illustrating the geology exposed on the surface of the Earth (Figs. 5, 6). Interpretation of geologic features in the subsurface rely on these geologic maps in addition to geophysical methods (such as gravity data and electrical resistivity data, the latter presented in Myers et al., 1994) and well data (i.e., cuttings and wireline logging) presented later in this report.

Groundwater movement and storage in the study area are strongly influenced by stratigraphic and structural features. Stratigraphic features pertain to subdivision of the Earth's upper crust into unique three-dimensional bodies (i.e., lithologic units). In stratigraphic studies, it is important to understand how these bodies (units) were originally formed and their present-day spatial relationships. Structural features (e.g., folds or fault lines) are a consequence of past forces (stresses) in the Earth's crust that have deformed lithologic units. Most geologic structures discussed in this report are due to extensional stresses over the past 36 million years (minimum age from Cather, 1990), which also formed the Rio Grande rift to the east.

Structure

The upper Alamosa basin, West San Agustin basin, and East San Agustin basin overlie geologic structures called grabens. A graben is a block of the Earth's crust, bounded by faults on one or both sides, which has slid down relative to the adjoining crust (Fig. 7). These faults are typically "normal faults," in which the upper block of a dipping fault plane has slid downward relative to the underlying block (Fig. 7). Normal faults and grabens commonly are a consequence of extension of the Earth's crust. Moreover, grabens are commonly asymmetric (Landon, 1994), that is, they are tilted more on one side than the other (half-graben in Fig. 7). The upper Alamosa basin coincides with a single graben (Harrison, 1994; Myers et al., 1994; Koning, 2012). We interpret three grabens underlie the East San Agustin basin. Note that a graben is commonly named after a coinciding geographic feature (e.g., C-N embayment and C-N graben).

Upper Alamosa Basin

The upper Alamosa basin coincides with the 40 mile long, 6–11 mile wide, north-trending Winston graben of Harrison (1992, 1994) and Koning (2012). Myers et al. (1994) refer to this structure as the Cuchillo Negro graben, but we elect to use the name Winston graben because of precedence in the literature (e.g., Chapin et al., 1978; Harrison, 1992), with Kelley (1955) calling it the Winston-Hillsboro trough. Note that the Winston graben extends south past the town of Winston, but our study area only includes the northern part of the Winston graben, north of ~33° 37' N latitude (Fig. 5). Sparse gravity data and bedding attitudes indicate that the northern Winston graben is asymmetric and tilted to the west towards the north-striking, west-down Black Range fault (Gilmer et al., 1986; Koning, 2012) (Figs. 5, 8, 9). Comparison of relative differences of Bouguer anomally gravity data in areas having deep well control (i.e., 4–6 mi east of Datil) with the upper Alamosa

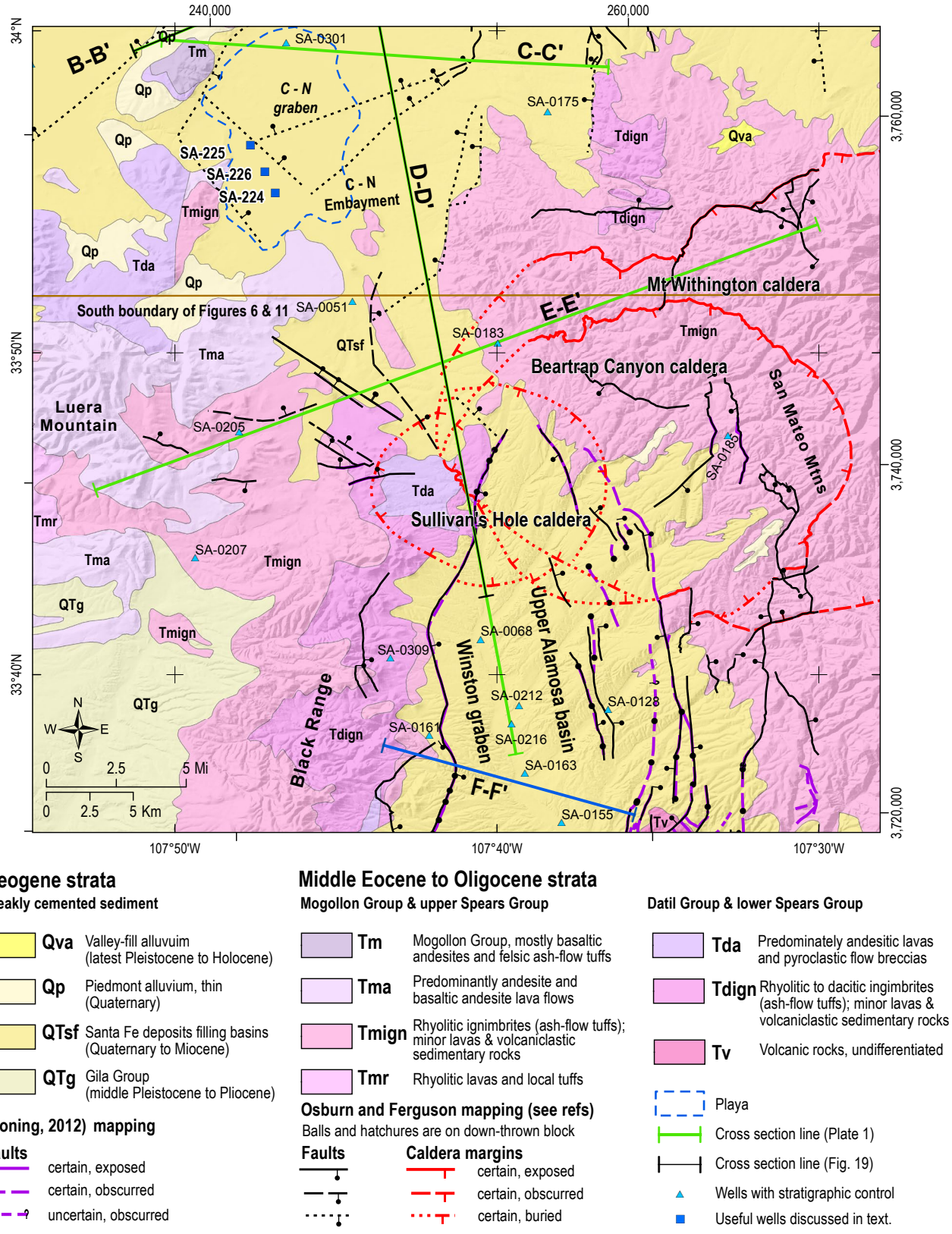

Neogene strata

Weakly cemented sediment

- **Qva** Valley-fill alluvuim (latest Pleistocene to Holocene)
- **Qp** Piedmont alluvium, thin (Quaternary)
- **QTsf** Santa Fe deposits filling basins (Quaternary to Miocene)
- **QTg** Gila Group (middle Pleistocene to Pliocene)

(Koning, 2012) mapping

Faults

- certain, exposed
- certain, obscurred
- uncertain, obscurred

Middle Eocene to Oligocene strata

Mogollon Group & upper Spears Group

- **Tm** Mogollon Group, mostly basaltic andesites and felsic ash-flow tuffs
- **Tma** Predominantly andesite and basaltic andesite lava flows
- **Tmign** Rhyolitic ignimbrites (ash-flow tuffs); minor lavas & volcaniclastic sedimentary rocks
- **Tmr** Rhyolitic lavas and local tuffs

Osburn and Ferguson mapping (see refs)

Balls and hatchures are on down-thrown block

Faults

Caldera margins

- certain, exposed
- certain, obscurred
- certain, buried

Datil Group & lower Spears Group

- **Tda** Predominately andesitic lavas and pyroclastic flow breccias
- **Tdign** Rhyolitic to dacitic ingimbrites (ash-flow tuffs); minor lavas & volcaniclastic sedimentary rocks
- **Tv** Volcanic rocks, undifferentiated

- Playa
- Cross section line (Plate 1)
- Cross section line (Fig. 19)
- Wells with stratigraphic control
- Useful wells discussed in text.

Figure 5. Geologic map of the C-N embayment and upper Alamosa Creek. The D-D' line (Plate 1) is overlain by a thinner black line representing the cross section shown in Figure 19. Names of calderas denoted by red text follow Ferguson et al. (2012). Unless otherwise noted, the geology is from NMBGMR (2003). The blue cross section line (labeled F-F') is not included in Plate 1.

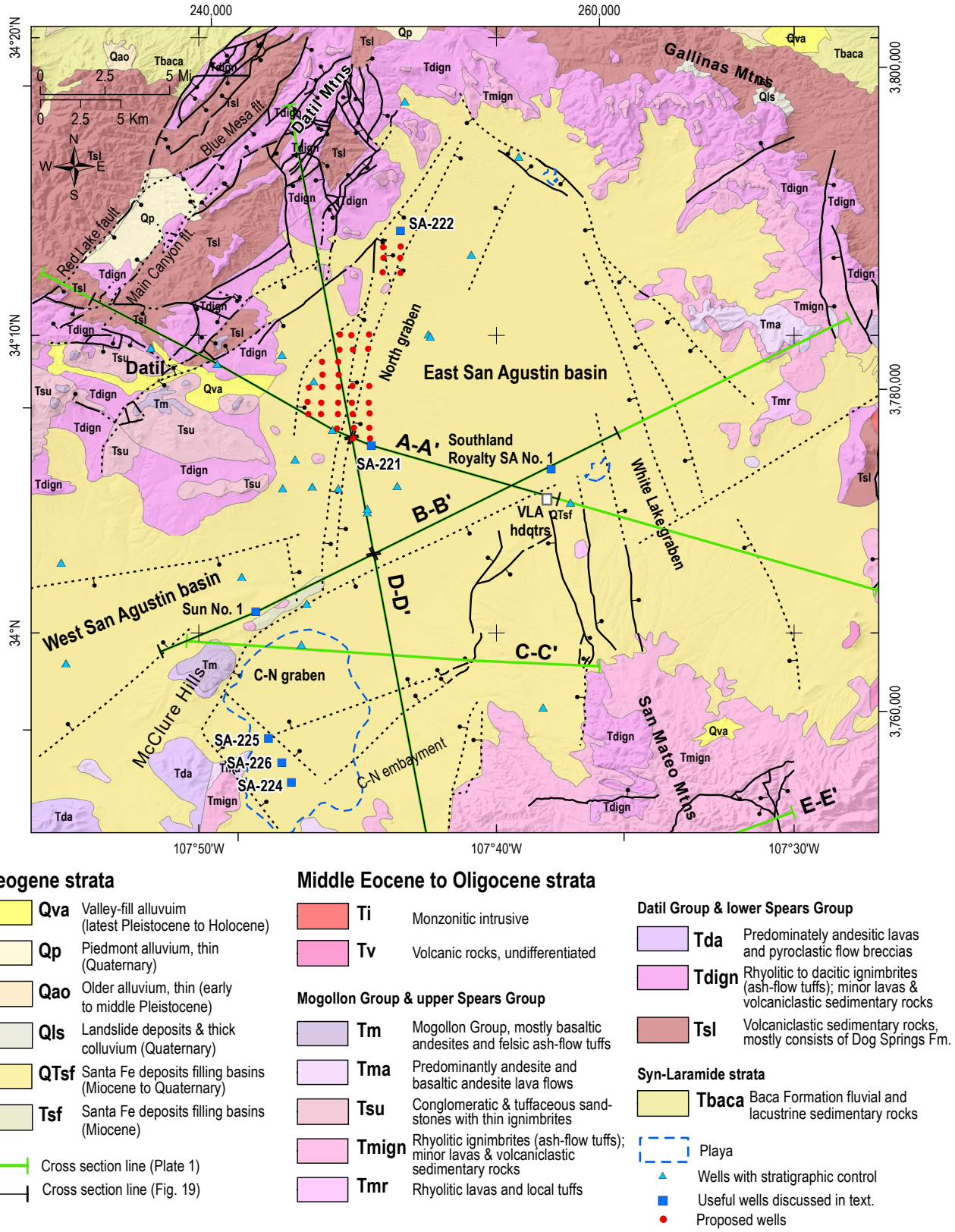

Neogene strata

- **Qva** Valley-fill alluvium (latest Pleistocene to Holocene)
- **Qp** Piedmont alluvium, thin (Quaternary)
- **Qao** Older alluvium, thin (early to middle Pleistocene)
- **Qls** Landslide deposits & thick colluvium (Quaternary)
- **QTsf** Santa Fe deposits filling basins (Miocene to Quaternary)
- **Tsf** Santa Fe deposits filling basins (Miocene)

Cross section line (Plate 1)
Cross section line (Fig. 19)

Middle Eocene to Oligocene strata

- **Ti** Monzonitic intrusive
- **Tv** Volcanic rocks, undifferentiated

Mogollon Group & upper Spears Group

- **Tm** Mogollon Group, mostly basaltic andesites and felsic ash-flow tuffs
- **Tma** Predominantly andesite and basaltic andesite lava flows
- **Tsu** Conglomeratic & tuffaceous sandstones with thin ignimbrites
- **Tmign** Rhyolitic ignimbrites (ash-flow tuffs); minor lavas & volcaniclastic sedimentary rocks
- **Tmr** Rhyolitic lavas and local tuffs

Datil Group & lower Spears Group

- **Tda** Predominately andesitic lavas and pyroclastic flow breccias
- **Tdign** Rhyolitic to dacitic ignimbrites (ash-flow tuffs); minor lavas & volcaniclastic sedimentary rocks
- **Tsl** Volcaniclastic sedimentary rocks, mostly consists of Dog Springs Fm.

Syn-Laramide strata

- **Tbaca** Baca Formation fluvial and lacustrine sedimentary rocks

Playa
Wells with stratigraphic control
Useful wells discussed in text.
Proposed wells

Figure 6. Geologic map and well locations of the East San Agustin basin. Thick, black lines denote faults (dotted where concealed); thinner black lines enclosing colored polygons are lithologic contacts. Cross-section line locations (green) are for cross-sections depicted in Plate 1. These are superimposed by thinner black lines representing cross sections shown in Figure 19. The small red circles are the proposed wells of the Augustin Plains Ranch LLC. Wells particularly important for stratigraphic interpretations are shown as blue squares; other wells (light blue triangles) also offer stratigraphic constraints via driller logs. The geology is from NMBGMR (2003).

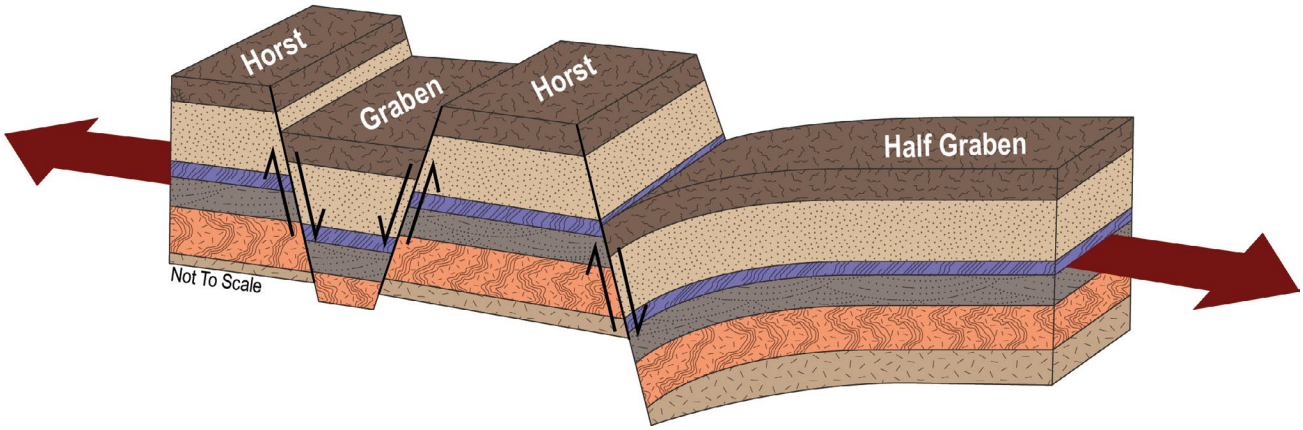

Figure 7. Schematic illustration of a full graben (left) and half graben (right). Grabens are formed by crustal blocks sliding downwards along normal faults. Small black arrows indicate direction of fault movment. Large red arrows show the direction of tectonic extension.

basin suggests a maximum basin-fill depth of 4,600 ft for the latter (Koning, 2012; Figs. 10, 11).

Santa Fe Group deposits that fill the northern Winston graben appear to be progressively less tilted up-section, indicating that westward tilting accompanied basin deposition (Koning, 2012, based on 1:24,000 scale mapping by C.A. Ferguson and G.R. Osburn listed in references). Lower (older) Santa Fe Group strata (probably 24–12? million years old) are tilted >15° westward, whereas middle-upper (younger) strata (12? to 5–2 Ma) dip 0–15°, with dips progressively decreasing up-section. Exposed playa deposits in upper Santa Fe Group strata indicate closed basin conditions in the northern Winston graben, and mapping east of the Monticello Box has not found evidence of an axial river draining the upper Alamosa basin prior to 5 Ma (D.J. Koning, unpublished data). This indicates that the rate of basin subsidence generally exceeded rates of sediment accumulation prior to open-basin conditions (i.e., Alamosa Creek extending downstream from the northern Winston graben into the Rio Grande).

East San Agustin Basin

The structure under the East San Agustin basin is less constrained compared to the upper Alamosa basin. Unlike the latter, the East San Agustin basin has remained topographically closed (endorheic) and thus basin fill has not been notably eroded. Therefore, sparse data provided by geophysical surveys and borehole data are particularly valuable (Figs. 9, 11). Geophysical data consist of gravity readings (PACES gravity database, 2014) as well as vertical electrical resistivity soundings (Myers et al., 1994).

We used these geophysical data in conjunction with lithologic data (from boreholes, wells, and geologic mapping) to interpret three grabens under the East San Agustin basin (Figs. 4, 11), which we call the North graben, White Lake graben, and C-N graben (clockwise from north). The North graben more or less coincides with the topographic Gallinas embayment of Myers et al. (1994), and is bounded by the Datil Mountains on the west and the Gallinas Mountains on the east. Narrowing to the north, its maximum dimensions are 13 miles long (north-south) and 11 miles wide (northeast-southwest). A subsurface bedrock high, located immediately north of the northeast-striking fault passing near the VLA observatory headquarters, separates the North graben from the C-N graben to the south (Figs. 6, 11).

Borehole, gravity, and resistivity data (Myers et al., 1994) indicate that the North graben is asymmetric, being tilted to the west against a north- to northeast-trending, east-down fault zone that bounds the eastern side of the Datil Mountains (Fig. 6, 11). Locally, these faults have created scarps as high as 5 m in middle (?) Pleistocene alluvium (Machette, 1978; Machette and McGimsey, 1983; Machette et al., 1998). Deep basin fill is localized immediately east of the fault zone. For example, well SA-221, located only 0.6–1.2 miles east of the eastern fault, bottomed at 3500 ft depth in basin fill (Fig. 11). Basin fill progressively thins to the east. Beyond 5–6 miles east of the fault zone, the geologic structure approximates a bench or platform with less than 1,000 ft of basin fill (Figs. 4, 11). Lithologic interpretations of boreholes drilled 3–4 miles northeast of the VLA observatory

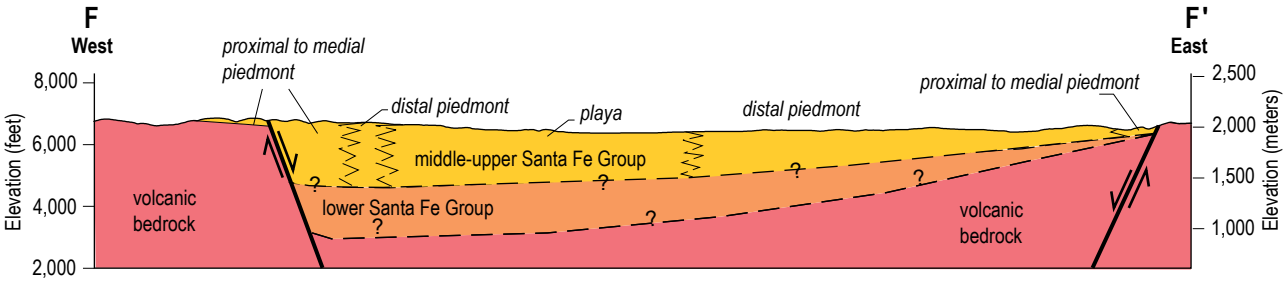

Figure 8. A west-east cross-section across the Winston graben near the southern boundary of the study area (Figs. 5, 10). The asymmetric nature of this basin, a result of more displacement along the western border fault compared to the eastern border fault, results in Santa Fe Group basin fill thickening to the west. The internal stratigraphy of the Santa Fe Group is also depicted. Modified from Koning (2012).

indicate that basin-fill there is 500–650 ft thick (G.R. Osburn, unpublished report to Mobil Alternative Energy Inc., 1984, cited in Chamberlin et al., 1994a, p. 15), consistent with gravity data (Fig. 11). Inclusion of a single low Bouguer gravity value in the northern part of the North graben (-243.3, Fig. 9) with the structural contouring of the base-of-basin fill suggests that the North graben may be subdivided into two "sub-grabens" separated by a bedrock saddle (ridge) 3 miles south-southeast of well SA-222 (Fig. 11). More data (i.e., gravity, electric resistivity, seismic, or boreholes) are needed to confirm the existence and geometry of the bedrock saddle and possible northern sub-graben.

Lacking resistivity soundings and drill holes, White Lake graben is poorly understood (Figs. 4, 11). It extends south-southeast from White Lake towards the low topographic divide (7,087–7,680 ft elevation) separating the East San Agustin basin from Milligan Gulch (Fig. 1). Three miles east of the VLA headquarters, the White Lake graben bends from north-northwest–south-southeast (to the north) to east-southeast (to the south). Mapped east-down faults extending north from the northern end of the San Mateo Mountains (part of the VLA fault zone; Machette and McGimsey, 1983; Machette et al., 1998) probably define the west boundary of the White Lake graben. Electrical resistivity soundings suggest that the base of basin fill is deeper at a location 3.5–4.0 miles (~6 km) northeast of the VLA observatory headquarters compared to ~1.2 miles to the east and west of the headquarters (Fig. 11; Myers et al., 1994). In the VLA area, a borehole (Southland Royalty SA No. 1) encountered the base of basin fill at a relatively shallow depth of 715 ft (Figs. 11, 12). Thus, we infer the west-bounding faults of the northern tip of the White Lake graben lies about 2–2.5 miles northeast of this borehole and the VLA headquarters (Figs. 6, 11).

The C-N graben is rectangular, being 8–9 miles long in the northeast direction and 4 miles wide in the southeast direction (Figs. 4, 11). The topographic high between the Datil and the Luera Mountains (McClure hills) bounds the graben on its west side, the Luera Mountains on its southwest side, and the northwestern San Mateo Mountains on its southeast side. The C-N graben is inferred to be bounded on all sides by faults, with its western floor likely dipping to the east (Fig. 11). The western fault is drawn using the linear eastern foot of the southern McLure hills, the northern fault is based on a relatively steep, southward Bouguer gravity gradient (Fig. 11), and the southern bounding fault is based on notable differences in bedrock elevations inferred from electrical resistivity sounding data (6,057 ft versus 4,777 ft across 2.5 mile distance, Fig. 11; Myers et al., 1994). The eastern bounding faults correspond with the VLA faults of Menges et al. (1984), which have offset middle(?) Pleistocene alluvium as much as 130 ft. The most recent movement along one of the VLA faults is inferred to be ca. 100,000 years ago, based on offset geomorphic surfaces and fault scarp morphology (Machette et al., 1998; McFadden et al., 1994). Maximum basin-fill thickness in the C-N graben is poorly constrained, but relative differences in Bouguer anomaly gravity values suggest ~4,000 ft, comparable with maximum basin-fill thicknesses in the adjoining North graben.

The northeast orientation of the West San Agustin basin and the C-N graben under the East San Agustin basin is likely controlled by older crustal structures that coincide with the southern limit of the Mogollon Slope (Chamberlin and Cather, 1994; Chamberlin, 1974). Chapin (1971) named this structure the San Augustine lineament and described it as a series of en echelon, northeast-trending fault zones and grabens. This lineament appears to approximate the northwestern boundary of the northeast-trending,

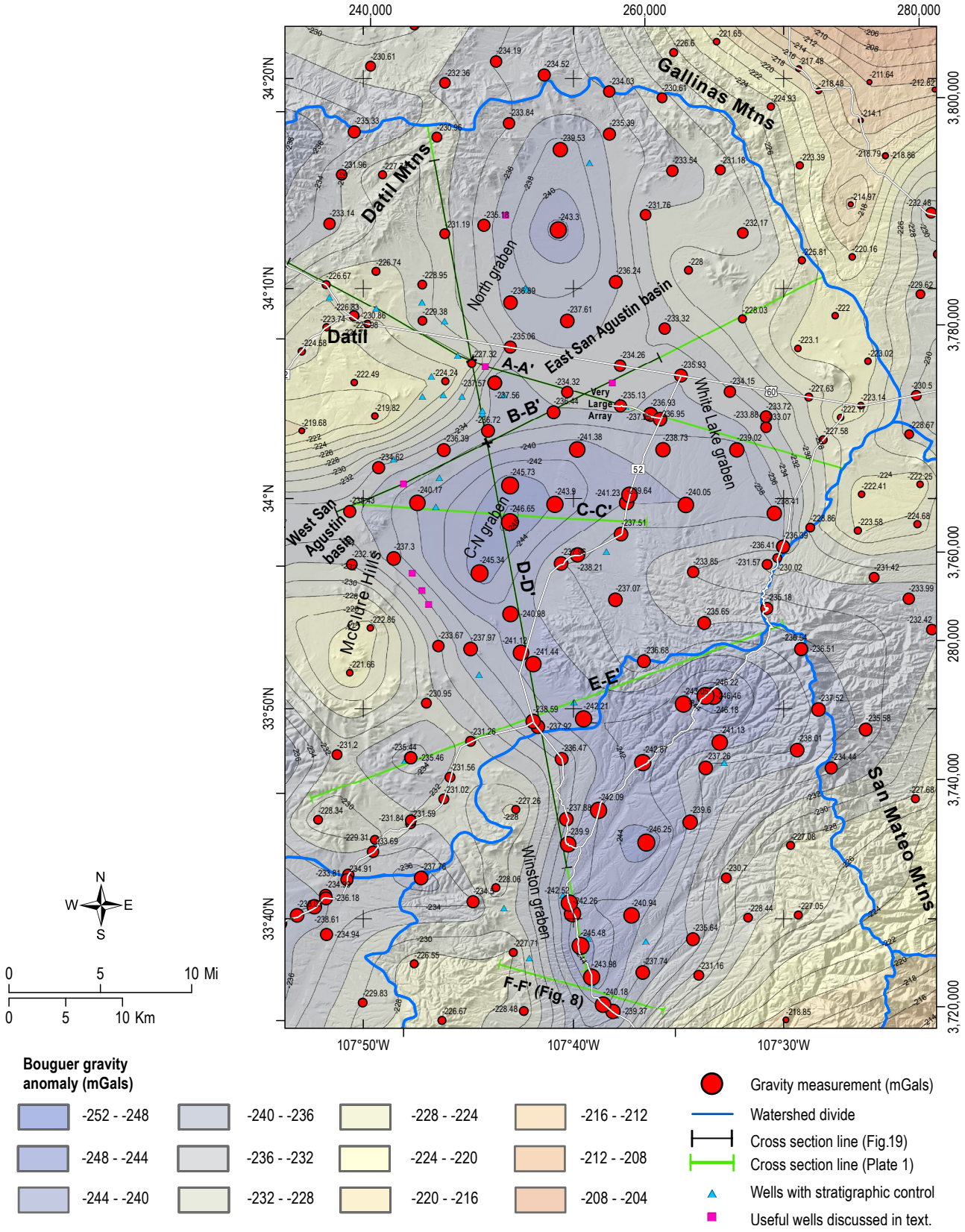

Figure 9. Gravity station locations in and near the study area. Gravity data were obtained from the PACES gravity database (2014) and reduced to show the terrain-corrected Bouguer gravity anomaly (Figs. 10, 11). White lines are roads. Note that the red circles are gravity measurement stations sized proportional to the magitude of the anomaly.

Laramide-age Morenci uplift of Cather and Johnson (1984), based on the apparent restriction of Laramide-age, clastic sedimentary strata (i.e., the Baca Formation) to the north of it. Northeast of the San Agustin Plains and north of Magdalena, left-lateral oblique slip is interpreted on the lineament's northeast trending faults (where the net left-lateral slip is as much as 4,000 ft; Chapin, 1971). There, the northeast-trending faults are offset by younger, north-trending normal faults (Chapin, 1971).

The structural relations observed along the San Augustine lineament north of Magdalena likely extend into the West and East San Agustin basins, but lack of exposure there makes interpretations uncertain. Buried, inferred northeast-trending faults on the northern and southern sides of the West San Agustin basin likely explain the northeast-trend of this structural low, even though buried north-trending faults may also be present. In the East San Agustin basin, a prominent northeast-trending fault (inferred based on gravity gradients), possibly stepping ~5 km to the right near the VLA observatory, approximately coincides with the terminations of north-south faults associated with the North, White Lake, and C-N grabens (Fig. 11). Southwest of the VLA observatory, this northeast-striking fault is interpreted to be southeast-side-down based on southeastward-down gradients in the Bouguer anomaly gravity data (Fig. 11). Available data does not allow observation of detailed cross-cutting relations, as seen north of Magdalena (Chapin, 1971), but these apparent fault terminations are consistent with a pre-existing, northeast-trending fault reflecting a larger-scale, northeast-striking structural fabric in the crust. The northeast alignment of volcanoes southwest of the Luera Mountains also attest to northeast-striking structural weaknesses in the crust. Note that Chamberlin (1974) interprets another structural trend (350°) in the Proterozoic basement east of the East San Agustin basin. Within the basin, this particular trend coincides with the trends of faults bounding the White Lake graben and faults near the foot of the Gallinas Mountains.

A number of north-northeast trending faults lie northwest and northeast of Datil, including the Red Lake, Blue Mesa, and Main Canyon faults (Fig. 6; Chamberlin et al., 1994a and 1994b; Lopez and Bornhorst, 1979). The Red Lake fault had a reversal of vertical motion between the late Laramide orogeny (~50–36 Ma), when the east side was uplifted, and post-36 Ma extension, when the east side subsided ~1,200 ft (Cather and Johnson, 1984; Cather, 1990). These faults trend more northerly than the San Augustine lineament and are not directly related to it.

Inferences may be made about the relative age of fault activity based on offset surfaces. Similar to north of Magdalena (Chapin, 1971), in the East San Agustin basin the northerly striking faults appear to be younger than the northeast-striking faults. The northerly faults locally form fault scarps in middle to late Quaternary alluvium, and thus would be post 800,000 years old. But movement along the northeast-trending faults is sufficiently old that there is no corresponding surface expression.

Calderas

Calderas are kilometer-scale, circular to slightly elliptical areas that have subsided over a rapidly depleting magma chamber, a process accompanied by explosive volcanic eruptions of ash and other debris (Fig. 13). This subsidence typically occurs on geologic structures that ring much of the caldera, which move similar to normal faults.

Geologists are relatively confident that three calderas exist in the study area (Ferguson et al., 2012, and references therein), although it is possible that more are buried underneath the Plains of San Agustin. The confirmed calderas are located near the topographic saddle between upper Alamosa basin (upper Alamosa Creek) and drainages flowing northward into C-N playa (Figs. 5, 10). The oldest and smallest is the Sullivan's Hole caldera (~34 million years old), which had the eastern half later down-dropped into the much larger Mount Withington caldera (27.73 ± 0.07 million years old). The youngest caldera is the Beartrap Canyon caldera (24.65 ± 0.06 million years old). The ignimbrites (ash-flow tuffs) sourced from these calderas are discussed in more detail below, and radiometric dating of these ignimbrites provides the aforementioned ages for their source calderas (Table 1).

Stratigraphy Background

The properties and extent of bedrock and sedimentary units under the Plains of San Agustin and upper Alamosa basin are important for groundwater studies and tell a fascinating geologic story. Strongly cemented bedrock layers are overlain by non- to moderately cemented sediment deposited mainly by water (with some wind-blown deposits) over the past ~26 million years. Most of this non- to moderately cemented sediment lies under basins, and hence is termed "basin fill." This section presents a

Tuff unit (source caldera*)	Datil Mountains (Harrison, 1980)	Luera Mountains-Mt. Withington area (compiled from mapping of Ferguson and Osburn)	Age (Ma)**
Turkey Springs (Beartrap Canyon)	Not preserved	Welded to non-welded, phenocryst content increases upwards from 3 to 15%, light gray to pink, 20% pumice lapilli, 5–10% lithic lapilli.	24.65 ± 0.06
South Canyon (Mount Withington)	Not preserved	Mostly welded. Phenocryst content increases up-section from 5% to 15%. Five to six subunits can be differentiated based on phenocryst content and compositions.	27.73 ± 0.07
Lemitar (Hardy Ridge)	Not preserved	Densely welded with 10–35% phenocrysts and 5–25% pumice lapilli.	28.36 ± 0.16
Bloodgood Canyon	Not preserved	Poorly to nonwelded, contains intracaldera Blue Canyon Tuff. 2–10% phenocrysts w/ abundant (1–2%) biotite. Slight pinkish color. Relatively thin (0–15 m thick)	28.41 ± 0.06
Vicks Peak (Nogal Canyon)	Light gray and very crystal poor, moderately pumice-rich, moderately welded. Local paleorelief at base. Well-developed eutaxitic structure. 1–3% tchitoyant sanidine phenocrysts, with trace phenocrysts of biotite, pyroxene, quartz, & plagioclase. 2–5% andesitic lithic clasts.	Densely welded, 1–15% phenos & 2–25% strongly flattened pumice lapilli. Lower part (up to 65 m) is poorly welded. Very thick within the Nogal Canyon caldera, its source.	28.93 ± 0.06
La Jencia (Sawmill Canyon)	Crystal poor, with 3–7% phenocrysts composed of sanidine, <0.5% quartz, <0.5% plagioclase, <0.5% biotite. 2–5% lithic fragments.	Densely welded with 2–10% phenocrysts, light to dark gray w/ 5–15% strongly flattened pumice lapilli up to 1 m long, 5% lithic lapilli. Lower part is poorly welded.	29.23 ± 0.07
Hells Mesa (Socorro)	Crystal-rich & quartz-rich. Base is 20 ft thick, white, quartz-poor, and poorly welded. Upper 250–350 ft is buff-colored, quartz-rich, moderately to poorly welded, and columnar jointed overlying a platy-fractured zone. 35–40% phenocrysts that include: 25–30% feldspar (mostly sanidine), 5–8% quartz, 2–4% biotite.	Densely welded with 20–35% phenocrysts; reddish brown to orange, sparse lithic lapilli, <10% pumice lapilli <10 cm long.	32.48 ± 0.10
Blue Canyon (Sullivan's Hole?)	Tan to light gray, moderately to poorly welded, and moderately crystal rich. 15–21% phenocrysts that include: 6–8% plagioclase, 8–10% sanidine, 1.5–3% biotite, <1% clinopyroxene, <1% hornblende.	Moderately phenocryst-rich tuff containing 10–15% plagioclase and 1–3% biotite; sparse pumice-lapilli; locally contains abundant lithic lapilli and blocks up to several meters.	34.10 ± 0.06
Rockhouse Canyon (Skeleton Ridge)	White to light gray. Poorly to non-welded at top and bottom. Partially welded middle part that is mostly densely welded and has columnar joints on either side of a platy layer. Pumice (up to 5 mm) content is variable (10–30%). Phenocrysts: 3–9% sanidine, ≤1% biotite, ≤1% plagioclase.	Caldera-fill that is moderately phenocryst-rich, typically dark gray, and contains 10–20% plagioclase (1–4 mm) and abundant biotite (1–3 mm).	34.61 ± 0.08***
Datil	Light gray & moderately welded. Grades up from crystal poor to crystal-rich. The upper part has 20–25% phenocrysts that include: 18–22% tchitoyant sanidine, 1–2% apple-green pyroxene, & 1% euhedral biotite. 10% pumice. Basaltic and lithic fragments common.	Not present.	35.43 ± 0.19***

* Calderas are from Ferguson et al. (2012).
** Unless noted otherwise, age is from McIntosh et al. (1991, 1992) and adjusted for the new Fish Canyon Tuff standard of 28.201 Ma.
*** Age is from McIntosh and Chamberlin (1994) and adjusted for the new Fish Canyon Tuff standard of 28.201 Ma.

Table 1. Description of regional ignimbrites in the eastern San Agustin Plains and upper Alamosa Creek.

summary of stratigraphic concepts and terms, and the next section describe the stratigraphic sequence in the study area from oldest to youngest. Detailed descriptions of the rock units are given in Appendix 1. Descriptive terms related to bedding thickness and shapes are illustrated in Figure 14, and gravel and sand size terms are given in Table 2 (note that gravel includes pebbles, cobbles, and boulders). This report only discusses geologic units that post-date 66 million years (i.e., the Cenozoic Era) because these rocks are closest to the Earth's surface and most germane for groundwater studies. Appendix 2 expounds on the geology of rocks in the study area predating 66 million years ago. Names relating to geologic time divisions are illustrated in Figure 15. In the following, the abbreviation "Mega annums" (Ma) represents "millions of years" in age.

The discipline of stratigraphy studies how rocks or variably consolidated sediment relate to each other in terms of space and time. There are a number of stratigraphic terms and concepts that we will employ in this section that are illustrated in Figure 16. First, in a pile of layered rocks, called strata (an individual layer is called stratum), the oldest layer lies on the bottom and is successively overlain by younger layers (law of superposition). Second, a rock body (commonly igneous) that cross-cuts another rock body is younger than the one it cross-cuts. Third, the boundary between two units of rock is called a contact. The contact might represent a minimal time gap, in which case it is conformable, or an appreciable amount of time might have passed before the younger rock was laid down over the older rock. The latter is an unconformity, which could be subdivided into different types. A nonconformity involves time gaps of at least tens of millions of years and very different rock types are juxtaposed across it (e.g., granite bedrock overlain by sedimentary rocks). In contrast, a disconformity involves less of a time gap and the rocks on either side are generally the same type (e.g., both sedimentary or both lava flows). In an angular unconformity, rock layers are tilted different amounts across the contact. These examples all involve vertical relations. A buttress unconformity, in contrast, is a lateral juxtaposition of rocks across an inclined or vertical contact that represents a geologic time gap (Fig. 16).

Stratigraphers attempt to group rocks and lesser-cemented sediment into a hierarchal system of units (Fig. 17). The fundamental unit is called a "formation," which is a package of lithologically similar rocks or sediment that can be readily mapped in the field. Formations may be subdivided into members.

Size term		Abbrev.*	Size (mm)
Boulder			>356
Cobble	coarse	c	128-356
	fine	f	64-128
Pebble	very coarse	vc	32.0-64.0
	coarse	c	16.0-32.0
	medium	m	8.0-16.0
	fine	f	4.0-8.0
	very fine	vf	2.0-4.0
Sand	very coarse	vcU	1.410-2.000
		vcL	1.000-1.410
	coarse	cU	0.710-1.000
		cL	0.500-0.7100
	medium	mU	0.350-0.500
		mL	0.250-0.350
	fine	fU	0.177-0.250
		fL	0.125-0.177
	very fine	vfU	0.088-0.125
		vfL	0.0625-0.088
Silt			<0.0625

*Abbreviations occasionally used in figures and appendices. Note that L=lower and U-upper. Grains sizes follow a modified Wentworth (1922) scale.

Table 2. Nomenclature for grain and gravel size.

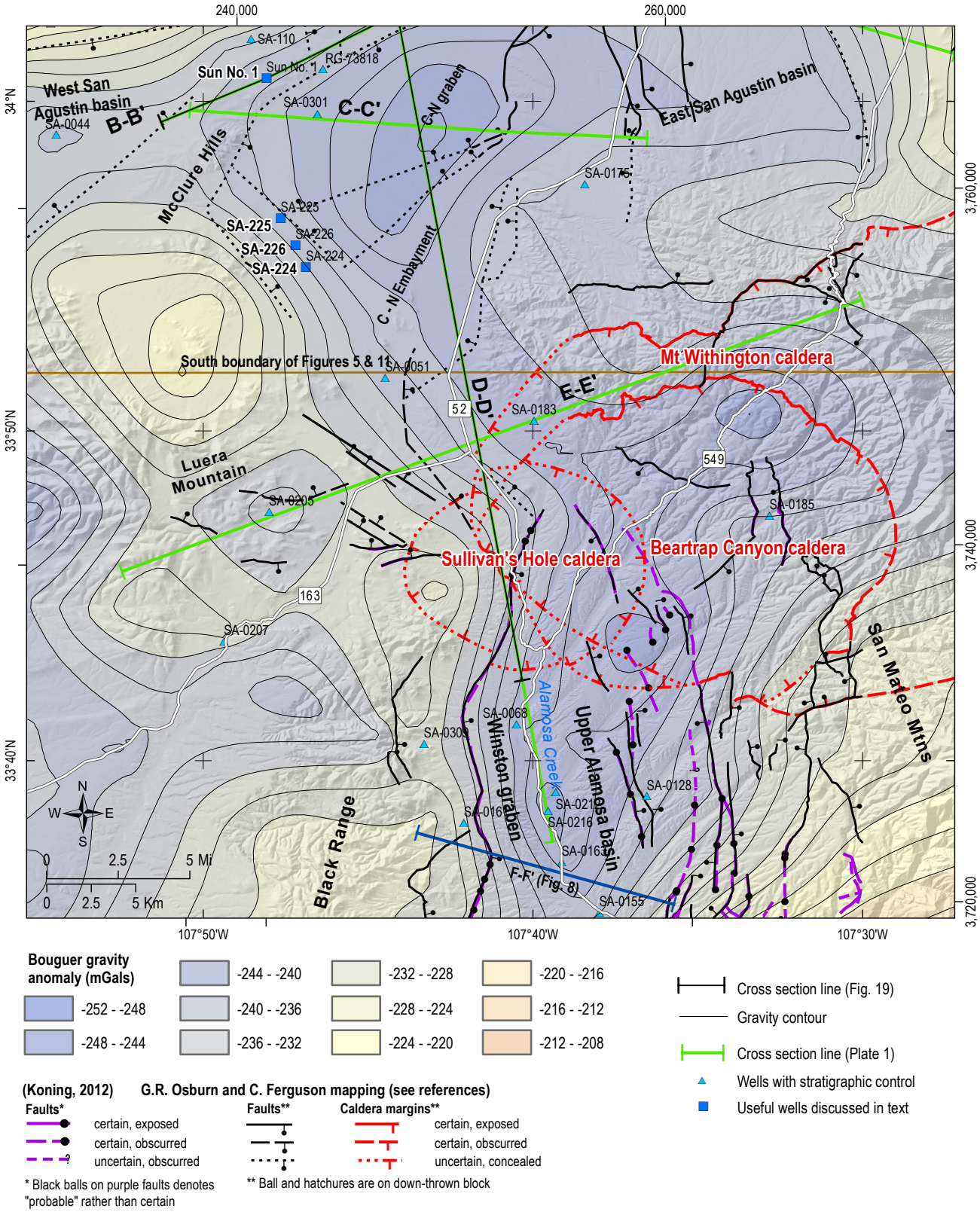

Figure 10. Map showing the Bouguer anomaly gravity data (via shading; values in milligals), faults (heavy black lines), and caldera margins (red lines) in the southern C-N embayment and upper Alamosa basin. Names of calderas that are denoted by red text follow Ferguson et al. (2012). Green lines denote locations of cross sections of Plate 1 with superimposed dark thin black lines depicting cross section lines of Fig. 19. White lines are highways. Figure 9 shows labels for the gravity data contouring.

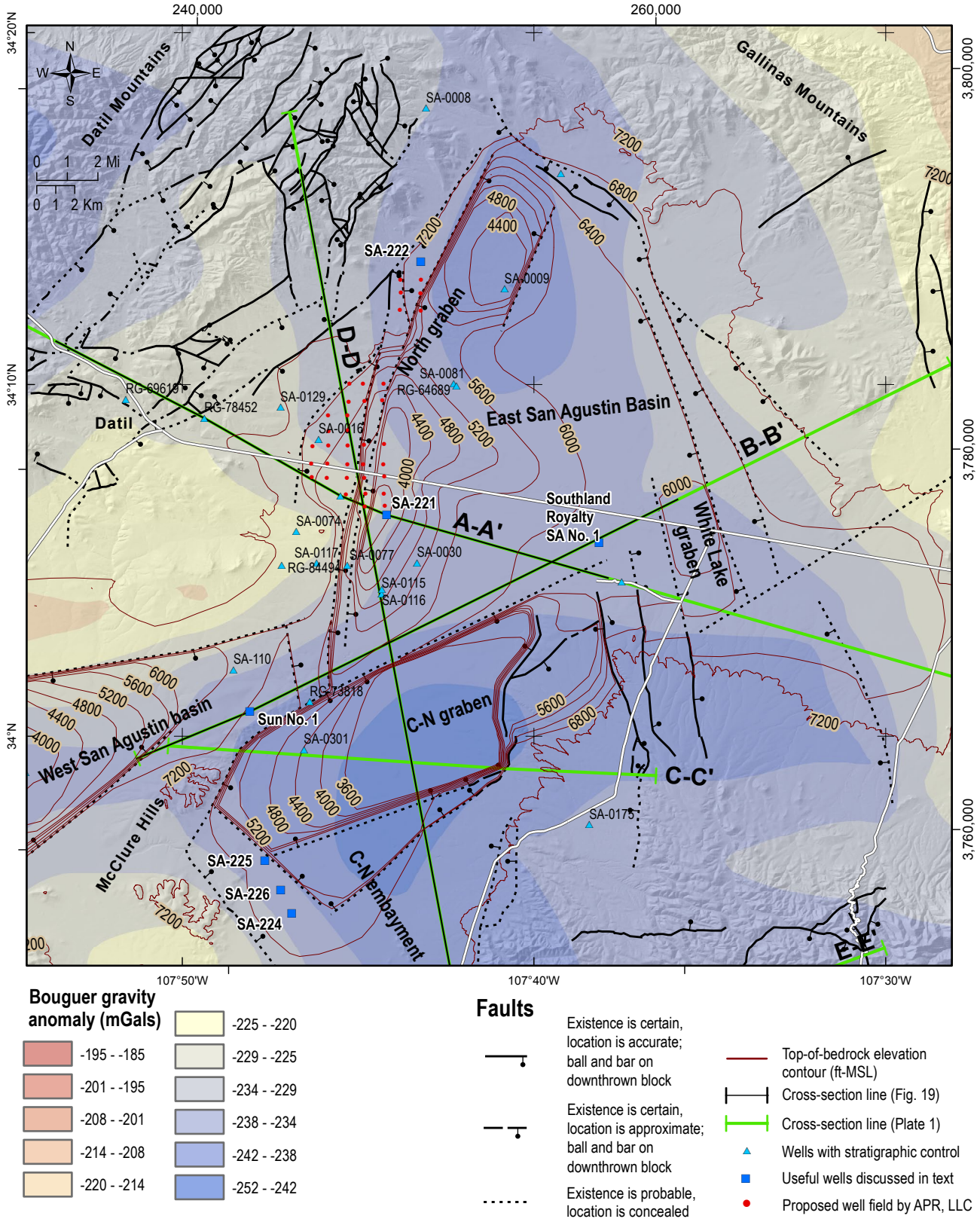

Bouguer gravity anomaly (mGals)

-195 - -185	-225 - -220
-201 - -195	-229 - -225
-208 - -201	-234 - -229
-214 - -208	-238 - -234
-220 - -214	-242 - -238
	-252 - -242

Faults

- Existence is certain, location is accurate; ball and bar on downthrown block
- Existence is certain, location is approximate; ball and bar on downthrown block
- Existence is probable, location is concealed

- Top-of-bedrock elevation contour (ft-MSL)
- Cross-section line (Fig. 19)
- Cross-section line (Plate 1)
- Wells with stratigraphic control
- Useful wells discussed in text
- Proposed well field by APR, LLC

Figure 11. Map of the East San Agustin basin showing Bouguer anomaly gravity data (via shading; values in milligals), faults, and inferred depth-to-bedrock under basin fill (using contours). The structural contours were interpreted using electrical resistivity soundings (see Myers et al., 1994, for associated data and interpretations), sparse well data, and interpretation of gravity data (Fig. 9). These contours define three grabens: North, White Lake, and C-N grabens. Green lines denote locations of cross sections of Plate 1, with superimposed, thinner black lines depicting cross section lines of Fig. 19.

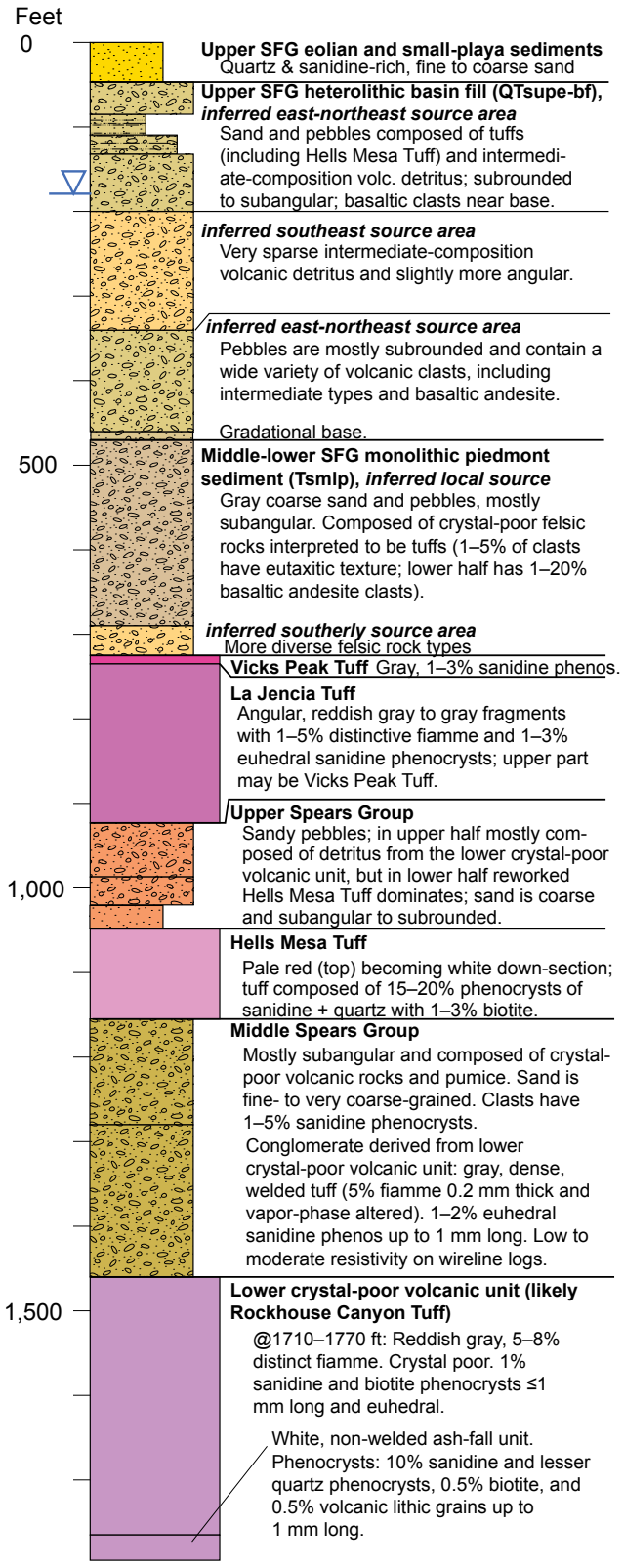

Members are noteworthy and usually lithologically distinctive, but to a lesser degree than formations; as such, they are more difficult to map. A distinctive layer (stratum), typically involving thicknesses of 1-10 m, within a formation or member is called a bed. Formations might be grouped together into more regional units called "groups" (Fig. 17).

Stratigraphy of Bedrock

Middle Eocene Sedimentary Rocks

Baca Formation

The Baca Formation consists predominately of reddish mudstones and red to light gray sandstone deposited in a closed basin in the late-early to middle Eocene. This unit is found only in the northern part of the study area, where it is 755–1,900 ft thick (Chamberlin, 1981; Cather, 1980; Cather and Johnson, 1986). Baca Formation sandstones are moderately to well-cemented by calcite and lesser silica, and are inferred to make better aquifers than the stronger-cemented sediments of the overlying Spears Group (Chamberlin et al., 1994b; S. Cather, personal commun., 2014).

The Baca Formation crops out on the north end of the Datil and Gallinas mountains. This unit was encountered in the Sun No. 1 well in the McLure hills (Figs. 6, 11, 18), where it is ~1,490 ft thick. In the Sun No. 1 well, this unit has a triparte, coarsening upward character. The lower 705 ft is largely composed of mudstone with a few thin beds of arkosic, fine to coarse sandstone. In the middle 480 ft, sandstone is more abundant, but there is still subordinate to mudstone and siltstone; the sand is mostly very fine- to fine-grained (locally medium to very coarse), and composed of quartz, feldspar, and chert. In the upper 310 ft, sandstone is subequal to mudstone-siltstone and composed of quartz and quartzite grains that are commonly frosted (thicknesses and descriptions are from New Mexico Bureau of Geology and Mineral Resources, unpublished records for the Sun No. 1 well).

The Baca Formation ranges in age from 51 to 38 Ma (Prothero et al. 2004; Lucas, 2015),

Figure 12. Illustration of the stratigraphic units encountered in the Southland Royalty SA No. 1 well, located 1.3 mi north of the VLA (NE 1/4 of SW1/4 of SW1/4, Section 35, Township 2S, Range 8W). Orangish-yellow shades represent sedimentary strata and pink-purple shades are ignimbrites. Water table depth shown by blue triangle. Well location shown in Figures 6 and 11.

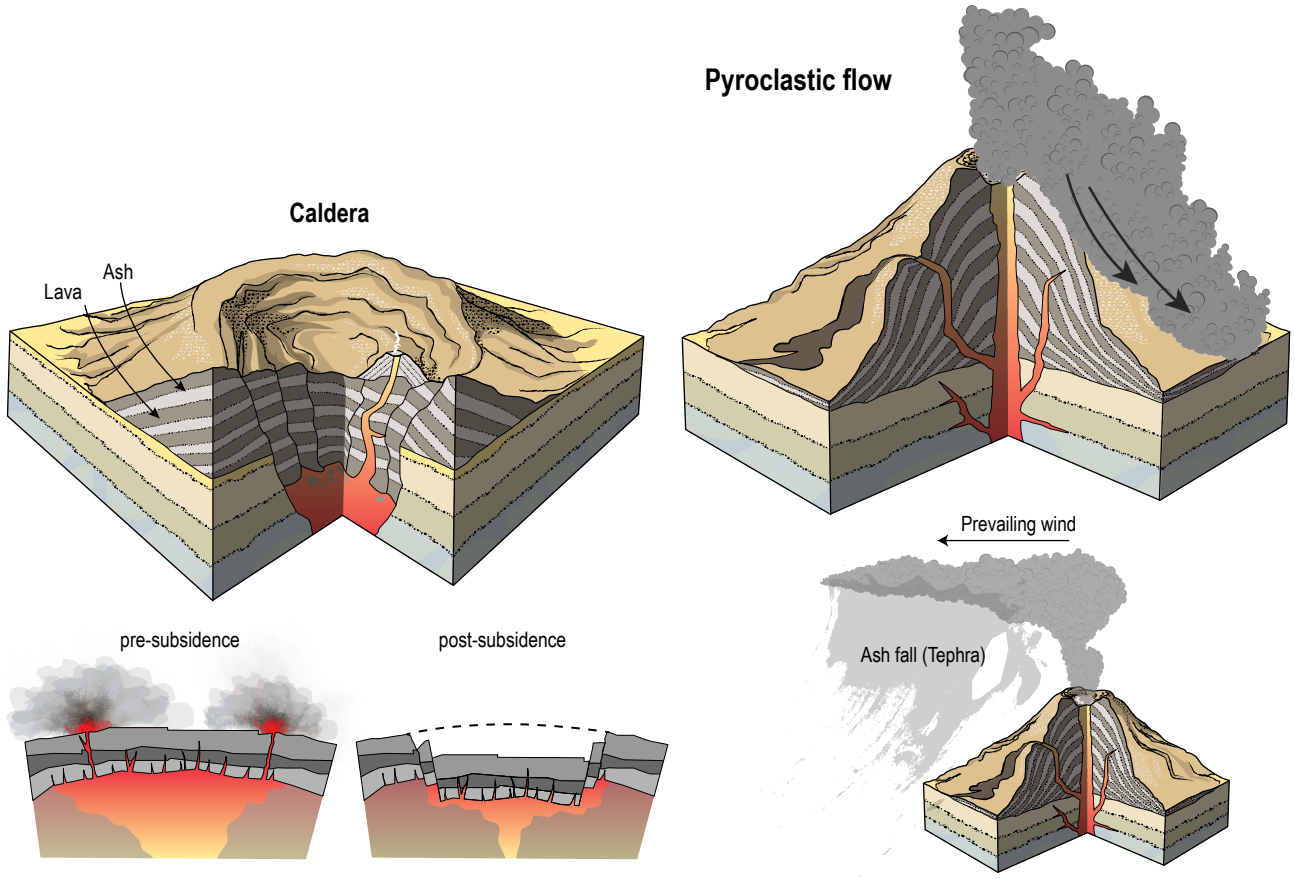

Figure 13. Illustration of volcanic calderas (top left) and how they are formed (bottom left). Eruption of ash and pyroclastic debris continues during subsidence. Expulsion of ash is commonly so voluminous that ignimbrites (ash flow tuffs) occur. On right is an example of a stratovolcano and a pyroclastic flow from that volcano. Ash and pyroclastic debris can flow downslope as density currents (forming ignimbrites or ash flow tuffs) or "rain out" as ash fall.

disconformably overlies Cretaceous strata (mostly Crevasse Canyon Formation), and is conformably overlain by the Spears Group, with the upper contact gradational over 5–10 m. The sedimentology and stratigraphy of Baca Formation was studied by Wipolt et al. (1946), Potter (1970), Snyder (1971), Johnson (1978), Schrodt (1980), and Cather (1980, 1982, 1983) — with an excellent summary given by Cather and Johnson (1984, 1986). More discussion of the age, sediment character, and paleoenvironments of the Baca Formation is given in Appendix 2.

Late Eocene and Early–Late Oligocene Volcanic and Volcaniclastic Strata

Intense volcanic activity between 38 and 24 million years ago formed a stack of volcanic rocks 3,300–4,900 ft thick. These rocks extend across the study area (Figs. 5, 6), and their stratigraphic relations are illustrated in Figures 18–20. The volcanic rock includes thick layers and tongues of volcaniclastic sediment (i.e., sediment derived from erosion of volcanic highlands) that is designated as the Spears Group (Cather et al., 1994), consolidated ash (tuffs and ignimbrites), and lava flows. The landscape at this time was characterized by volcanic highlands, which included stratovolcanoes (like modern-day Mt. Vesuvius or Mt. Fuji) and volcanic calderas (both illustrated in Fig. 13), surrounded by basin(s) in which volcaniclastic sediment accumulated. Caldera subsidence is accompanied by explosive volcanic eruptions producing ignimbrites, ash and other pyroclastic debris (Fig. 13).

Ignimbrites are prevalent in both the Datil and Mogollon Groups (Figs. 18, 19; Plate 1). Ignimbrites are a hot suspension of ash, pumice, and gas ejected into the atmosphere by immense volcanic eruptions, such as those forming calderas (Fig. 13). This hot mixture flows rapidly away and downward as a

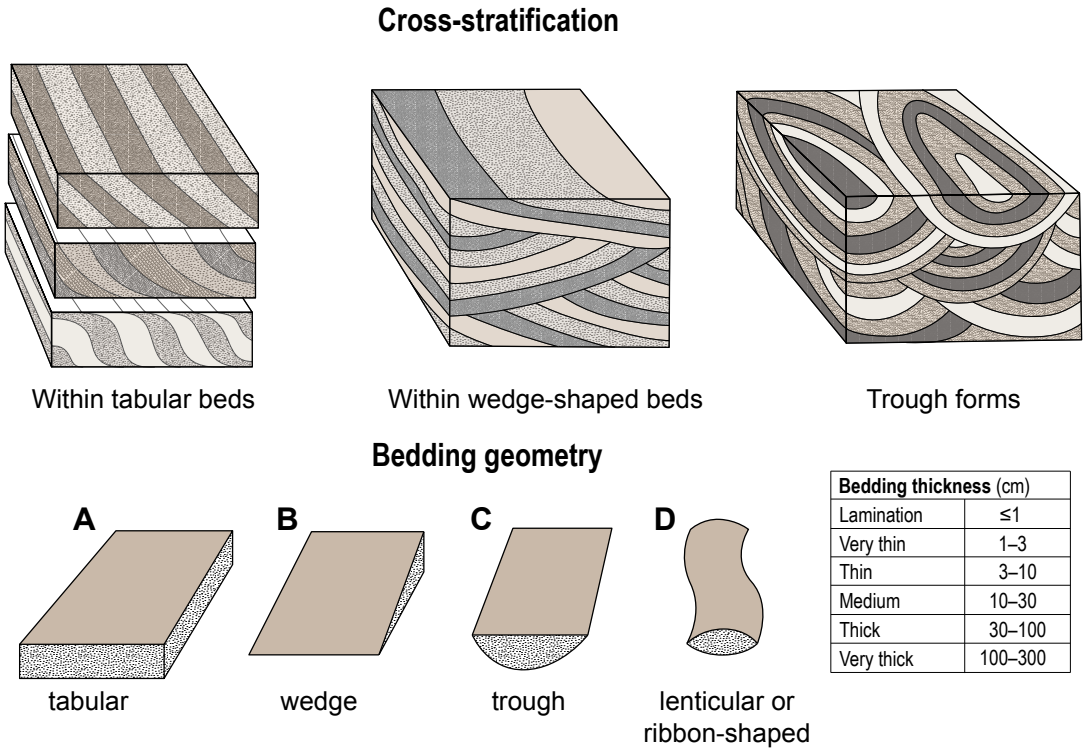

Figure 14. Illustration of various types of bedding. The top row depicts cross-stratification (cross bedding). The bottom row illustrates other types of bedding geometry (shapes). Thickness terms are listed on the lower right; thickness terminology follows Ingram (1954).

density current because it is denser than the surrounding atmosphere (Fig. 13). Ignimbrites can blanket the landscape up to 100 miles from the volcano. If sufficiently hot, the deposited material can fuse together, forming a welded tuff. Because they can travel long distances, ignimbrites make useful, laterally extensive, stratigraphic markers in the volcanic bedrock that are commonly 10–300 ft thick. Important ignimbrites in the study area are listed and described in Table 1.

Cather et al. (1994) proposed a regional stratigraphic framework in which an extensive volcaniclastic sedimentary sequence, the Spears Group, interfingers laterally with two thick intervals dominated by ignimbrites and volcanic flows, called the Datil and Mogollon Groups. Although lava and volcaniclastic sediment layers are typically discontinuous (an exception being the lower Spears Group), there are relatively distinctive ash-flow tuffs (ignimbrites) that extend across the study area. Correlation of these units have been aided by $^{40}Ar/^{39}Ar$ geochronology and paleomagnetic reversal stratigraphy (McIntosh et al., 1990, 1991, 1992, 1994). The Datil and Mogollon groups are separated by an extensive disconformity at the top of the Hells Mesa Tuff, encompassing a pause in, or erosion of, 32.5–29.5 Ma geologic strata. The Datil Group lies below this disconformity and the Mogollon Group lies above it. Below, we discuss these three stratigraphic groups in more detail. Photos of these volcanic rocks are shown in Figures 21 and 22. In the following, we use four common descriptive terms for volcanic rocks: porphyritic and phenocrysts (relating to rock texture) and felsic, intermediate, and mafic (relating to composition). Porphyritic means that conspicuously large crystal sizes are present in a matrix of finer minerals. These large crystals are called phenocrysts. Felsic rocks are usually light-colored and relatively rich in sodic or potassium feldspar and/or quartz; also, the silica content is relatively high, typically ≥ 63%. Mafic rocks are typically dark-colored and rich in minerals containing magnesium and iron; silica content is typically ≤ 52%. Intermediate rocks are in-between felsic and mafic in terms of color and silica content.

Spears Group

The Spears Group, as defined by Cather et al. (1994), includes all thick intervals of volcaniclastic sediment that interfinger with both the Datil and Mogollon groups. Note that before Cather et al. (1994), the

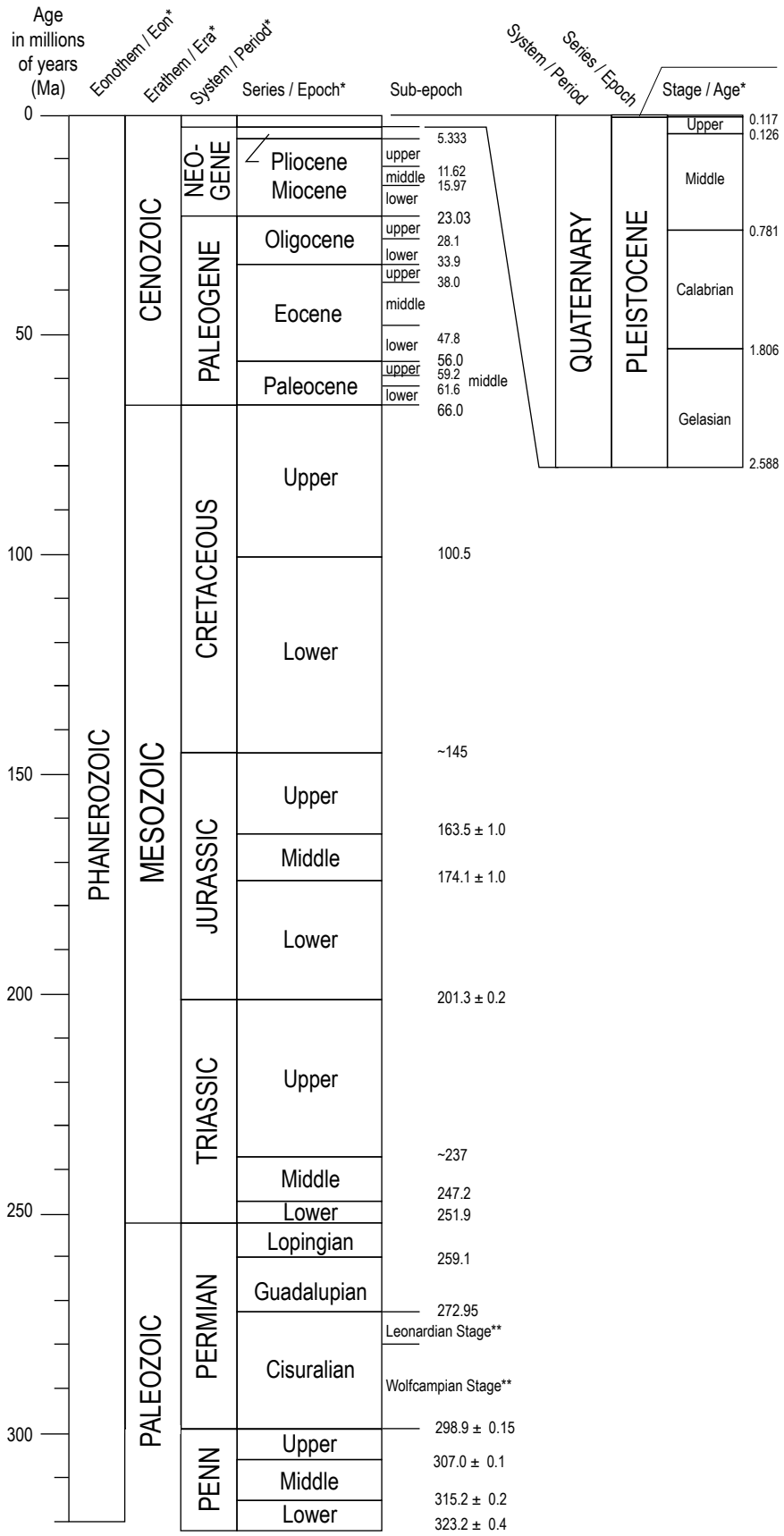

NOTES:

* The two-fold division of time has its basis in chronostratigraphy versus geochronology. For example, "system" is a chronostratigraphic term and refers to segments of rock; "period" is a geochronologic term and refers to a time span. The small-font numbers on the right side of the chart are the ages of the boundaries between epochs, sub-epochs, or ages. Note that sub-epochs and ages are only shown for the Cenozoic Era. As noted in Cohen et al. (2013), the numerical ages are subject to revision; this reference and Gradstein et al. (2012) provide more information about how these units are defined.

** North American stages

Figure 15. Illustration of the geologic time scale (Cohen et al., 2013).

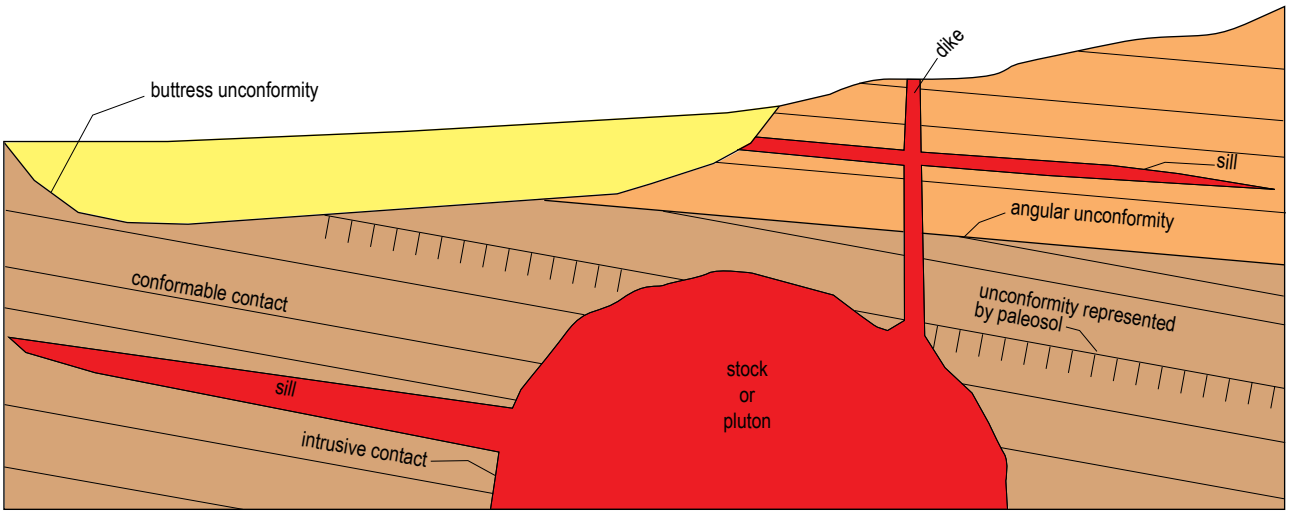

1. The layered rocks are called strata. The lower layers are the oldest and progressively higher layers are progressively younger.
2. Stocks, plutons, sills, or dikes are examples of intrusive rocks. These are younger than rocks they cut across.
3. Boundaries between rock units are called contacts. A conformable contact means that little to very little time is represented by the contact. An unconfomable contact means that the contact contains a significant time gap in the geologic record. Common unconformable contacts on this figure involve intrusions, paleosols, as well as buttress or angular relations.

Figure 16. Schematic figure illustrating stratigraphic terms and concepts.

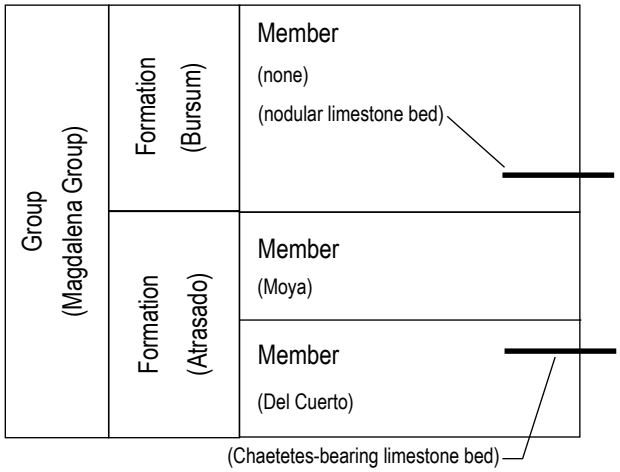

Figure 17. Hierarchal system of categorizing units of rocks and variously consolidated sediment, with an example from the Magdalena Group in parentheses Except for the term "Magdalena Group," this follows stratigraphic nomenclature proposed for the Mud Springs Mountains by Lucas et al. (2012).

Spears Group was considered as a formation-rank unit. This sediment consists of conglomerate, sandstone, and minor mudstone (Cather and Chapin, 1989). This unit ranges in color from gray, buff purple, to reddish-gray (Cather et al., 1987). The Spears Group excludes caldera-fill deposits, which are particularly abundant on the northern and eastern sides of the upper Alamosa basin. Three lithologic units are mapped in the Spears Group in the Datil and Gallinas Mountains (listed from lower to higher stratigraphic level): Dog Springs, Chavez Canyon, and Rincon Windmill members (Fig. 18; Harrison, 1980; Coffin, 1981; Brouillard, 1984; Osburn and Chapin, 1983) that were later raised to formation status by Cather et al. (1994). Away from the Datil Mountains, the Spears Group can be subdivided as follows (Fig. 20): lower Spears Group (equivalent to the Dog Springs Formation); middle Spears Group (volcaniclastic strata interbedded with ignimbrites older than the Hells Mesa Tuff, equivalent to the Chavez Canyon and Rincon Windmill Formations); and upper Spears Group (volcaniclastic sedimentary strata between the Hells Mesa Tuff and the Santa Fe Group).

The Dog Springs Formation (Fig. 21a) is dominated by tuffaceous debris flows and mud flows, where the matrix includes mineral grains of plagioclase, sanidine, hornblende, biotite, and pyroxene (Harrison, 1980; Osburn and Chapin, 1983). These minerals are also present as phenocrysts in most of the volcanic gravel (Osburn and Chapin, 1983). In addition, there are minor ash-flow tuffs (Harrison, 1980). Bedding is massive, tabular, or highly contorted and chaotic (Fig. 21a; Harrison, 1980; Osburn and Chapin, 1983). Chaotic bedding and large-scale folding are interpreted to be due to penecontemporaneous soft sediment-deformation folding (Osburn and Chapin, 1983; Cather and Chapin, 1989). Large blocks of Paleozoic limestone were transported via

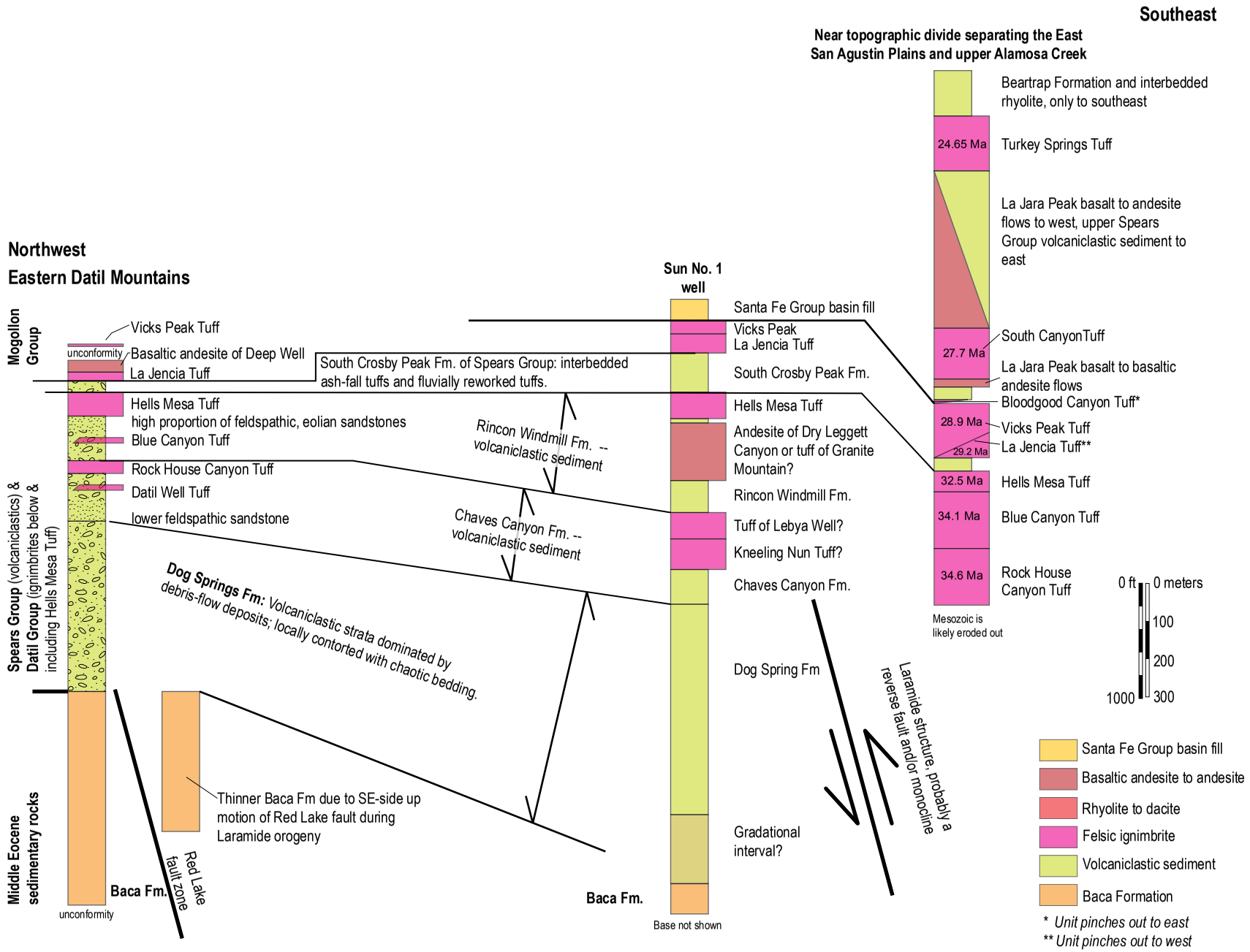

Figure 18. Stratigraphic correlation diagram illustrating stratigraphic units in volcanic bedrock, oriented northwest to southeast. Stratigraphic columns were assembled for three locations: eastern Datil Mountains (Harrison, 1980; Osburn and Chapin, 1983); Sun No. 1 well (unpublished lithologic and geophysical logs from the Petroleum Records office at the New Mexico Bureau of Geology and Mineral Resources), and the topographic divide between the C-N embayment of the East San Agustin basin and the upper Alamosa basin (cross section D-D' and Osburn and Ferguson, 2010). Thicknesses of volcanic units are highly variable, depending on location. Additional references for the three stratigraphic columns are as follows. Left column: Chamberlin (1981); Cather and Johnson (1986); Harrison (1980); Osburn and Chapin (1983); Chamberlin et al. (1994b). Middle column: Chamberlin et al. (1994a, table 1.2). Right column: Osburn and Ferguson (2007, 2010); Ferguson and Osburn (2011, 2012).

Figure 19 A. Cross-sections A-A' and B-B' across the East San Agustin basin. Cross-sections are vertically exaggerated by a factor of 4. See Figures 6 and 11 for cross-section location. Longer, non-exaggerated versions of these cross-sections are shown in Plate 1. Cross-sections C-C' and E-E' are only presented on Plate 1.

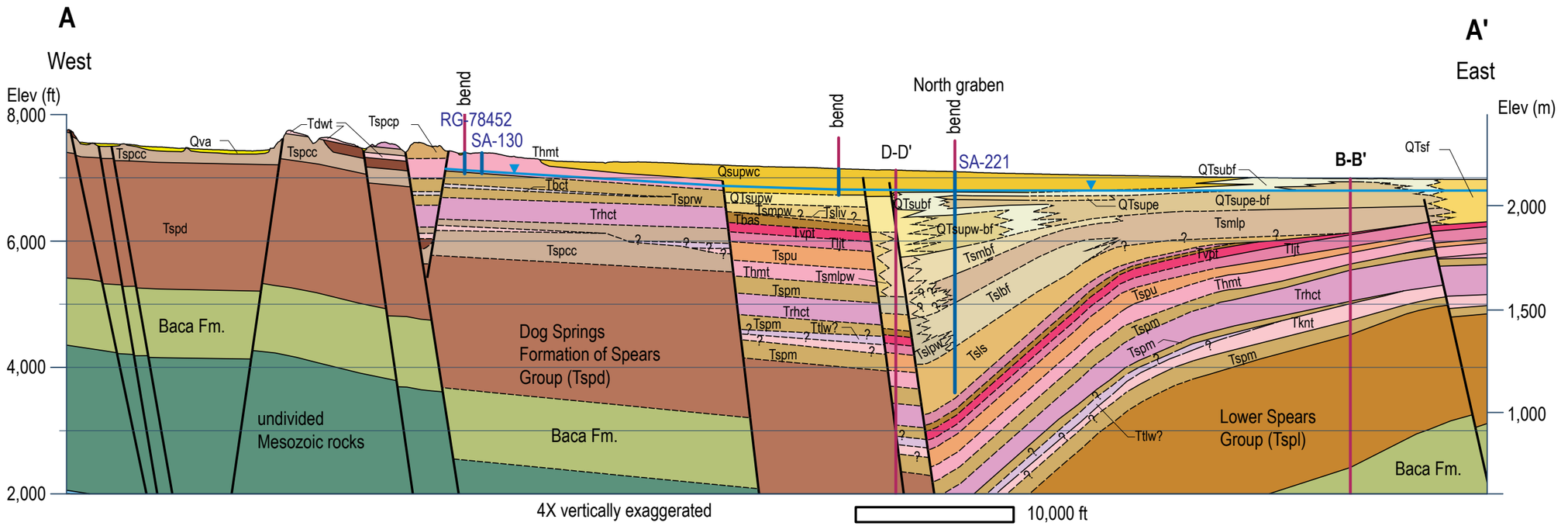

Note: although the depicted succession of bedrock units is reasonable, their thicknesses and depths are poorly constrained away from bedrock-penetrating wells; there may also be additional volcanic units and faults in the subsurface that are not exposed on the surface. Fault dips may shallow with depth.

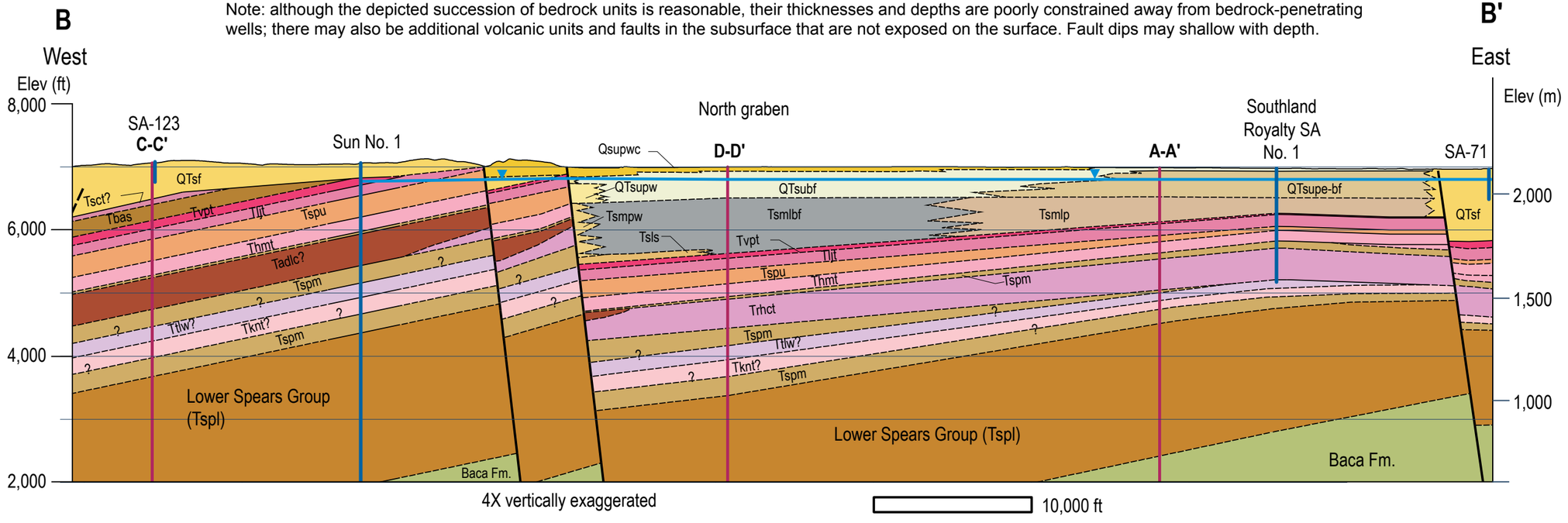

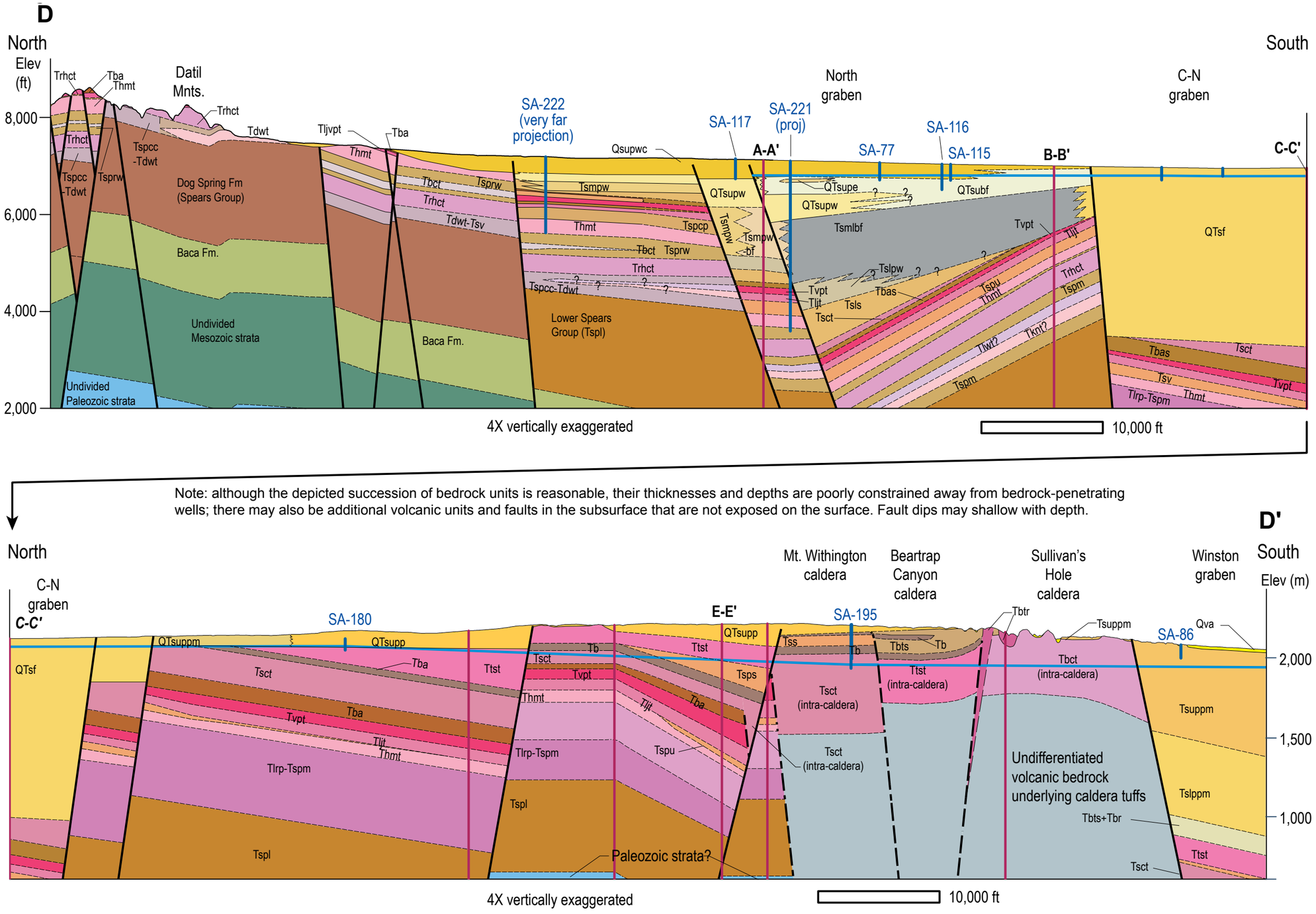

Note: although the depicted succession of bedrock units is reasonable, their thicknesses and depths are poorly constrained away from bedrock-penetrating wells; there may also be additional volcanic units and faults in the subsurface that are not exposed on the surface. Fault dips may shallow with depth.

Figure 19 B. Cross-section D-D' that trends SSE from the Datil Mountains to the Upper Alamosa basin. Shown as two segments, with the top being the northern half. Cross-section vertically exaggerated by a factor of 4. See Figures 5, 6 and 10, 11 for cross-section location. Non-exaggerated version shown in Plate 1.

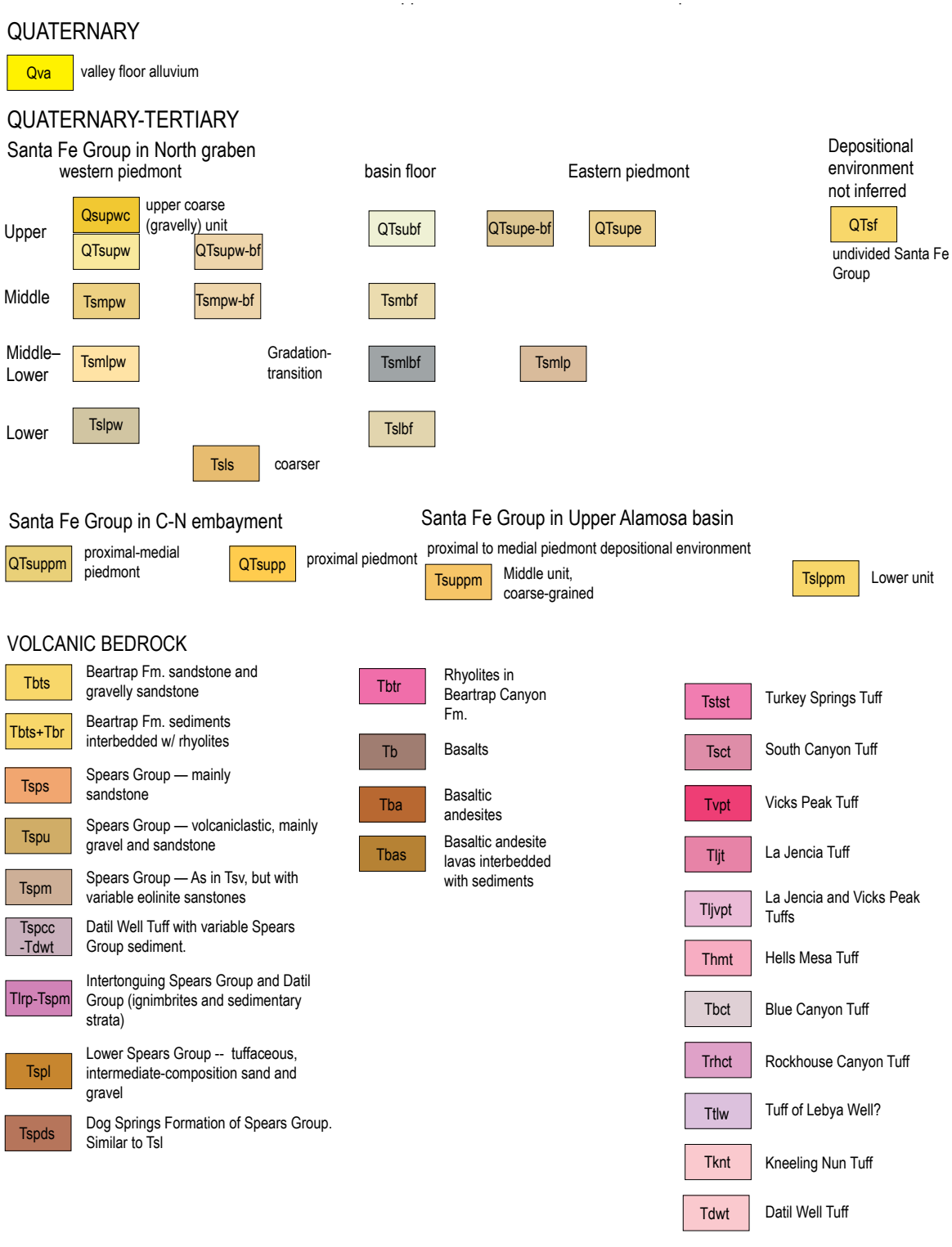

Figure 19 C. Geologic unit colors and symbols for cross sections.

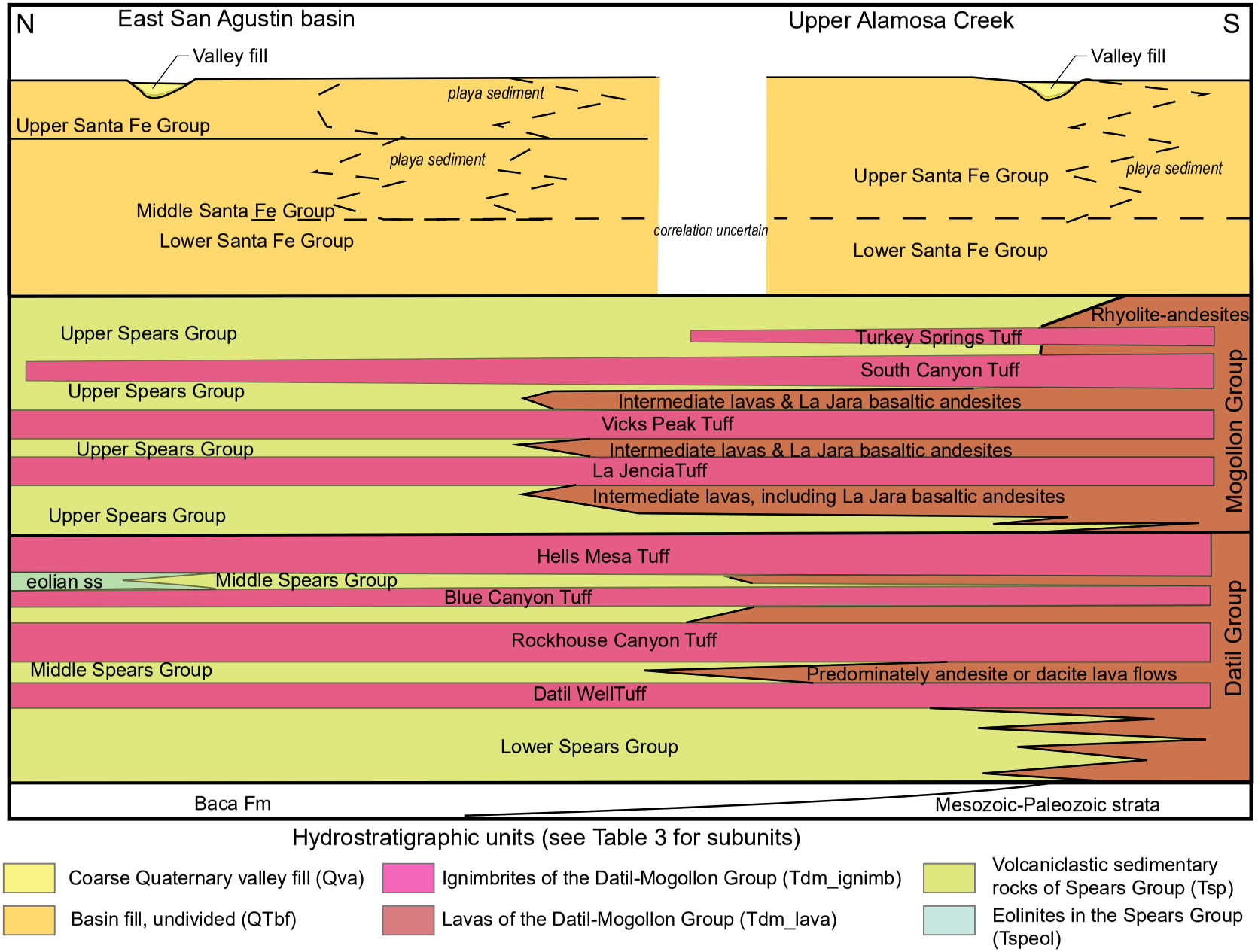

Figure 20. Schematic diagram illustrating the stratigraphic relations of the major geologic units in the study area. Shading of these units is according to hydrostratigraphic unit (see Table 4); note that hydrostratigraphic subunits are not shown.

debris flows (Harrison, 1980; Broulliard, 1984; Cather and Chapin, 1989).

The Chavez Canyon and stratigraphically higher Rincon Windmill Formations are separated by the Rockhouse Canyon Tuff (Figs. 18, 19, 22). To the west, feldspathic sandstones, many of eolian (wind-blown) origin, occupy the lower 175–200 ft of the Chavez Canyon Formation and the upper third of the Rincon Windmill Formation (Fig. 18). The remainder of these two units consist of volcaniclastic conglomerates and sandstone (Fig. 21).

An upward gradation is present in the composition of the Spears Group. The lower two-thirds contains non-volcanic detritus, virtually identical to sand and gravel compositions of the Baca Formation, mixed with volcaniclastic sand and gravel dominated by andesites with plagioclase and amphibole phenocrysts (Cather et al., 1987). The upper third of the Spears Group lacks non-volcaniclastic detritus and the volcanic gravel is characterized by phenocrysts of plagioclase and clinopyroxene (Cather et al., 1987).

The Spears Group is remarkably well-cemented and underlies the mountains surrounding the western and northern Plains of San Agustin. Cementing agents include zeolites, clay, silica (quartz and opal-CT), and calcite (Harrison, 1980; Cather and Chapin, 1989; Chamberlin et al., 1994b). Propylitic alteration (characterized by the mineral assemblage of epidote-chlorite-sericite-calcite) is locally found near igneous intrusions (Cather and Chapin, 1989). The Spears Group accumulated in the same basin as the earlier Baca Formation. Volcaniclastic deposition occurred on coalesced, laterally extensive, low-gradient alluvial fans; lacustrine deposition in the northeastern part of the Baca basin, outside of the study area, continued into early Spears time (Cather and Chapin, 1989).

Datil Group

The Datil Group is comprised of lavas and ignimbrites that interfinger laterally with thick volcaniclastic sediments of the Spears Group (Cather et al., 1994) (Figs. 18, 19, 20, 22; Table 1). Across the northern and middle parts of the study area, the Datil Group consists mainly of rhyolitic ignimbrites that have a relatively low silica content. Subordinate andesitic lava flows are present in the highlands flanking the east margin of the East San Agustin basin (Chamberlin, 1974; Wilkinson, 1976). Four ignimbrites are distinctive and mappable: the Datil Well Tuff, Rockhouse Canyon Tuff, Blue Canyon Tuff, and the Hells Mesa Tuff (Table 1; Figs. 18–20, 22). Of these, the Rockhouse Canyon Tuff and Hells Mesa Tuff are particularly thick and extensive. The Rockhouse Canyon Tuff is a white to light gray, dense, crystal-poor (<10% visible crystals composed primarily of sanidine), welded tuff (Table 1; Fig. 22b). The densely welded Hells Mesa Tuff represents a simple cooling unit; it is readily distinguishable based on its porphyritic texture, abundance of conspicuous crystals (phenocrysts), and the abundance of quartz (except near its base) (Fig. 22a, 22c; Table 1).

Mogollon Group

The Mogollon Group includes mafic to intermediate lavas and ash-flow tuffs associated with the latter phase of ignimbrite volcanism in the Mogollon-Datil field (Cather et al., 1994; McIntosh et al., 1992). Most of the ignimbrites have high silica contents. Four major regional ignimbrites were erupted and preserved between 29.3 and 24.6 Ma (Table 1): La Jencia, Vicks Peak, South Canyon, and Turkey Springs tuffs (Figs. 18–21). Mafic to intermediate lavas are present in the Mogollon Group and include the La Jara Peak basaltic andesites.

Three calderas have been recognized in the upper Alamosa basin, three of which extend into the low topographic divide separating Alamosa Creek from the C-N embayment (Ferguson et al., 2012; Table 1; Figs. 5, 11; Plate 1). These calderas are important to consider for hydrogeologic investigations because their boundaries may correspond with ring fractures or ring faults, and subsidence-related fracturing may initially have increased permeability. However, the initial high permeability may have facilitated circulation of hydrothermal fluids that, over time, may precipitate silica or other cements—eventually "plugging up" the fractures. The older and western of these calderas is called Sullivan's Hole caldera; it might be the source of the Blue Canyon Tuff (34.1 Ma; Ferguson et al., 2012).

The large Mountain Withington caldera dominates the geology of the northern San Mateo Mountains (Deal, 1973; Deal and Rhodes, 1976; Ferguson, 1991, Ferguson and Osburn, 1994). This 27.7 Ma caldera is filled by at least 1 km of South Canyon Tuff (an estimated volume of ~700 km^3). The phenocryst content of this tuff increases gradually upwards from <5% to ~15% (Ferguson et al., 2012). Along the southern caldera margin, overlying the South Canyon Tuff, is 200 m of caldera moat-fill composed of conglomerate and sandstone, much of which is eolian (Ferguson, 1986a,b).

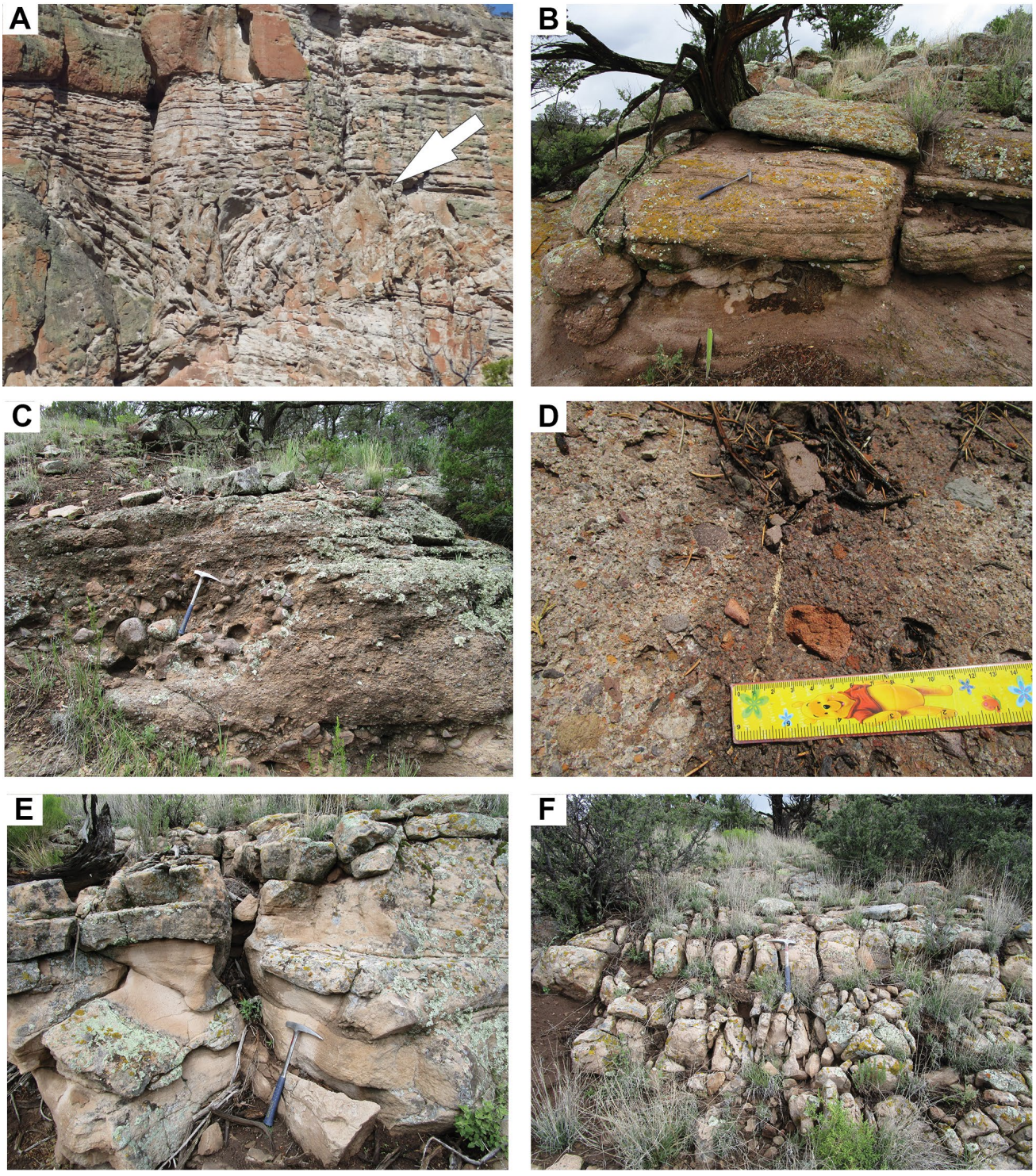

Figure 21. Photographs of various volcaniclastic sedimentary rocks near the eastern San Agustin Plains, all of which belong to the Spears Group. A) The Dog Springs Formation showing folded strata probably related to soft-sediment deformation due to rapid debris flow emplacement. Above the white arrow, sedimentary beds are tabular and non-deformed. Except near fault zones, this formation generally lacks well-developed joint sets. ~10 m-tall vertical exposure. B) Cross-stratified, pebbly sandstone of the upper Rincon Windmill Formation; well-cemented by silica and possibly zeolites. Hammer for scale. C) Photograph of volcaniclastic conglomeratic sandstone of the Rincon Windmill; note the cobbly channel fill (near the hammer) corresponding to a debris-flow deposit. D) Volcanic gravel of the Chaves Canyon Formation and a fracture filled by silt (this infilling is likely a recent phenomena). E) Photographs of eolian facies in the upper Rincon Windmill Formation, taken in the northeastern Datil Mountains. Hammer for scale. F) Fractures developed in eolian sediment of the upper Rincon Windmill Formation; photograph taken in the same area as Photo E. Hammer for scale.

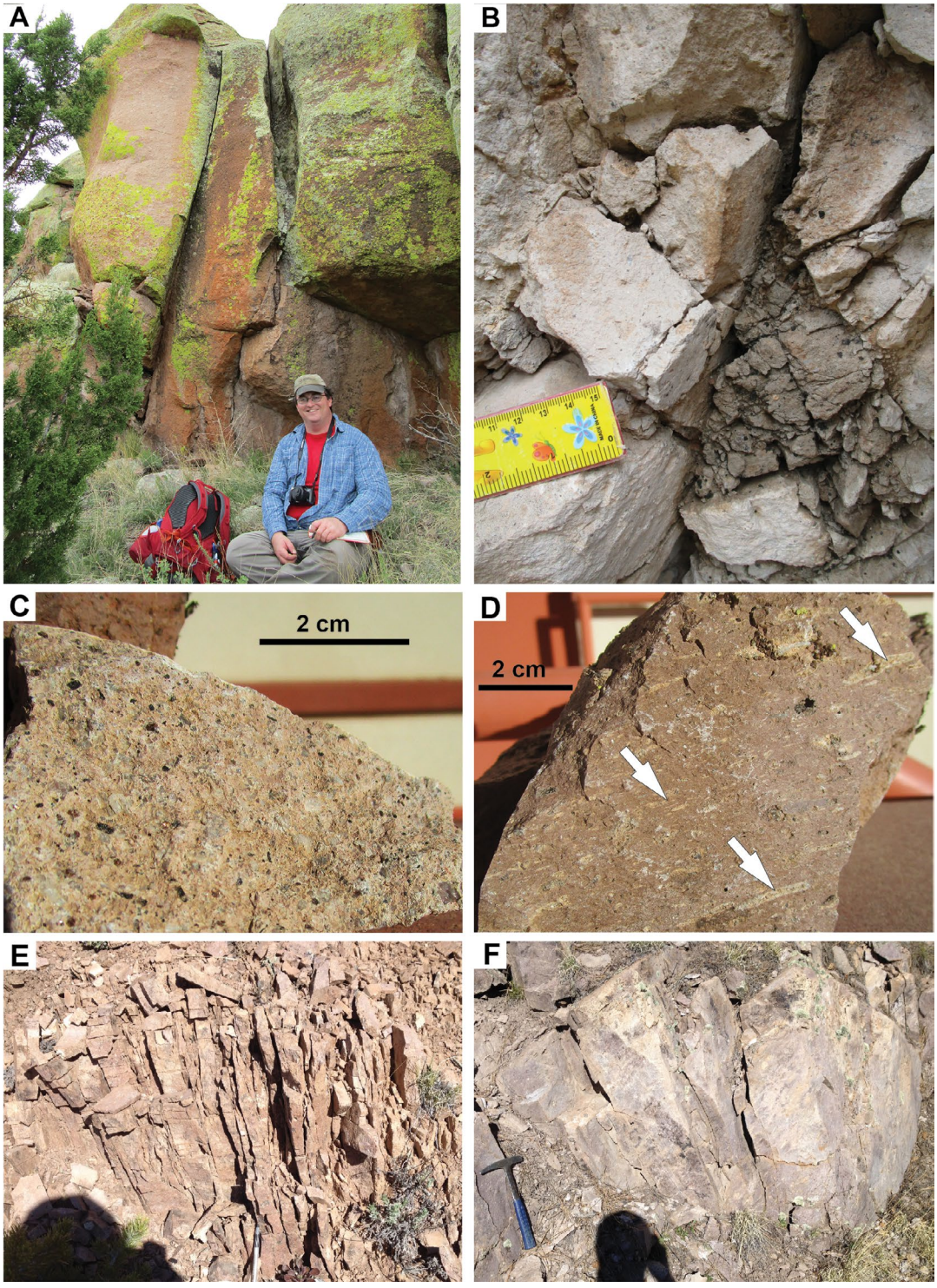

Figure 22. Photographs of ignimbrites of the Datil and Mogollon groups. A) Fractured Hells Mesa Tuff. Alex Rinehart for scale. B) Close-up of open fractures in the Rockhouse Canyon Tuff. Where observed in the northeastern Datil Mountains, this ignimbrite is generally extensively fractured. Top of ruler is in centimeters. C) Close-up of the Hells Mesa Tuff. This tuff is distinctive because of its abundance of macroscopic crystals (phenocrysts), which include quartz, sanidine, biotite, and hornblende. D) Close-up of the La Jencia Tuff, which is an example of a welded tuff; arrow points to pumices that have been compacted. Differences between degrees of welding and crystal composition allows one to recognize and map different ignimbrites in the field (cf. photos C and D). E and F). Photographs illustrating varying degrees of fracture development in the South Canyon Tuff, as observed along Forest Service Road 476 (Section 18, T5S R7W).

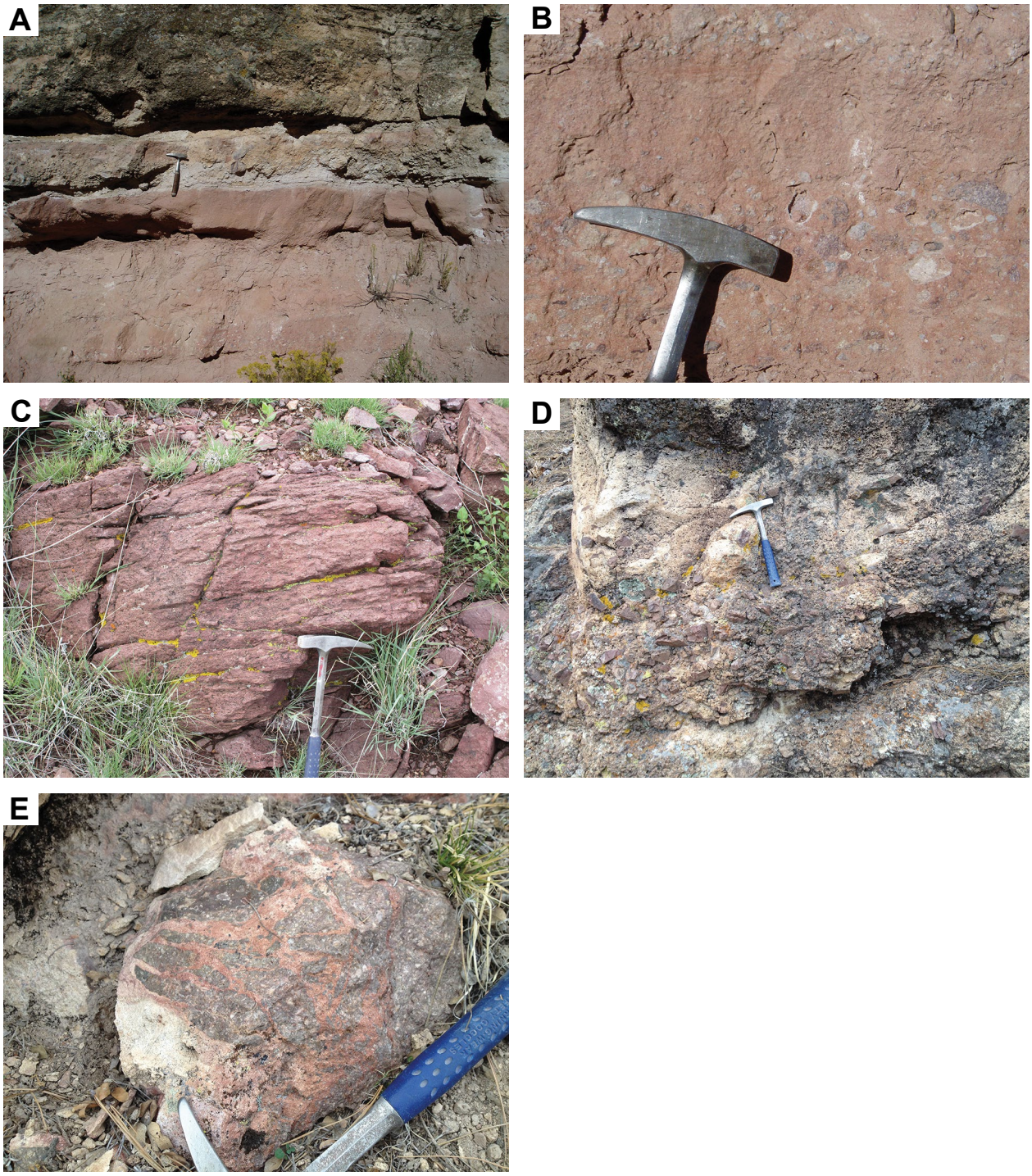

Figure 23. Features related to the Beartrap Canyon caldera and its margin, which has been dated at 24.33 Ma; thus, this is the youngest caldera to have formed in the study area (Ferguson et al., 2012). Photographs A through C show the Beartrap Canyon Formation, which fills the caldera. A) Medium to thick, tabular beds of sandstone and pebbly sandstone cemented by silica and clay. B) Close-up photograph of a debris-flow bed. Note the matrix-supported pebbles and massive texture. Both Photos A and B were taken near UTM coordinates (zone 13, NAD83): 258,780 m E, 3,742,262 m N. C) Well-cemented sandstone exhibiting very thin to thin, lenticular to tabular beds; cemented agent is largely silica. Photograph is from the topographic saddle between the upper Alamosa Creek drainage and the C-N topographic embayment. Photographs D through E were taken along a short transect across the caldera margin, which trends east-west at this locality on the north slope of Limestone Canyon (UTM coord: 261,088 m E, 3,748,982 m N; zone 13, NAD83). D) Angular, monolithic cobbles probably representing a locally derived debris flow from the caldera margin. This dipping deposit is just inside (south of) the caldera margin. E) Older clasts of volcanic rock (dacite?) intruded by a white-orange rhyolite; note the penetrative fabric of the younger rhyolite with the older volcanic rocks. The rhyolite intruded along the caldera margin.

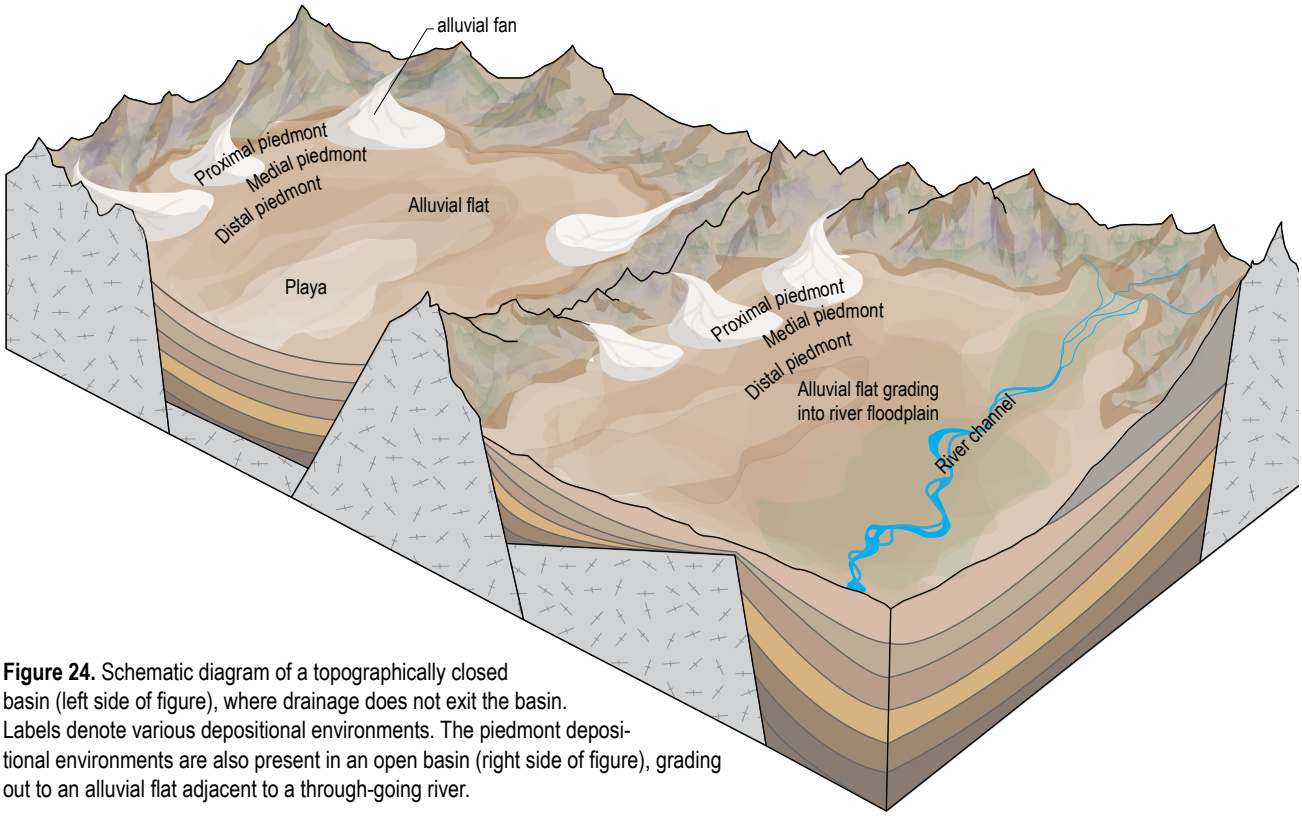

Figure 24. Schematic diagram of a topographically closed basin (left side of figure), where drainage does not exit the basin. Labels denote various depositional environments. The piedmont depositional environments are also present in an open basin (right side of figure), grading out to an alluvial flat adjacent to a through-going river.

The 24.65 Ma Beartrap Canyon caldera is superimposed over the western half of the Mount Withington caldera and the eastern half of the Sullivan's Hole caldera (Ferguson et al., 2012). The Beartrap Canyon caldera is filled by >2,300 ft of the Turkey Springs Tuff overlain by the Beartrap Canyon Formation, the latter being as much as 1,000 ft thick (Fig. 23; Ferguson et al., 2012). The rhyolitic Turkey Springs Tuff contains about 15% phenocrysts (increasing up-section from 3–5% at the base to about 15% near the top). The Beartrap Canyon Formation consists of volcaniclastic sediment interbedded with, and locally overlain by, rhyolite and dacite lava flows and domes (Osburn and Ferguson, 2010). The volcaniclastic sediment includes sandstone, conglomerate and subordinate mudstone and non- to poorly welded, buff- to tan-colored, felsic ash-flow and ash-fall tuff (Deal and Rhodes, 1976; Osburn and Ferguson, 2007, 2010; Ferguson and Osburn, 2007; Ferguson et al., 2012; Koning, 2012). The Beartrap Canyon Formation is generally in medium to thick tabular beds and is strongly cemented by silica and clay (Fig. 23a, 23b; Koning, 2012). Much of the formation appears to have been deposited by debris flows or hyperconcentrated flows (Koning, 2012).

Stratigraphy of Neogene Basin Fill

Basin-fill sediment that overlies cemented, volcanic bedrock is correlated to the Santa Fe Group or Gila Group. We elect to call the basin fill in the West and East San Agustin basins as Santa Fe Group, following the New Mexico State Geology map (NMBGMR, 2003 and Givens, 1957) and the concept that the San Agustin Plains are a structural arm of the Rio Grande rift (Chapin, 1971). Furthermore, Santa Fe Group has been used in the extensional basin corresponding to the Alamosa Creek drainage (Willard, 1957; Koning, 2012). This sediment locally may contain interbedded volcanic flows. Santa Fe Group basin fill is generally non- to moderately cemented, with cementation probably increasing by border faults and with depth (based on comparison with exposed Santa Fe Group basin fill of the Rio Grande rift). A gravelly equivalent of the Santa Fe Group, called the Gila Group, is restricted to the Gila watershed (per original definition by Gilbert, 1875), including the upper reaches of the Gila River drainages west of the Black Range (QTg in Fig. 5). Note that the Gila Group was used for the San Agustin Plains by Myers (1994). But we elect to extend the term “Santa Fe Group” to the San Agustin Plains to have a single, unified term in this

publication for these basin fill deposits. We do not advocate having the Santa Fe Group be used west or northwest of the West San Agustin basin.

Santa Fe Group deposition began 26–24 Ma in this area and, for the Plains of San Agustin, continues to the present-day. Streams in the upper Alamosa drainage basin (i.e., Alamosa Creek) connected (integrated) with the Rio Grande in the Pliocene or early Pleistocene. This stream connection allowed most sediment to be transported out of the upper Alamosa drainage basin, likely slowing down deposition rates. When the Rio Grande began incising around 0.8–0.9 million years ago (Mack et al., 1993, 1998, 2002), large tributaries like Alamosa Creek also probably incised, effectively ending Santa Fe Group deposition. In the upper Alamosa basin, Santa Fe Group deposition post-dates the caldera-filling Beartrap Canyon Formation. Therefore, the Santa Fe Group in the upper Alamosa basin is younger than 24 Ma (approximate age of Beartrap Canyon Formation, which overlies the 24.65 ± 0.06 Ma Turkey Springs Tuff), consistent with interbedded basalts in the lower part of basin fill that are 18.73 ± 0.13 Ma and 18.75 ± 0.16 Ma (Koning, 2012; McLemore et al., 2012). A maximum age of 26–24 Ma is permissible in the West and East San Agustin basins, given that the highest preserved tuff in the bedrock alongside the eastern flanks of the East San Agustin basin is the 27.73 ± 0.07 Ma South Canyon Tuff.

Santa Fe Group sediment accumulated in topographically closed drainage basins that locally coincided with tectonic basins. Depositional components of a closed basin are illustrated in Figure 24. A sediment subunit is designated a particular "facies" when a depositional environment (such as the depositional components in Fig. 24) can be deduced using various features or properties of the sediment. On the flanks of a stereotypical basin are surfaces that slope away from adjoining highlands towards the middle of the basin; these sloping surfaces are called piedmonts (Fig. 24). In the proximal (upper) part of the piedmont (nearest the sediment source), relatively coarse sediment is commonly deposited as alluvial fans. Here, gravel and sand generally dominate the sediment. In the middle (medial) part of a piedmont, the alluvial fans commonly have coalesced laterally downstream to form a relatively smooth surface. Here, finer sediment (commonly very fine- to medium-grained sand and clayey-silty very fine to medium sand) is found as tabular beds interspersed with beds of coarser sand and gravel. Further downstream, towards the center of the basin, the distal piedmont is characterized by a lower-gradient, relatively smooth slope. Fine-grained sediment (very fine- to medium-grained sand and clayey-silty very fine to medium sand) dominates on a distal piedmont, where it is deposited as broad sheets interspersed with minor coarser sediment (sand and minor gravel). On a piedmont, coarse sand and gravel are deposited in paleochannels (forming trough- or lenticular-ribbon bed geometries, see Fig. 14) or as lobes (small alluvial fans) at the mouths of discontinuous paleochannels (that in outcrop form broad lenticular bodies, with an upper surface that is usually convex-up, that interfinger laterally with adjoining sand). Being more abundant in the proximal piedmont, coarse sediment bodies are typically better connected there than elsewhere on the piedmont, increasing overall permeability and the likelihood of more productive aquifers.

Slopes are very low-gradient at the bottom of a closed basin, corresponding to an alluvial flat that adjoins playa lake(s) in the lowest surface-elevation part of the basin. (Fig. 24). On an alluvial flat, surface water flows slowly towards the playa, commonly as a broad, unconfined sheet or in channels. A playa is characterized by clayey-silty sediment in its center that grades outwards into very fine- to fine-grained sand and silty-clayey very fine- to fine-grained sand.

In the upper Alamosa basin and elsewhere in mountainous-hilly areas of the study area, canyons (such as White House Canyon near Datil, Fig. 1) that have incised during the past ~500,000 years were later backfilled by relatively coarse-grained sediment. This is similar to what is observed on the southeastern Colorado Plateau to the north (Love and Connell, 2005). This time period had particularly strong glacial-interglacial cycles that could have notably changed precipitation intensity (driving the incision) and vegetation density (providing resistance to incision; cf. Connell et al., 2005). In Alamosa Creek, incision may have also been facilitated by river base level drops downstream of the upper Alamosa basin, since the Rio Grande system was incising in southern New Mexico since 800–900 Ma (e.g., Mack et al., 1993, 1998, 2002; McCraw and Williams, 2012). In many areas of southern New Mexico, notable incision occurred at the height of the last glacial maximum, and backfilling occurred in the transition to warmer climates 15,000 to 5,000 years ago (e.g., Gile et al., 1981; Jochems and Koning, 2015). This backfill consists largely of sand and gravel, with subordinate silty or clayey sand.

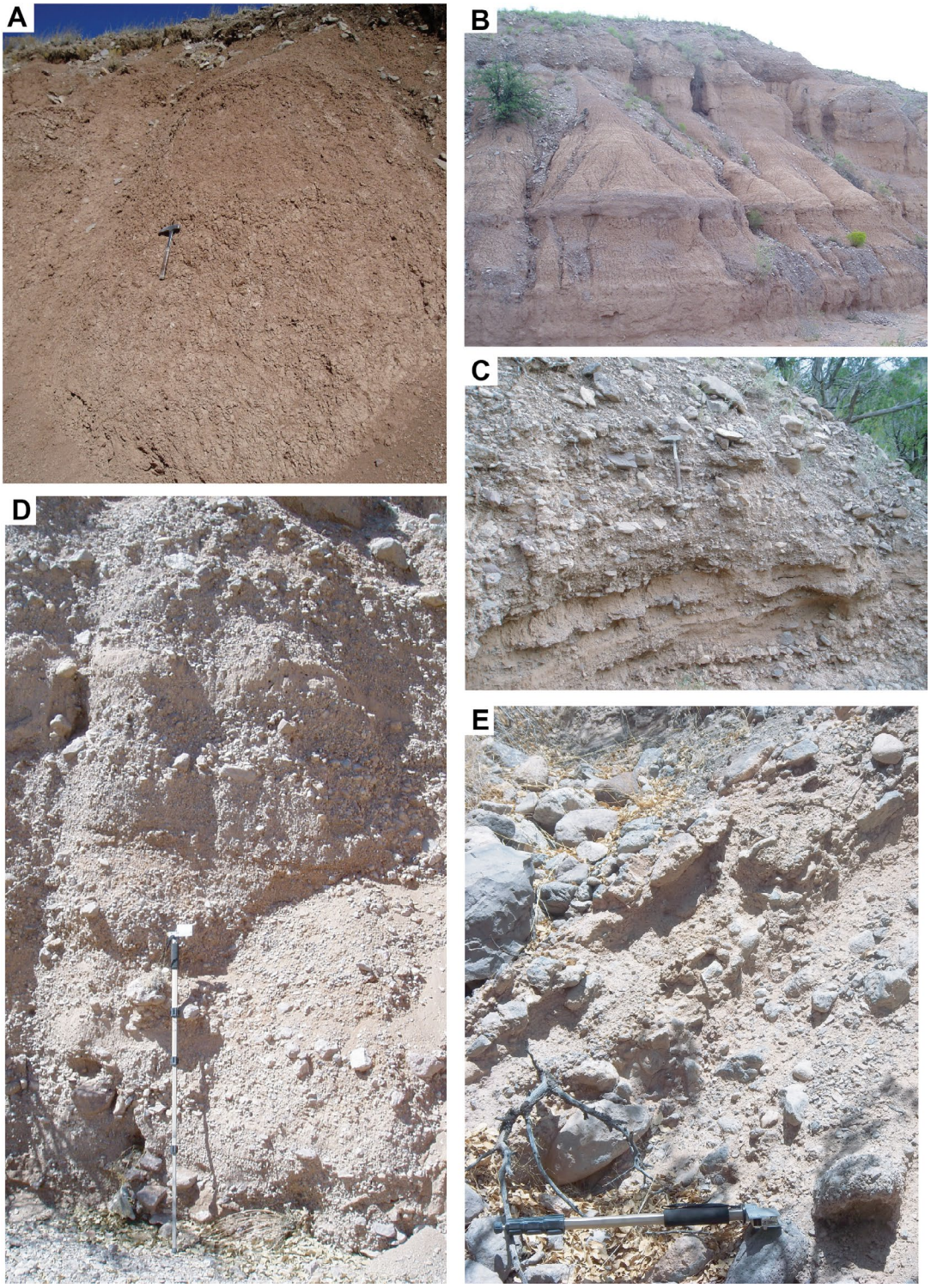

Figure 25. Photographs illustrating various facies of the upper Santa Fe Group exposed in the upper Alamosa basin (modified from Koning, 2012). A) Photograph of massive clay-silt interpreted as playa facies; hammer for scale (UTM coord: 253,180 m E; 3,721,332 m N; zone 13, NAD83 here and for subsequent site locations). B) Photograph illustrating distal piedmont facies, where gravelly sediment is subordinate to non-gravelly sediment (UTM coord: 253,080 m E; 3,726,037 m N (zone 13; NAD83). Here, the non-gravelly sediment is in thin to thick, tabular beds and composed of silt and very fine-grained sand. C) Western proximal-medial piedmont facies showing minor, finer-grained extra-channel sediment near the base of the exposure, hammer for scale (UTM coord: 251,265 m E, 3,722,792 m N, zone 13, NAD83). D) Eastern proximal-medial piedmont facies in West Red Canyon, 1.5 m-tall Jacob staff for scale (UTM coord: 257,500 m E, 3,726,666 m N). E) Steeply tilted strata near the southern boundary of the study area, correlated with the lower Santa Fe Group (proximal-medial piedmont facies). Here, bed attitudes average 350°\40°W; folded Jacob staff (60 cm long) for scale.

Upper Alamosa Basin

The upper Alamosa basin corresponds with the west-tilted, northern Winston graben of Koning (2012), who conducted a sedimentologic and paleocurrent study of its Miocene-Pliocene sediments. There are two informal stratigraphic units above the ~24 Ma Beartrap Canyon Formation: the lower and middle–upper Santa Fe Group. These units are generally tilted westward towards normal faults on the western side of the basin (Fig. 8). The lower Santa Fe Group unit is only exposed in the eastern part of the basin, near bedrock outcrops at the foot of the San Mateo Mountains, and is interpreted to be early to middle Miocene in age. Here, it is steeply tilted (>15° W; Fig. 25e), unconformably overlies the Beartrap Canyon Formation and fills local paleovalleys, exhibits westward paleoflow, and is interpreted to have been deposited on a west-sloping piedmont (Koning, 2012). Compared to the underlying Beartrap Canyon Formation, this stratgraphic unit contains more rounded gravel, a higher ratio of stream-flow versus debris-flow sediment, and has a lower degree of cementation. The lower Santa Fe Group unit consists of pebbly sand and sandy pebble-cobble conglomerate (pebbles>cobbles) (Fig. 25e). Gravel clasts in the conglomerate are poorly imbricated and composed of rhyolite, welded tuff, and minor non-welded tuff. Strata are moderately to well consolidated and weakly to strongly cemented by silica or clay (Koning, 2012). It is likely that the lower Santa Fe Group unit grades laterally westward into distal piedmont facies and then to playa facies, similar to the middle-upper Santa Fe Group unit in the upper Alamosa basin, but this is not exposed and facies relations remain somewhat uncertain.

The overlying middle-upper Santa Fe Group layer (unit) is characterized by gently dipping (<15°) or horizontal strata (Fig. 8) and non- to weak cementation. Three laterally adjacent facies are recognized (Fig. 25a-d; Plate 1): 1) proximal-medial piedmont (where gravel and coarse sand beds dominate or these coarse beds are proportionally subequal to fine- to medium-grained sand and muddy sand in a given 15 m thickness interval), 2) distal piedmont (where gravel and coarse sand are subordinate to finer sand and muddy fine sand), and 3) playa facies. The western piedmont is relatively narrow in extent compared to the eastern piedmont, a consequence of westward tilting of the Winston half-graben and corresponding westward shifting of depositional components towards the area of maximum subsidence (Fig. 8; e.g., Leeder and Gawthorpe, 1987; Gawthorpe and Leeder, 2000). Paleosols are observed in many exposures, particularly in the distal and medial piedmont facies. The middle-upper Santa Fe Group unit is interpreted to be middle(?) to late Miocene, and the upper part is possibly as young as the Pliocene (Koning, 2012). Its thickness is very poorly constrained, likely ranging between 1,000 and 2,000 ft.

The proximal-medial piedmont facies contain abundant gravelly beds with thicknesses and geometries that are typically very thin to medium and tabular, with lesser medium to thick, lenticular beds (Figs 14, 25c-d). Gravels are composed of clasts (fragments) of rhyolite, welded tuffs, and minor white, non-welded tuff; however, minor andesite clasts are seen along the western basin margin. The very fine-medium sand and clayey-silty very fine-medium sand beds in the proximal-medial facies occurs as medium to thick, tabular beds. Clay and silt content is estimated to range up to 25%. Scattered within the fine sand are minor grains of coarse to very coarse sand, as well as 1-15% very fine to very coarse pebbles. Strata are moderately to well consolidated and generally non- to weakly cemented by calcium carbonate. The proportion of fine sediment appears to increase up-section, as does the relative abundance of paleosols (Koning, 2012).

Very fine- to medium-grained sand and clayey-silty very fine- to medium-grained sand dominate in the distal piedmont facies, where the sediment is typically massive or in thick beds (Fig. 25b). Very thin to thick, lenticular to tabular bodies of pebbly sand or sandy pebbles-cobbles (paleo-channel fills or gully-mouth fan deposits) are interbedded within the finer sediment. Where present, cementation is weak and dominated by calcium carbonate, although locally cementation is moderate to strong (Koning, 2012).

At least 100 ft of playa sediment is exposed 3.7–5.0 miles northwest of the Monticello Box. It consists of brown to reddish brown clay interbedded with minor, very fine- to fine-grained sand and clayey sand beds (Fig. 25a). The sand beds are very thin to thick and tabular, but the clay is generally massive (Koning, 2012). Geologic mapping in gently tilted strata immediately east of the Monticello Box, inferred to be middle-late Miocene and probably correlative to the middle–upper Santa Fe Group unit in the upper Alamosa basin, did not find evidence for a river flowing out of the upper Alamosa basin. Therefore, the upper Alamosa Basin was a closed basin for at least part of (possibly all of) Miocene time. The depth (thickness) of the playa sediment would depend on how long the basin was closed.

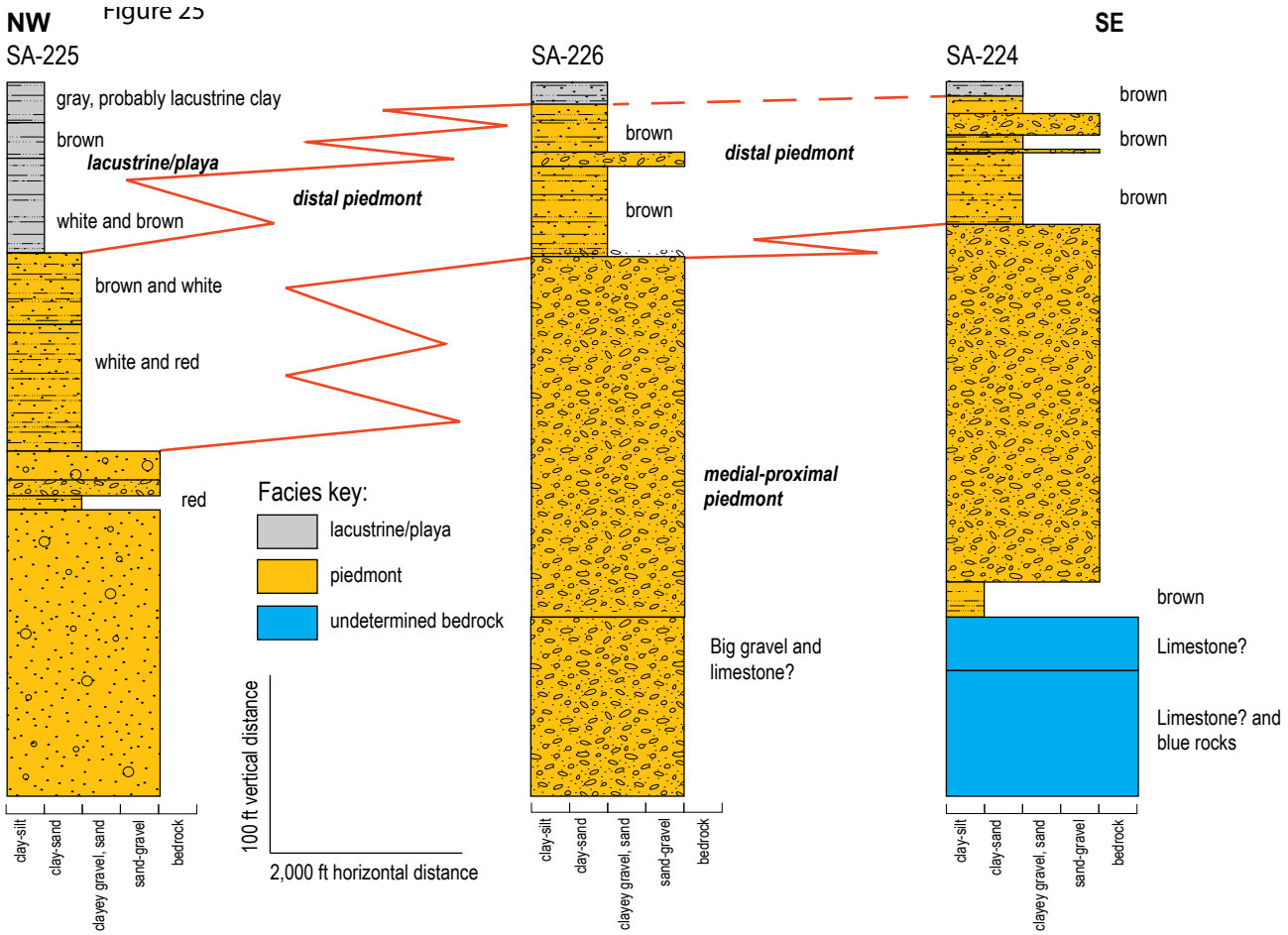

Figure 26. Well log correlation diagram using NM State Engineer well records (i.e., cuttings logs) for 3 water wells at C-N playa. See Figures 6 and 11 for the locations of these wells.

East San Agustin Basin

Unlike the upper Alamosa basin, the East San Agustin basin has remained topographically closed to the present-day and basin fill has not been notably incised. Based on available well data, the sedimentary architecture is probably relatively similar to that found in the upper Alamosa basin, where coarse channel fills or gully-mouth fan deposits (containing coarse sand or gravel) are interbedded with very fine- to medium-grained sand and silty-clayey sand. In the North graben, examination of available well data indicate a lateral fining trend of the sediment from the mountainous source areas to the deepest part of the graben, and this presumably is the case for the C-N graben as well. Three ~300 ft deep wells on the south side of C-N playa allow stratigraphic interpretations for the shallow subsurface in that part of the C-N embayment (Figs. 6, 26). North of the C-N embayment, interpretation of three deep wells (SA-221, SA-222, Southland Royalty No. 1) with relatively good subsurface data give a preliminary characterization of the Santa Fe Group there (Figs. 11, 27, 28). Below, we separately describe playa deposits and basin fill in the North graben (including near the VLA). The lack of subsurface data precludes description of basin fill in the White Lake graben and most of the C-N graben.

Playa Deposits

Thick (>50 ft) lacustrine or playa deposits are known to be present in shallow strata under and near the modern playa in the C-N graben—where they are composed of clay, silt, and fine sand—but have not

been confirmed for depths greater than 100 ft in that graben nor in the North and White Lake grabens. The apparent paucity of convincing playa/lacustrine facies in well SA-221 (Fig. 28), which was drilled in the structurally deeper part of the southern North graben (Fig. 11), suggests that ancient playas were not present in this graben or were of limited spatial extent and thickness (i.e., small and north or south of SA-221). If playa sediment is indeed absent in the North graben, then paleodrainage during most of Santa Fe Group deposition (Miocene through Quaternary) may have flowed southward from the North graben into the C-N graben. During the Quaternary, large lakes episodically occupied the West San Agustin basin, leaving lacustrine deposits up to ~1,000 ft thick (Foreman et al., 1959; Markgraf et al., 1983, 1984) and shorelines (Weber, 1994). Based on consultation with geologists who have reviewed the work of Weber (1994), including John Hawley and Bruce Allen (emeritus and current employee, respectively, of the N.M. Bureau of Geology and Mineral Resources), there is large uncertainty regarding the existence of the highest two of Weber's shorelines (elevations of 7,005 and 7,050 ft). The next lowest shoreline (6,940 ft) is relatively certain and indicates that the largest late Pleistocene lake(s) spilled into the lower part of the C-N embayment (near the modern-day playa) from the West San Agustin basin.

Deposits associated with the playa in the C-N embayment continue down to at least 100 ft depth within a mile of the modern C-N playa. Figure 26 is a northwest-southeast trending well-log correlation diagram that illustrates the interfingering nature of playa, distal piedmont, and medial-coarse piedmont lithofacies under and near the C-N playa. The three wells in the stratigraphic correlation diagram are on the southwest part of the playa, where they form a northwest-southeast line about 3.2 miles long (Fig. 6). Thick playa or lacustrine sediment may be limited to the gray and brown, upper clay of SA-225, although a thin layer of playa sediment very likely extends across all three wells (since all three wells lie in the current playa) but was not captured in the driller logs. Note that thick lake-playa facies do not extend from SA-225 to SA-226, but the underlying finer-grained, inferred distal piedmont facies does extend southwards, where it is 80–100 ft thick and overlies coarser sediment interpreted as medial-proximal piedmont facies. These stratigraphic relations indicate that the C-N playa has expanded or laterally shifted southward with time during the late Quaternary, causing the distal piedmont facies to correspondingly shift southward (Fig. 26).

Basin Fill in the North Graben

Background

Analysis of cuttings and geophysical logs from three deep wells allows partial characterization of the Santa Fe Group in the North graben, under the general area of the proposed Augustin Plains Ranch well field and near the VLA headquarters.

The Southland Royalty SA No. 1 well is located 1.3 miles north of the VLA headquarters (Figs. 6, 11). This well lies west of the White Lake graben and in the shallow, southeastern edge of the North graben. Relative to faults, this well is located 1.2–2.4 miles west of the east-down faults bounding the western White Lake graben and just north of the northeast-trending fault that bounds the north side of the C-N graben (Figs. 11, 19). The Southland Royalty SA No. 1 well penetrated 725 ft of relatively non-cemented Santa Fe Group strata before encountering the following interpreted bedrock units (descending order): relatively phenocryst-poor tuffs correlated to the Vicks Peak and La Jencia Tuffs; upper Spears Group strata; crystal-rich tuff with notable quartz grains, correlated to the Hells Mesa Tuff; middle Spears Group strata; and a phenocryst-poor volcanic rock that is likely the Rockhouse Canyon Tuff (Fig. 12). Total depth is 1,795 ft.

Interpretations of wells SA-221 and SA-222 suggest that the basin fill of the North graben can be subdivided into three layers, at least locally, that we call the upper, middle, and lower Santa Fe Group. Note that these layers do not necessarily correlate with the middle–upper and lower Santa Fe Group in the Winston graben. Each of these layers is 200–1,400 ft thick (Figs. 27, 28). The lateral extent of these three layers remains to be determined, and in the Southland Royalty SA No. 1 well and SA-222 only two layers can be readily distinguished. Within these layers at SA-221 and SA-222, the composition of sand and pebbles plus the character of geophysical curves allow us to infer the following depositional environments that interfinger with one another: a western piedmont derived from the Datil Mountains, basin floor, and an eastern piedmont deposit derived from a highland(s) underlain mainly by a phenocryst-poor tuff. This phenocryst-poor tuff looks very similar to the upper phenocryst-poor tuff (i.e., Vicks Peak Tuff) encountered in the shallow bedrock of the Southland Royalty SA No. 1 well. Thus, a preliminary correlation is established between the eastern piedmont detritus and a highland underlain by Vicks Peak and/or La Jencia tuffs in the vicinity of the Southland Royalty SA No.

1 well, but additional geochemical and geochronologic analyses are needed for verification. An interval of detritus comprised of phenocryst-poor tuff in SA-221 (unit Tsmlp) may have been derived from the aforementioned source or possibly elsewhere, such as the southern Datil Mountains.

In order to interpret the three depositional environments from properties of the basin fill sediment, one needs to consider the bedrock composition of the surrounding mountains (Fig. 6). The Gallinas and Datil Mountains flank the North graben and would be expected to contribute sediment into a subsiding graben. Both of these highlands are composed of interbedded volcaniclastic sedimentary rocks, felsic ignimbrites, and minor basaltic andesite flows. The volcaniclastic rocks are composed primarily of intermediate volcanic detritus and feldspar grains, but quartz sand grains are a notable component above the Hells Mesa Tuff (such as in the South Crosby Peak Formation) and in the upper Rincon Windmill Formation immediately below the Hells Mesa Tuff (Fig. 18; Harrison, 1980).

It is important to note that the proportion of intermediate-composition volcaniclastic sediment is currently at least twice as abundant on the eastern flanks of the Datil Mountains compared to the southwestern flanks of the Gallinas Mountains and the northern part of Mount Withington (35–50% versus <20% based on visual estimation of geologic mapping of Lopez and Bornhorst, 1979; Coffin, 1981; Harrison, 1980; Osburn and Ferguson, 2010, 2011; Osburn et al., 1993; Ferguson and Osborn, 2011). Roughly half of the drainage area of White House Canyon, the largest canyon draining the Datil Mountains and hosting the town of Datil, is underlain by the intermediate volcaniclastic sediment of the lower Spears Group (Dog Springs Formation; Fig. 18, Tsl in Fig. 6). However, the lower Spears Group, and intermediate-volcanic detritus higher in the section, is not exposed on the southwestern flanks of the Gallinas Mountains (Fig. 6; Osburn et al., 1993) nor on the northern flanks of Mount Withington (Fig. 6; Osburn and Ferguson, 2010, 2011; Ferguson and Osborn, 2011), although intermediate volcanic detritus is relatively abundant near Highway 60 on the eastern topographic divide of the East San Agustin Basin (Wilkinson, 1976).

A distinctive volcanic rock is the phenocryst- and quartz-rich Hells Mesa Tuff. However, it is not that useful as a sediment-source marker because of its widespread distribution. The Hells Mesa Tuff is widely exposed in the eastern foothills of the Datil Mountains, including the lower part of White House Canyon (Lopez and Bornhorst, 1979; Harrison, 1980). It also crops out on the lower slopes of drainages flowing into North Lake playa from the northern Gallinas Mountains (Coffin, 1981). However, further south in the Gallinas Mountains, the Hells Mesa Tuff is less spatially abundant and stratigraphically higher tuffs are more abundant (Osburn et al., 1993). The Hells Mesa Tuff is relatively abundant (20% modern-day outcrop area) on the northern flanks of Mount Withington (Osburn and Ferguson, 2010, 2011; Ferguson and Osburn, 2011).

In addition to lateral changes, the composition of Santa Fe Group basin fill from a certain source area (e.g., Datil vs western Gallinas Mountains) would be expected to change with depth. This is because basin fill strata become progressively older with depth (based on the geologic principle called the Law of Superposition) and the composition of the upland source areas changes over time due to exhumation (erosion) causing older, initially deeper rocks to be removed later. In other words, older basin fill was eroded from upland rocks that may have since eroded away. The volcanic stratigraphy developed by Cather et al. (1994) can be used to infer how the rocks exposed on the Datil and Gallinas Mountains would change with time. However, there might have been bedrock layers that have been completely eroded away and thus not incorporated into the known bedrock stratigraphy of Osburn and Chapin (1983) and Cather et al. (1994). Just prior to Rio Grande rifting and associated normal faulting, one could envision a paleo-landscape underlain by ignimbrites interbedded with local volcanic flows and varying amounts of volcaniclastic rocks of the upper Spears Group. These ignimbrites thin to the north and west and include (from top to bottom, with thickness ranges noted from Osburn and Chapin, 1983): South Canyon Tuff (0–650 ft; seen in the southern Gallinas Mountains and thickening southward to Mount Withington, its source area); Vicks Peak Tuff (0–500 ft); La Jencia Tuff (0–300 ft); Hells Mesa Tuff (160–410 ft); Blue Canyon Tuff (0–500 ft); Rockhouse Canyon Tuff (0–500 ft); and Datil Well Tuff (0–80 ft). Note that we interpret the Rockhouse Canyon Tuff to be 300–500 ft under the southern part of the East San Agustin basin, based on an inferred correlative in the Southland Royalty SA No. 1 well. The youngest ignimbrite, the Turkey Springs Tuff (Fig. 18; Table 1), has not been observed near the North or White Lake grabens but perhaps it has been completely eroded away. The major volcanic rock units exposed at (or near) the land surface at the beginning of the Miocene (23 Ma) would have been the Turkey Springs Tuff(?),

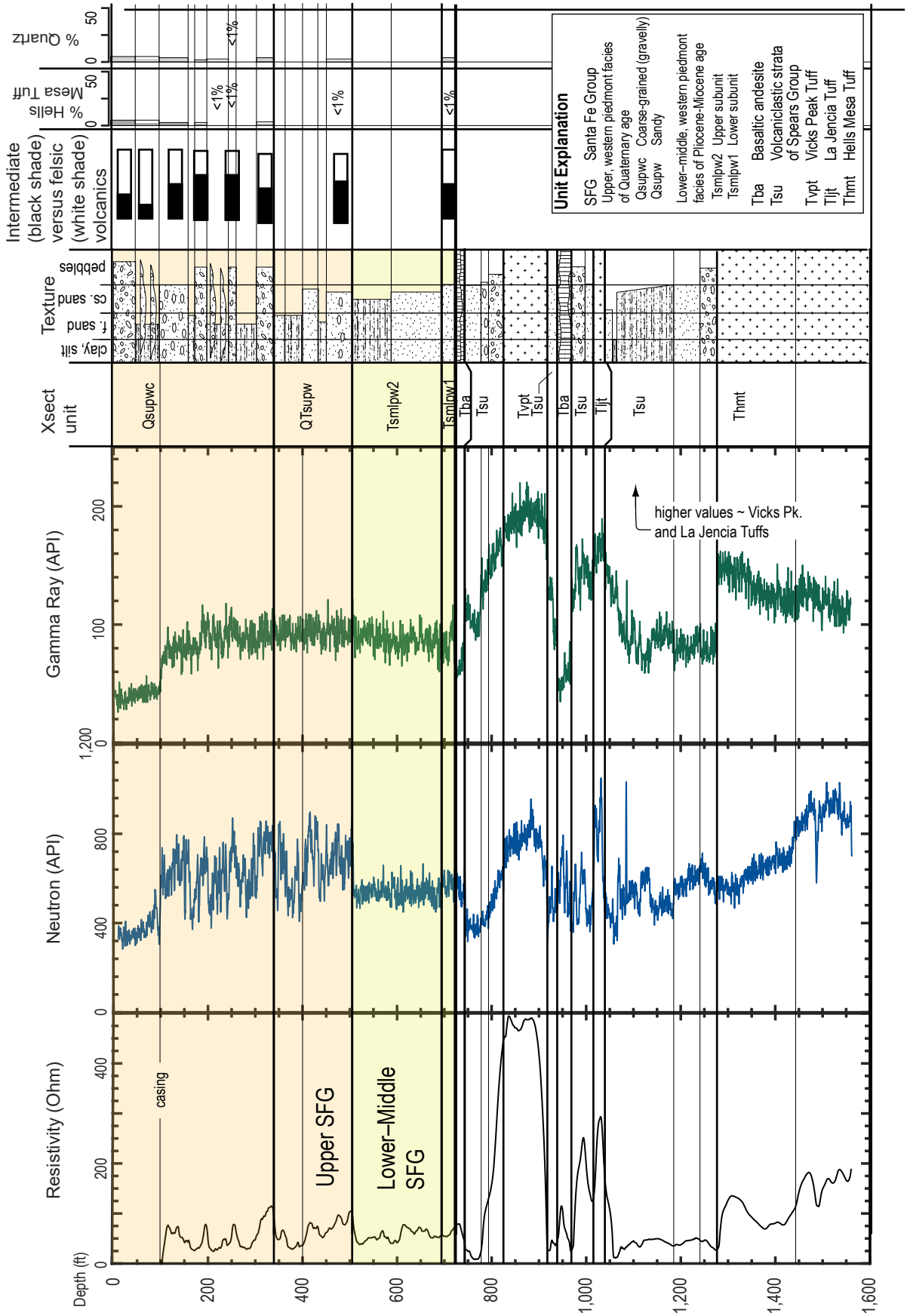

Figure 27. Subsurface data for well SA-222, which was drilled on a fault-bounded, structural bench on the western margin of the North graben about 6.8 mi north of Hwy 60 (Fig. 11). To the left are resistivity, neutron, and gamma-ray curves. On the right are inferences regarding texture and sand composition, based on interpretation of the curves and close examination of cleaned cuttings (using a high-powered hand lens) on chip boards provided by John Shomaker and Associates (complete descriptions are in Appendix 4). Plotted compositional parameters include: the approximate ratio of intermediate volcanic detritus versus felsic detritus (the latter mainly tuffs); the percent of Hells Mesa Tuff, and the percent of quartz. The Hells Mesa Tuff was assigned to porphyritic (crystal-rich) tuff grains containing quartz; intermediate volcanic grains for dark-colored grains (locally with mafic phenocrysts); and tuffs for light-colored grains containing quartz or sanidine phenocrysts. Most single quartz grains are likely derived from erosion of the Hells Mesa Tuff, which is the most extensive and thickest unit containing notable quartz crystals.

South Canyon Tuff, La Jara Peak basaltic andesites, Vicks Peak Tuff, and perhaps La Jencia Tuff. There also could have been felsic to intermediate volcanic flows near the top of the volcanic rock package that have been completely eroded away, analogous to the rhyolite of Piñon Well that is still preserved in the southern Gallinas Mountains (Osburn et al., 1993). As extensional faulting progressed in the Miocene and the Datil and Gallinas Mountains were formed, one would expect a progressive increase in the exposure of older rocks. For example, the Hells Mesa Tuff would appear and become progressively more abundant in mountain outcrops as a result of erosion and unroofing of earlier strata. In the basin fill record, lower sandy strata would be expected to have abundant detritus from the South Canyon, Vicks Peak, and La Jencia Tuffs. With further unroofing of the mountains, in the middle part of the basin fill one would expect increased amounts of Hells Mesa Tuff detritus and then, in an up-section direction, felsic tuff detritus mixed with intermediate volcanic detritus derived from the South Crosby Peak, Rincon Windmill, Chavez Canyon, and Dog Springs Formation (all of the Spears Group).

Well Log Methodology and Interpretation

Considering the geology bedrock source areas, adequately interpreting well cuttings from the three deep wells in North graben basin fill depends on petrologic study of the sand grains. The lead author did this petrologic assessment using a binocular microscope and high-powered hand lens on samples provided by John Shomaker and Associates and stored at the New Mexico Bureau of Geology Subsurface Library. The noted grain size of these described samples (Appendices 3, 4) is not a true reflection of the formation texture, since the samples are captured by screening the mud-slurry from the well (i.e., very fine sand, silt, and clay mostly pass through the screen). Clay fraction analyses are presented later in this report. Descriptions of sand composition and texture are in Appendices 3 and 4. One could do a more detailed examination, however, by making thin section slides of the cuttings and doing petrographic analyses on these slides. Another powerful tool would be radiometrically dating sandine grains and tuff fragments from the cuttings to confirm correlations to particular tuff units. This study lacked the funding to do these more thorough analyses. However, we encourage that such a study be conducted, and we would expect some of the details of the interpretations offered below to change as a result.

Resistivity and gamma-ray logs are available for the Southland Royalty SA No. 1 well (Appendix 5). Resistivity, neutron, density, gamma, and sonic wireline logs are available for both SA-221 and SA-222 drill holes and complemented the cuttings examination (Appendices 6, 7). Geophysical wireline logs measure physical and chemical properties of rocks, sediments, and fluids in and around a well bore. These are measured using a variety of sensors on the end of a wireline that is lowered into a well.

In this report, we will use data from five types of geophysical logs. ***Resistivity tools*** measure how much a material (bedrock or sediment) opposes the flow of electric current. It is a function of salinity in the formation fluid (i.e., the fluid filling the pore spaces and cracks in a formation) and also the mineral matrix (primarily clay, where cations in the crystal lattice allow conduction of electricity). If the groundwater salinity is relatively constant with depth, or changes in a gradual manner, sharp variations of the resistivity tool with depth will primarily be a function of the clay content in a layer (bed) of sediment. ***Neutron logs*** involve emitting neutrons into a formation. As these neutrons collide with atoms they lose energy. Most of the energy loss is due to collisions with hydrogen nuclei; therefore, the loss of neutron energy is primarily a function of the water and clay content of the rock (because water and clay have a relatively high proportion of hydrogen atoms). Because they are influenced by clay content, resistivity and neutron curves can allow one to: (1) estimate sand versus mud (silt-clay) ratios, and (2) assess if sand bodies fine-upward to more clayey sediment or coarsen upwards from more clayey sediment.

Density logs measure the electron density of a formation. A gamma-ray source emits gamma rays into the formation, where they experience Compton scattering, which is a function of the density of electrons in the formation. Such electron density can be related to the bulk density of a formation.

Given an assumed density of the formation matrix and an assumed density of pore-filling fluids (e.g., fresh groundwater at 1 g/cm^3), a ***density-porosity log*** can be readily calculated. Unfortunately, the SA-221 wireline log does not list the formation matrix density used in the calculation. The density of quartz sand (2.65 g/cm^3) is commonly used by logging companies for drilling in sandy basin fill, but the rhyolitic (felsic ignimbrite) sand that dominates the cuttings of SA-221 may range from 2.4–2.7 g/cm^3. (http://geopixel.co.uk/lab3/

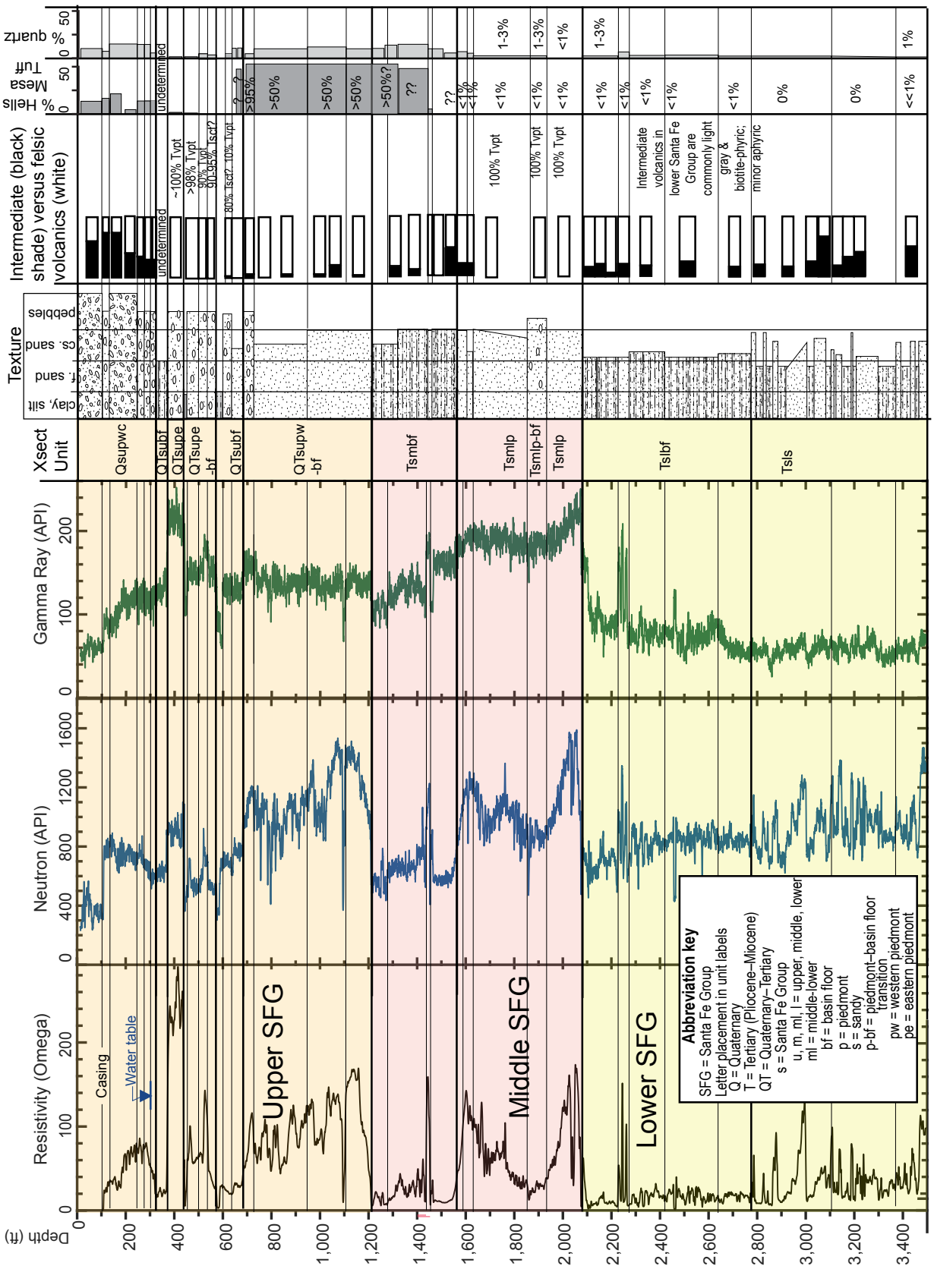

Figure 28. Subsurface data for well SA-221, which was drilled in the southern sub-basin of the North graben about 1.2 mi south of Hwy 60 (Fig. 11). To the left are resistivity, neutron, and gamma ray curves. On the right are inferences regarding texture and sand composition, based on interpretation of the curves and close examination of cuttings via binocular scope and hand lens (complete descriptions are in Appendix 4). Plotted compositional parameters include: the ratio of intermediate volcanic detritus versus felsic detritus (mainly tuffs; Tvpt = inferred Vicks Peak Tuff, Tsct = possible South Canyon Tuff); the percent of Hells Mesa Tuff, and the percent of quartz. The Hells Mesa Tuff was assigned to porphyritic (crystal-rich) tuff grains (commonly 1–2 mm long) containing quartz; intermediate volcanic grains for dark-colored grains containing biotite, hornblende, or pyroxene; and tuffs for light-colored grains containing sanidine or quartz phenocrysts. Most single quartz grains are likely derived from erosion of the Hells Mesa Tuff, which is the most extensive and thickest unit containing notable quartz crystals.

Densities_of_Typical_Rock_Types_and_Minerals.pdf). Using an average density of 2.5 g/cm^3 for the formation matrix rather than 2.65 g/cm^3 may result in error percentages of up to ~20% in the calculated porosity.

Different types of rock or sediment emit different amounts and different spectra of natural gamma radiation, which are measured by ***gamma-ray wireline logs***. Gamma rays are primarily produced by radioactive decay of certain potassium, thorium, and uranium isotopes. Thus, rock types that have higher concentrations of these isotopes, such as granite or clays or felsic tuffs, tend to produce higher gamma-ray signatures.

Sonic logs measure the time it takes for a sound wave to travel vertically through the formation, measured in μs/ft, and will be particularly useful in the discussion below regarding depth-changes in porosity and clay fraction. The transit time is sometimes referred to as "slowness" and is dependent on both lithology and porosity. The calculated porosities for Well SA-221 is shown in Figure 30, where a 100-ft moving window was used to smooth the data. Because sonic logs are highly sensitive to small changes in the sediment, such as fluid content and architecture of the sediment, they often contain sharp spikes in responses that are difficult to rectify with other, more smoothly varying logs. Using a moving average allows for these comparisons. Slower travel times would be associated with less compacted and less cemented strata, including clayey strata, and faster times would be associated with higher degrees of compaction and cementation as well as lower proportions of clay. Compaction is a function of the maximum post-burial depth as well as lithology. Porosities of volcaniclastic sediment tend to change more rapidly with depth compared to quartz-dominated sands (Nagtegaal, 1978).

Of particular interest in our investigation was the correlation of a high gamma ray signature with a monolithic sand composed of light gray, phenocryst-poor (aphanitic) tuff in SA-221 and the Southland Royalty SA No. 1 well. We interpret that this sand is eroded from the Vicks Peak Tuff and, to a lesser extent, the La Jencia Tuff, because these tuff grains have <10% phenocrysts and they bear a lithologic similarity to in situ Vicks Peak and La Jencia Tuff in Well SA-222 and the Southland Royalty SA No. 1. The Vicks Peak Tuff in nearby highlands tends to be light gray, whereas the La Jencia Tuff is often redder. Note that where the Vicks Peak and La Jencia Tuffs are present in the subsurface, they produce a notably high gamma ray signature (Fig. 27). Another phenocryst-poor volcanic unit (inferred to correlate to the Rockhouse Canyon Tuff) is interpreted to lie near the bottom of the Southland Royalty SA No. 1 well; this unit is reddish gray and has a high gamma-ray signature as well (Appendix 5). However, it alone is unlikely to have been a sole sediment source because this tuff is relatively low in the stratigraphic pile—requiring unusually high amounts of localized uplift to expose it to erosion—and, if exposed, canyon-cutting would likely result in a sand-mixture of this phenocryst poor tuff with phenocryst-rich tuffs derived from the overlying Hells Mesa Tuff. It is noteworthy that the topmost bedrock stratigraphic unit encountered in SA-222, Southland Royalty No. 1, and the Sun No. 1 well is the Vicks Peak Tuff. In the absence of high amounts of localized uplift, the Vicks Peak Tuff is more likely to be a sole sediment source than the Rockhouse Canyon Tuff.

Collectively, these observations support the inference that grayish, crystal-poor, monolithic sand producing a high gamma-ray signature is most likely to have been derived from erosion of relatively low highlands underlain by Vicks Peak Tuff and possibly La Lencia Tuff. The presence of this sand immediately above the Vicks Peak Tuff in the Southland Royalty SA No. 1 well (Fig. 12), where it is relatively angular, is consistent with the interpretation that a paleotopographic highland underlain by these upper phenocryst-poor tuffs was located on the east flank of the North graben (Fig. 29a). However, it is also possible that early erosion of the eastern Datil Mountains could have produced thick intervals of detritus derived from originally thick Vicks Peak Tuff bedrock strata. Future radiometric dating of this detritus would be necessary to varify the tuff correlations and test this paleogeographic model.

Table 3 summarizes the wireline log criteria we used to recognize the three aforementioned environments: western piedmont, basin floor, and eastern piedmont. Petrographic criteria that could be obtained via binocular scope or hand lens include the estimated proportion of quartz (1–10% estimated error), the estimated proportion of Hells Mesa Tuff (which is relatively porphyritic and quartz-bearing;

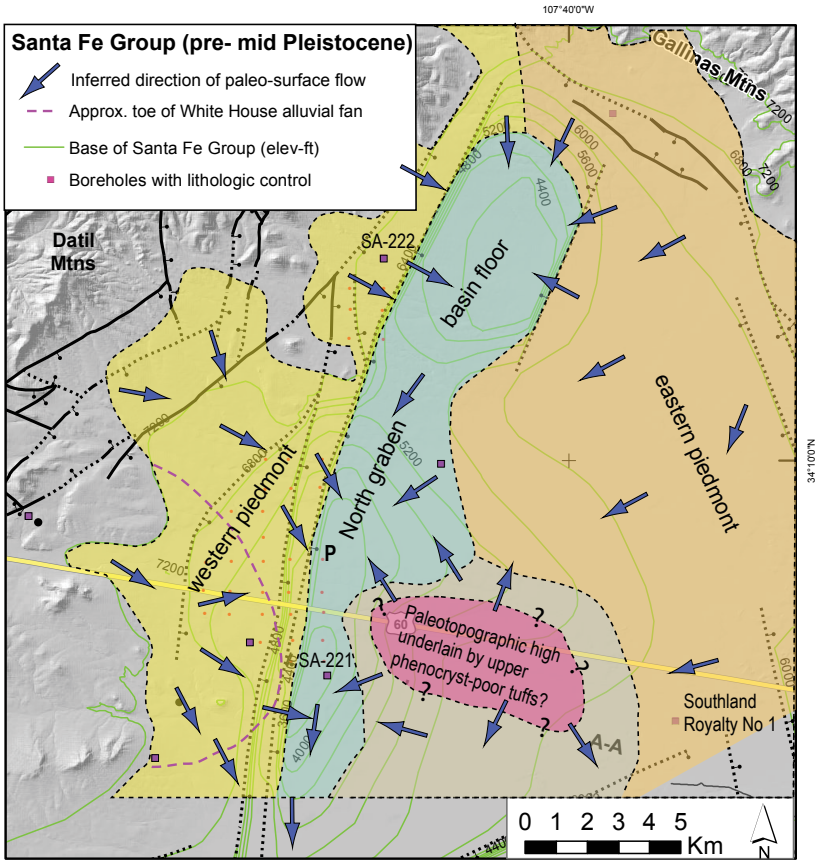

Figure 29A

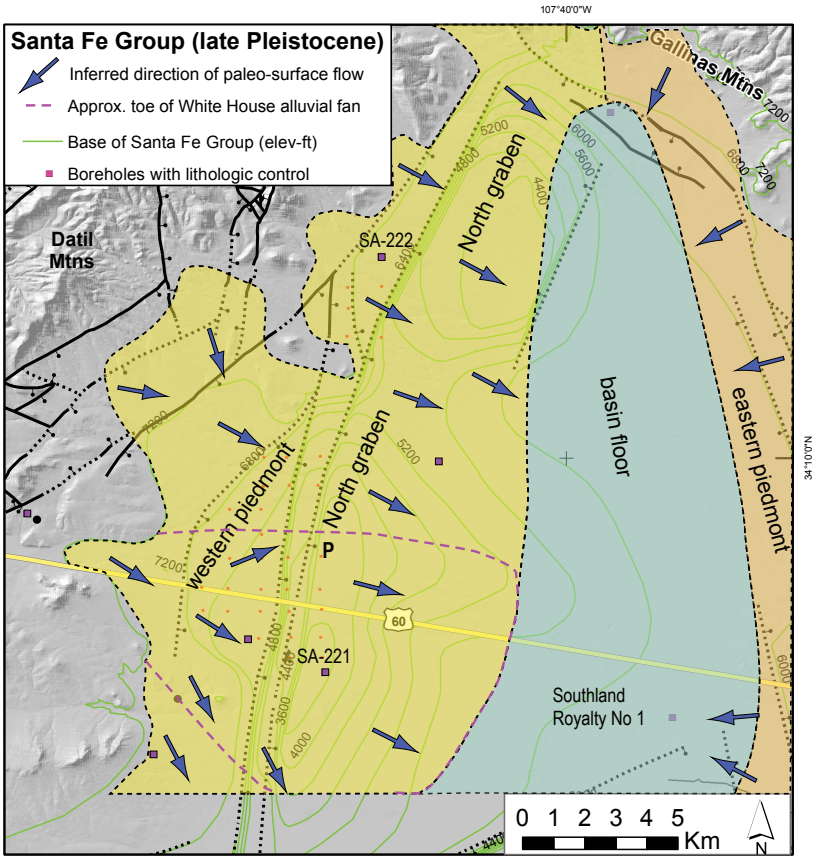

Figure 29B

Figure 29. Schematic paleo-geographic map of the North graben, showing authors' interpretations of paleo-environments during deposition of the middle Santa Fe Group (Figure 29A) and latest Santa Fe Group (Figure 29B). During middle to late Quaternary time, the western piedmont prograded eastward and the basin floor deposits moved eastward as well. Consequently, middle-late Quaternary basin fill deposits mainly lie east of the deepest part of the North graben (Figure 29B).

5–20% estimated error), and the estimated ratio of tuffs versus intermediate volcanic rocks (20% estimated error for the sand fraction). An interpretation of felsic or tuff sand grains is applied to lighter-colored grains that typically feature sanidine, quartz, and/or biotite phenocrysts. Most of these grains are likely tuffs, rather than rhyolite flows, because such flows are less common than rhyolitic tuffs in the Datil and Gallinas Mountains (Fig. 5; Osburn and Chapin, 1983; Harrison, 1980; Coffin, 1981), with an exception of a thick rhyolite flow present in the southern Gallinas Mountains (rhyolite of Piñon Well; Osburn et al., 1993). An interpretation of intermediate volcanic sand is assigned to grains that lack quartz or sanidine phenocrysts and typically feature black-colored pyroxene, hornblende, or biotite phenocrysts.

Another criteria for recognizing the depositional environments is the abundance of sand bodies and up-section trends in grain size (Table 3). The proportion of medium- to very coarse-grained sands and gravels increases away from the center of a basin (especially a closed basin) towards the proximal part of the piedmont. Moreover, the center of an alluvial flat is predominately clay, silt, and very fine to fine sand. A playa is mostly clay-silt, with the proportion of very fine to fine sand increasing towards the margins. Alluvial fans on a piedmont commonly show an overall coarsening-upward trend (Weissmann et al., 2011).

Quantification of Porosity and Clay Percentage

The availability of sonic and density curves for Well SA-221 allows us to quantify porosity and the proportion of formational clay as a function of depth. We are unable to use the neutron log for this analysis because of the lack of a reliable calibration curve relating the neutron log to porosity. For most basin fill across the world, gamma ray logs are often used in conjunction with density logs to estimate the clay fraction of sediments. However, in SA-221 using gamma ray logs to calculate clay is complicated by copious radiogenic sand of felsic composition, which like clay, results in relatively high gamma ray readings. Calculating the clay fraction from the SP curve is hindered by changing salinity levels of formation water with depth plus the lack of a SP response for inferred clayey beds in SA-221, the latter likely due to thinness of the clayey beds.

Formational clays could be detrital (deposited by water on the Earth's surface before subsequent burial) or formed by chemical alteration (diagenesis) of volcanic grains after the sediment was buried. Such diagenesis can be pronounced for the high amounts of lithic grains observed in volcaniclastic sediment (e.g., Nagtegaal, 1978). Possible evidence of this diagenesis was locally observed in the lower Santa Fe Group in SA-221 (below 2,075 ft depth), based on discoloration and chemical alteration of some sand grains. However, higher in SA-221 there is little notable alteration of sand grains, except for a reddening at 1,253–1,628 ft depths. The apparent lack of clay diagenesis for the middle to upper Santa Fe Group may be due to the relative dryness of central New Mexico in the past 16 million years (Chapin, 2008). A collabatory observation is the lack of notable diagenesis in Middle Miocene through Pleistocene strata of the Palomas Basin (lead author observation during geologic mapping; Koning et al., 2015; Koning et al., 2018; Jochems and Koning, 2016). Thus, we infer that most of the clay in the subsurface is likely of primary origin (non-diagenetic), particularly above 2,075 ft.

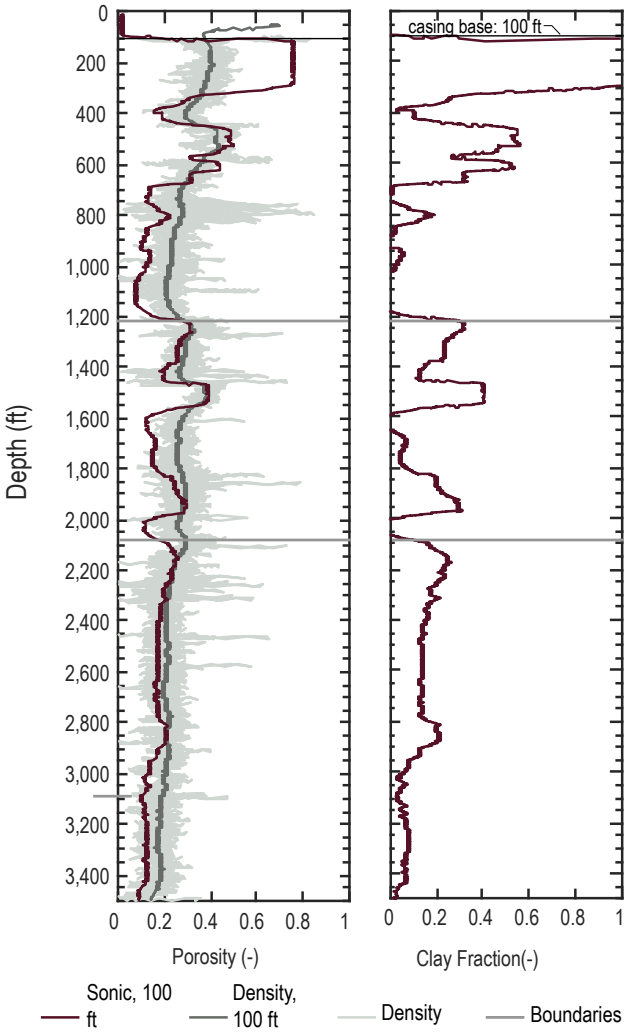

Figure 30. Plots of porosity (left column) and clay fraction (right column) for the SA-221 well. In the left column, porosity was calculated using a 100-ft smoothing window of sonic logs and density logs. Depth is shown on the left. The two horizontal lines are boundaries between the upper, middle, and lower Santa Fe Group.

To estimate the clay fraction from the combination of sonic and density logs, porosity must first be estimated. The porosity from the density logs, n_d, was calculated by the logging company; it should be noted that the density logs do not state what density values were used by the logging company for the formation matrix. The porosity from the sonic logs, n_s, was calculated from the 100-ft moving average of the sonic log (s_{log}) using:

$$n_s = \frac{1}{c_p} * [\frac{s_{log} - s_{min}}{s_{fluid} - s_{min}}]$$

where s_{min} is the slowness of the primary minerals (53.25 µs/ft; Crain, 2019), s_{fluid} is the slowness of fresh water (189 µs/ft; Crain, 2019), and c_p is the compaction factor (unitless). The compaction factor corrects the porosity estimate for the compaction of sands with increasing depth (Crain, 2019). It is given by:

$$c_p = max\ (\frac{c * s_{sand}}{100}, 1)$$

where c is an empirical factor usually given as 1, and s_{sand} is the maximum slowness of a sand interval. Sandy intervals from the following depth intervals of SA-221 were used to calculate a depth-dependent c_p: 320–374 ft, 440–450 ft, 596–626 ft, 1,210–1,315 ft, 1,452–1,555 ft, 2,075–2,226 ft, and 2,265–2,775 ft. For every depth that the porosity was calculated using the sonic data, we applied the compaction factor derived from the nearest of these sandy intervals.

The clay fraction, $v_{sh,dxs}$, is estimated from the sonic porosity response in a purely clay interval ($n_{s,\ sh}$) and the difference in compaction-corrected sonic (n_s) and the density (n_d) porosities using the following function (Crain, 1999):

$$v_{sh,dxs} = \frac{n_{s,sh} n_d - n_s n_d}{n_{s,sh} - n_d}$$

Because there may be a lack of pure clay beds in Well SA-221, we used the minimum sonic porosity ($n_{s,sh}$) from what we inferred to be the most clay-rich interval in the well (573–590 ft).

Figure 30 shows the porosity and clay fraction as a function of depth in Well SA-221. The clay fraction is anomalously high between 100 ft (bottom of casing and top of useful sonic data) and roughly 350 ft, consistent with the extremely high slowness in the sonic log. Ironically, cuttings data indicate that this interval is gravelly (Fig. 28), so the corresponding sediment must be a clayey gravelly-sand mix. This is not unusual in the region; such clayey gravel-sand is conspicuous in exposed post-2.5-Ma piedmont sediment, observed south of Socorro, derived from volcanic terrain (e.g., Koning et al., 2015, 2018; Jochems, 2015; Jochems and Koning, 2016, 2019). Inspection of the results in Figure 30 indicates low clay percentages (<15%) at 376–440 ft (QTsupe) and 680–1,210 ft (unit QTsupw-bf on Figure 28), consistent with relatively high resistivity and neutron log responses. Clay content is variable between 1,210 and 2,075 ft, but relatively high (18–40%) at 1,210–1,555 ft and 1,825–1,985 ft. At depths greater than 2,075 ft (lower Santa Fe Group), there is less clay variability and a relatively steady downhole trend to lower clay proportions (20% at top and 5% near the bottom).

Of the various ways to calculate porosity and clay fraction (including those using gamma-ray and neutron porosity data), those based on sonic logs are among the least accurate due to the large number of

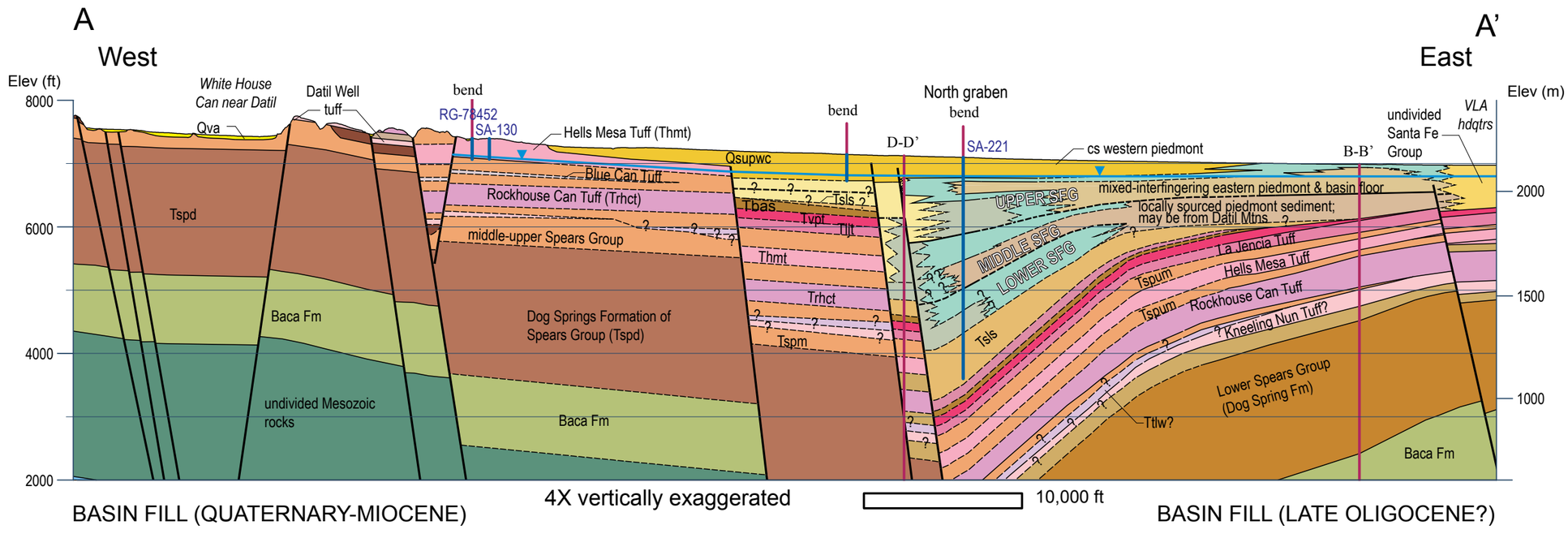

Note: although the depicted succession of bedrock units is reasonable, their thicknesses and depths are poorly constrained away from bedrock-penetrating wells; there may also be additional volcanic units and faults in the subsurface that are not exposed on the surface.

Figure 31. Simplified version of cross-section A-A' that passes through Datil and the southern part of the North graben (cross-section line in Figs. 6, 11).

non-porosity-related controls of sonic log responses. However, we have reasonable confidence in these results qualitatively and believe the data are adequate for comparative purposes within the well. For example, below 350-ft depth the intervals with high clay fractions commonly correspond to what was interpreted to be basin floor environments (Appendix 4). These environments are noted by "bf" at the end of the cross section (xsect) unit labels in Fig. 28 (c.f., Figure 28 and Appendix 4 inferred depositional environments with clay fraction in Figure 30).

Southland Royalty SA No. 1

Detailed descriptions of the cuttings of the Southland Royalty SA No. 1 well are given in Appendix 3. Scans of the electric, SP, and gamma-ray curves are provided in Appendix 5. Interpretation of these data indicate that a 725-ft-thick succession of relatively coarse, volcaniclastic sediment (sand and gravel of the Santa Fe Group) directly overlies light gray bedrock composed of fine-grained (phenocryst poor) ignimbrite correlated to the Vicks Peak Tuff and underlying reddish gray to gray La Jencia Tuff (Fig. 12).

The upper 47 ft of the Santa Fe Group consists of sand composed of quartz, sanidine, and plagioclase with 20% felsic-dominated volcanic grains and 5–7% black mafic grains (mostly biotite and hornblende). This interval has the lowest gamma-ray signature of the well (Appendix 5). The low gamma-ray signature and lack of volcanic lithics may reflect mineralogically mature sediments subjected to long-duration weathering cycles and/or lack of clays, although low resistivity at 18–20 ft and 44–58 ft may be due to clays associated with a local playa at what is now the VLA (i.e., the White Lake playa). We infer that the depositional paleoenvironment associated with the upper 47 ft of the well was predominately wind-blown (eolian) with localized playas.

The sediment at 47 to 470 ft depths consists of sand and pebbles, although low resistivity readings at 110–140, 170–175, 220–225, 235–240, 245–253 ft depths (Appendix 5) are likely due to clays or clayey sands. The sand and pebbles are subangular to subrounded. Pebbles and sand are composed of felsic volcanic rocks, hornblende- or biotite-bearing intermediate volcanic rocks, variable Hells Mesa Tuff, and, with depth, 1–20% basaltic andesite. The presence of intermediate volcanic rocks is best explained by a west-flowing drainage sourced in the topographic divide to the east, near where the divide is crossed by Highway 60, because the intermediate rocks are not common in bedrock strata near Mount Withington (Osburn and Ferguson, 2010, 2011); tributary drainages from the southern Gallinas Mountains could have provided the basaltic andesite. In contrast to the typical composition in the 47–470 ft depth interval, the 200–340 ft sub-interval is distinctive in that it lacks notable intermediate detritus and basaltic andesite; this is probably best explained by piedmont deposition from drainages sourced to the southeast (northern Mount Withington).

At 470–690 ft depths the sand and gravel are composed of a monolithic, light gray, crystal-poor tuff (1–5% show eutaxitic texture) with minor basaltic andesite (Fig. 12). The sand and gravel composed of tuff are slightly more angular than observed above and are lithologically similar to the underlying Vicks Peak Tuff. This sediment interval is inferred to represent deposition of detritus eroded from a nearby paleotopographic high (discussed above) underlain primarily by the Vicks Peak Tuff (some possible La Jencia Tuff) with minor capping basaltic andesite flows. At 690–725 ft, the sand and pebbles become lithologically more variable (heterolithic). Basaltic andesite is not observed at this depth, and there is abundant sanidine and quartz. In addition, the gamma ray readings decrease slightly at 690–725 ft. This lithologic change at the base of the Santa Fe Group may be attributable to deposition on the distal piedmont shed from the northern flanks of Mount Withington. The northern flanks have very little basaltic andesite, but does have notable rhyolite flows and crystal-rich tuffs (per Osburn and Ferguson, 2010, 2011). Another possibility for the heterolithic cuttings is slough or caving from the 47–470 ft depth interval.

SA-222 Results

The Upper Santa Fe Group unit (prefixed by Q or QT in Figures 19 and 27, since it is likely both Quaternary and Tertiary in age) is 507 ft thick in Well SA-222 and consists of a gravelly, upper subunit (Qsupwc) and a sandy, lower subunit (QTsupw). In these unit abbreviations, 'u' stands for upper, 'p' for piedmont, 'w' for western, and 'c' for coarse. Cuttings description text is given in Appendix 4. The original, detailed wireline logs are found in Appendix 6; lower-scale versions are presented in Figure 27 alongside graphics summarizing the cuttings descriptions.

The two Upper Santa Fe Group subunits are interpreted to be derived from the west (i.e., from the Datil Mountains) because of the hetereolithic nature

of the well cuttings (e.g., mixture of intermediate volcanic sand, tuffs, and quartz; Table 3; Fig. 27). This interpretation is bolstered by the position of this well on the modern, medial piedmont shed from the eastern Datil Mountains. The upper subunit (Qsupwc) is 340 ft thick and consists of pinkish gray to gray, sandy gravels interbedded with pink to light brown, clayey, fine-grained sands. Gravels are subangular to subrounded and are composed of intermediate volcanic rocks and tuffs. Some tuff gravels are large enough to correlate to the crystal-rich, quartz-bearing Hells Mesa Tuff. Finer-grained tuffs are likely the Datil Well or Rockhouse Canyon Tuffs (exposed in the bedrock to the west). The proportion of Hells Mesa Tuff and quartz decreases slightly down-hole. The lower, Quaternary-Tertiary piedmont unit derived from the west (QTsupw) is 167 ft thick (340–507 ft depths) and composed of light brown to pink, very fine- to coarse-grained sand and clayey sand. The bases of these subunits are sharp (marked by abrupt deflections in the wireline curves) and the sands overlying the two bases are coarse-grained and gravel-bearing; these sharp bases (contacts) may correspond to stratigraphic disconformities. Above these basal fining-upward sands, the remainder of the two subunits mostly consist of sand bodies 8–12 ft thick, which have a symmetrical expression on the resistivity and neutron curves (Appendix 6).

A somewhat perplexing phenomena is observed in the wireline data for the upper 175 ft of SA-222. The 75-ft interval of strata immediately underlying the base-of-casing (100–175 ft depth)—corresponding to the upper, coarse, western piedmont unit (QTupwc)—exhibits a coarsening upward trend, based on the upward-increasing resistivity curves and a subtle upward-decreasing gamma-ray curve. The gamma-ray curve decreases upwards within the casing. The neutron curve shows an upward decrease for the 75 ft below the casing and into the cased uppermost 100 ft of the well. The trends in the neutron and gamma curves may possibly be explained by an upward decrease in the proportion of felsic volcanic detritus (based on the gamma-ray curve) or upward-increasing vadose-zone moisture (based on the neutron curve; note that an upward increase in clay content is inconsistent with the upward-decreasing gamma-ray curve). However, our observations of the cuttings do not indicate an upward decrease in the proportion of felsic volcanic detritus, although this interpretation might change with detailed thin-section petrographic analyses.

The lower–middle Santa Fe Group (Tsmlpw1 and Tsmlpw2) is 217 ft thick (507–724 ft depth interval) and is composed of interbedded sand and clayey-silty sand. The sand is pinkish white and very fine- to coarse-grained (<15% very coarse sand). Compared to the upper Santa Fe Group, the resistivity and neutron curves show lower amplitudes and thinner peaks and troughs (~6 ft thick), the latter likely due to thinner bodies of sand and clayey-silty sand. The decrease in amplitude of the neutron curves in the lower-middle Santa Fe Group is much more dramatic than in the resistivity data. Compared to the lower upper Santa Fe Group (QTsupw), there is a notable left shift of the neutron curve and lower peaks in the resistivity curve. The lower amplitudes and lower general values of both curves suggests more uniform sediment that contains less clean sands than QTsupw; the slightly lower resistivity signal of the upper part of Tsmlpw2 suggests a slightly higher clay fraction or more saline groundwater. The sand in the cuttings contains about subequal intermediate volcanics versus tuffs (based on hand lens inspection of the John Shomaker and Associates chipboards), consistent with a piedmont depositional environment sourced from the Datil Mountains. The lowest subunit, Tsmlpw1, has a slightly higher neutron value and the sand in the cuttings are slightly coarser than overlying strata.

Bedrock below the Santa Fe Group in well SA-222 is readily interpretable in the cuttings on the John Shomaker and Associates chipboards. The following units are confidently recognized (listed from top to bottom, thicknesses in parentheses): basaltic andesite (18 ft), volcaniclastic strata (84 ft), Vicks Peak Tuff (93 ft thick; gray, ≤3% phenocrysts that include sanidine, plagioclase, biotite or hornblende), volcaniclastic strata with a tongue of basaltic andesite (97 ft), La Jencia Tuff (24 ft; eutaxitic texture, fine-grained, strongly welded), volcaniclastic strata of the South Crosby Peak Formation (238 ft), and Hells Mesa Tuff (>286 ft). Of importance to our stratigraphic interpretations of well SA-221 is the high gamma signature of the Vicks Peak Tuff in well SA-222 (180-230 API) followed by the La Jencia Tuff (~170 API). The thick basal unit, the Hells Mesa Tuff, has a gamma ray signature that decreases down-section from 150 to 110 API.

SA-221 Results

Well SA-221 penetrated 3,495 ft of Santa Fe Group without reaching bedrock. Cuttings descriptions are given in Appendix 4. Original wireline data are given in Appendix 7. In Figure 28, a summary of the description of cuttings (right side of figure) is shown

alongside small-scale resistivity, neutron, and gamma wireline data (left side of figure). The basin fill in this well can be subdivided into three vertically stacked layers: the upper, middle, and lower units of the Santa Fe Group (Figure 28). Correlation of the upper layer between wells SA-221 and SA-222 is relatively certain. Exactly how the middle and lower layers of SA-221 correlate with the lower layer in SA-222 is uncertain.

Based on our methods (discussed above) and available data, we preliminary differentiate strata into one of four stratigraphic facies reflecting specific depositional environments (in contrast to just the western piedmont depositional environment interpreted for well SA-222): western piedmont, basin floor, eastern piedmont, and lower-river facies. These facies extend across the three units (layers) of the Santa Fe Group. ***As noted above, more detailed study employing comprehensive sand petrography and radiometric dating of sand grains would likely result in refinement to our designation of facies and how they are depicted in the cross sections (Figures 19, 31); thus, facies interpretations for this well and cross-section interpretations near SA-221 should be considered as preliminary.***

Upper Santa Fe Group, gravelly upper unit (0 to 320 ft depth) — The Upper Santa Fe Group is divided into a 320-ft thick, gravelly upper unit overlying an 890-ft thick, lower unit comprised of several subunits with lesser proportions of gravel (compared to the gravelly upper unit). The gravelly upper unit consists of interbedded sandy pebbles, pebbly sand, and sand. The pebbles are angular to subangular, and composed of tuffs (including the crystal-rich Hells Mesa Tuff) and intermediate volcanic clasts. The sand in the gravelly upper Santa Fe Group is pinkish gray to pink, mostly medium- to coarse-grained, and subangular to angular. Like the gravels, the sand is composed of a mixture of tuffs and intermediate volcanic rocks. There are up to 20% Hells Mesa Tuff lithic grains and 10-30% quartz grains (probably derived mostly from weathering of the Hells Mesa Tuff, the eolianites of the upper Rincon Windmill Formation, or sandstones post-dating Hells Mesa Tuff). Sand bodies are relatively thin (2–8 ft thick). The lower 30 ft of the gravelly upper Santa Fe Group (290–320 ft depths) clearly coarsens up-section, based on both the neutron and resistivity curves.

For the gravelly upper unit (Qsupwc), the resistivity curve shows an overall symmetrical shape (with respect to depth) between 320 and 190 ft (Fig. 28; Appendix 7), which is located above the water table. In the unit labels of Figure 28, 'u' stands for upper, 'pw' for western piedmont, and 'c' for coarse-grained. Interpreting the overlying 100-190 ft interval is complicated by a slight wash-out—the caliper log indicates that the hole becomes 2–3 inches wider here compared to below 190 ft and this may result in the lower gamma ray values for 100–190 ft. The upper part of the resistivity curve progressively decreases up-section from 280 to 190 ft. The neutron curve remains at a relatively constant value from 270 to 190 ft. The wide spread in the 16-inch and 64-inch resistivity curves between 320 and 190 ft, where the deeper (64-inch) curves show increased resistivity compared to the shallower (16-inch) curves (see Appendix 7), indicate somewhat permeable conditions that allowed a diffusion of salinity associated with the drilling fluid to penetrate into the adjoining formation. However, there is abundant clay in this interval (Fig. 30), as well as the entire gravelly upper unit, decreasing what might have otherwise been high permeability associated with gravelly sediment. The progressive up-section decrease of resistivity and gamma-ray values above 270 ft may indicate a progressive up-section decrease of clay content (but still it is overall clayey, per Fig. 30); the fact that the neutron curve does not show a such a decrease may be due to complications by vadose-zone moisture content (note the leftward deflection of the neutron and gamma-ray curves above 100 ft is due to the 100-ft long surface casing).

The heterolithic composition of the cuttings in the gravelly upper unit (i.e., 30% to ~70% intermediate volcanic detritus mixed with 30-70% felsic volcanic detritus) is consistent with sediment derived from erosion of the Datil Mountains and deposited on a western piedmont (Table 3). Based on its location near the middle of the modern-day White House Canyon fan, we accordingly interpret that the Upper Santa Fe Group in SA-221 represents deposition on the medial part of the White House Canyon alluvial fan. The upward-coarsening inferred from the neutron and resistivity curves at 320–285 ft, corresponding to a slight upward decrease in gamma ray values (Fig. 28), is interpreted to reflect a progradation of the White House alluvial fan.

Upper Santa Fe Group, gravel-poor, lower unit (320 to 1,210 ft depth) — The less-gravelly, lower unit of the upper Santa Fe Group (320–1,210 ft) is composed of fine-grained sediment (unit QTsubf) interbedded with a relatively monolithic sand (unit QTsupe and QTsupe-bf) (Fig. 28; Appendix 4). In the unit labels of

Criteria	Western piedmont	Basin floor	Eastern piedmont*
Proportion of clayey-silty beds	Low to moderate	Moderate to high	Very low
Proportion of light gray, crystal-poor tuff in cuttings (probably Vicks Peak Tuff, but could possibly be Rockhouse Canyon Tuff)	<80%	<80%	<80%
Gamma ray (API)	80 to 160	80 to 160	>140
Proportion of Hells Mesa Tuff	5-70%	1-50%	<1%
Intermediate volcanic grains (int.) vs. felsic volcanic grains	10-75% (int.) vs 75-10% (felsic)	0-75% (int.) to 25-100% (felsic)	<1%
Proportion of quartz grains	1-30%	1-30%	≤1%

*Inferred to be on the eastern piedmont because of similar sediment in the lower Santa Fe Group at the Southland Royalty SA No. 1 well to the east (near the VLA headquarters). Sediment appears to be largely derived from the Vicks Peak Tuff. To the north, the eastern piedmont would be derived from the western face of the Gallinas Mountains and have a more heterolithic sand composition (probably like that seen in the upper half of the Santa Fe Group at the Southland Royalty No. 1 well). Using these criteria become more difficult with depth (especially for middle and lower Santa Fe Group) due to uncertain exposure of bedrock units and the possibility of bedrock types that have been completely eroded away with time.

Table 3. Wireline and cuttings criteria used to recognize depositional environments in Wells SA-221 and SA-222. int. = intermediate.

Figure 28, 'u' stands for upper, 'p' for piedmont, 'bf' for basin floor, and 'e' for eastern; a hyphen indicates inferred interfingering between adjoining depositional environments, such as the eastern piedmont and the basin floor.

Relatively finer-grained intervals are interpreted at 320–374 ft, 440–450, and 573–680 ft depths in Well SA-221 (Fig. 28; Appendix 7). Most of these are associated with wash-outs based on the caliper log, but the wash-out for the fine-grained layer at 440–450 ft is less pronounced. In addition to relatively high values (>30%) in the clay-fraction curves at these depths (Fig. 30), the fine-grained texture is interpreted using the corresponding low values of the resistivity and neutron curves together with slightly increased gamma ray values (slightly increased compared to gamma values of the western piedmont unit Qsupwc). Preserved sand in the cuttings is as coarse as medium- to very coarse-grained (minor very fine- to fine-grained sand preserved in samples), light gray to pinkish gray to white, angular to subrounded (mostly subangular), and composed of felsic tuff-dominated detritus and 1–5% quartz. Sand from within the lower finer-grained interval (626–680 ft) is white to light gray, fine- to coarse-grained (apparently coarsening-upward), subrounded to subangular, well-sorted, and composed of sanidine and other feldspar with 25–50% felsic tuff lithics (phenocryst-rich with feldspar, quartz, and biotite — possibly correlative to the Hells Mesa and/or South Canyon Tuffs), 10% quartz, and 7–10% biotite. The sand composition of these finer-grained intervals are compositionally more diverse than the monolithic sands seen elsewhere in the gravel-poor, lower unit of the upper Santa Fe Group (see next paragraph). This diversity and the relative abundance of fine-texture cuttings are used to infer deposition on a basin-floor (Table 3), and hence the corresponding depth intervals are labeled QTsubf ('bf' for basin floor).

Cuttings in the 376–440 ft depth interval consists of monolithic sand that is gray, medium to very coarse, angular, and has 5–10% very fine pebbles. The sand is composed exclusively of phenocryst-poor tuff with a phenocryst assemblage that includes trace amounts of vitreous feldspar (up to 2 mm long and probably sanidine) and biotite. This monolithic gray sand is very similar to the Vicks Peak Tuff at 826–919 ft depth in the SA-222 well and, like the Vicks Peak Tuff in SA-222, has a very high gamma ray value (200–240 API at 376–440 ft depth). We thus feel relatively confident in interpreting this monolithic sand to be an erosional product of the Vicks Peak Tuff (but this correlation needs to be confirmed by radiometric dating or geochemical correlation). High resistivity, neutron, and low density-porosity values at 376–440 ft may be due to a very low fraction of clay or due to cementation. We prefer the low-clay fraction alternative because no signs of cement were observed in the cuttings, and the clay fraction analysis indicates <10% clay (Fig. 30).

Similar monolithic sand is present at 450–537 ft depths but it is slightly diluted by other tuffs. Here, the monolithic sand is light gray to pinkish gray, angular to subrounded, and mostly medium- to very coarse-grained (15–20% pinkish, clayey very fine- to medium-grained sand is noted at 450–500 ft depths). Very fine to fine pebbles (10–25%) that are compositionally similar to the light gray, monolithic sand are also present. Both the grayish sand and pebbles are predominantly a phenocryst-poor tuff containing 1–5% phenocrysts of sanidine and quartz (up to

3 mm long), as well as biotite and hornblende. As at 376–440 ft, this tuff detritus is correlated to the Vicks Peak Tuff. Other tuff grains include a reddish brown, relatively phenocryst-poor, eutaxitic tuff likely correlative to the La Jencia Tuff (≤10% of detritus) and possible crystal-rich, whitish Hells Mesa Tuff (<1%). The gamma ray curve for this interval is still relatively high (140–170 API) but notably lower than at 376–440 ft; the resistivity and neutron curves exhibit low to moderate values, with two peaks at 460–470 and 520–535 ft interpreted as coarse-grained channel-fills or gully-mouth fan deposits (the one at 520–535 ft likely is a fan deposit due to its coarsening-upward trend and sharp upper contact). Discernable sand beds in the wireline data are thin (less than 5 ft thick) but when amalgamated, produce relatively thick sandstone packages. Although not obvious in the cuttings, the clay fraction analyses indicates about 50% clay (Fig. 30).

At 537–573 ft, the sediment is a fine- to very coarse-grained sand with 10–15% very fine to medium pebbles. The sand and pebbles are predominately composed of a moderately phenocryst-rich, welded tuff. In the tuff fragments, there are 20–25% phenocrysts that are 0.5–1.5 mm long and include feldspar, quartz, and biotite. This moderately phenocryst-rich tuff may possibly correlate to the South Canyon Tuff. In addition, there are 1–5% fragments of a phenocryst-poor tuff (probably Vicks Peak Tuff) and 1–3% quartz grains. Compared to the adjoining stratigraphic intervals, clay content is lower in the 537–573 ft interval (20–40%).

For the relatively monolithic sands (376–440, 450–537, 537–573 ft depths), we interpret deposition on an eastern piedmont, with sediment that was sourced from a paleogeographic high a short distance to the east or southeast. Exposed bedrock strata on this bedrock high was initially a moderately phenocrystic tuff (South Canyon Tuff?); the eroded detritus accumulated in the 537–573 ft depth interval. But further erosion then exposed a thick interval of Vicks Peak Tuff and minor La Jencia Tuff (accounting for the gray, monolithic tuff cuttings at 376–440 and 450–537 ft). Since the depth intervals of interest lie relatively high in the basin fill stratigraphy and likely are Quaternary in age, it is difficult to imagine how there could be a source that is solely underlain by Vicks Peak Tuff (and minor La Jencia Tuff) in the Datil Mountains, since these mountains were likely uplifted for several million years and canyon down-cutting would likely have exposed a variety of rock types, as is seen today, that would result in mixed volcanic compositions. We suggest that a more likely source of this detritus is a paleo-topographic bedrock high composed of Vicks Peak Tuff on the east or southeast side of the North graben, probably on the footwall of the northeast-trending fault that bounds the northern C-N graben (Fig. 29). Presumably, earlier Santa Fe Group deposition buried this particular source area so that it was not initially eroded, but it was uplifted and exposed later in the Neogene so that it could serve as a source of this monolithic sand. Sometime later in the Quaternary (middle to late Pleistocene), the source was buried again by basin fill. We place the outcrop of this Vicks Peak Tuff to the east or southeast because if it was located to the west or north; the sand would be mixed with other types of volcanic sand derived from the Gallinas and/or Datil Mountains. Bolstering this correlation is the presence of a similar monolithic sand in the 470–690 ft of the Southland Royalty No. 1 well, implying both SA-221 and the Southland Royalty No. 1 were close to this source of phenocryst-poor tuff sand (Fig. 29a).

The geophysical wireline data are consistent with a predominately piedmont depositional environment at 376–440 and 450–573 ft depths, with a tongue of clayey basin floor deposits at 440–450 ft. At these depths, resistivity and gamma ray curves are moderate, but particularly high values are observed at 376–440 ft. The neutron and resistivity curves indicate a coarsening-upward trend from 573–525 ft and then mostly fining-upward from 525–475, which in turn is overlain by a vertically symmetrical (in terms of textural trends) sand body at 475–450 ft. The composition of the 376–440 ft interval and the 475–573 ft interval is consistent with a piedmont depositional environment. The sand in these intervals was sourced from an area with abundant Vicks Peak Tuff (the sand is composed exclusively of Vicks Peak Tuff fragments in the 376–440-ft interval) originally capped by a phenocryst-rich, felsic rock (based on the composition of cuttings at 537–573 ft) that may correlate to the South Canyon Tuff.

Underlying the inferred basin-floor deposits at 573–680 ft depth, the lower part of the gravel-poor, lower unit of the upper Santa Fe Group layer (680–1210 ft depths) consists of sand that is white to light gray to pinkish white, mostly subangular, and as coarse as medium- to very coarse-grained (unit QTsupw-bf). This interval has >50% detritus from a whitish, phenocryst-rich tuff, minor intermediate detritus (<20%), and 5–15% quartz sand grains. The whitish tuff is interpreted as Hells Mesa Tuff because it contains 15–25% phenocrysts that are 0.2–3.0 mm long and include quartz, sanidine, and biotite. The 32-inch and 64-inch resistivity curves are commonly

not separated and the density curve is relatively high (2.2–2.3 g/cm^3), implying less permeability than higher sand bodies, likely due to more cementation or compaction. The lower 100 ft coarsens upward, but overlying strata in the lower unit progressively fines-upwards until 825 ft (based on neutron and resistivity curves); between 825 and 680 ft are three symmetrical sand bodies separated by likely finer sediment (clayey sand?). A sharp leftward deflection in the neutron, resistivity, and gamma ray curves at 1,093–1,100 ft, corresponding to a wash-out, is probably a tongue of clayey fine-grained sediment. The basal contact in the neutron curve is sharp at 1,210 ft, but more gradual in the resistivity and gamma ray curves (Fig. 28; 1,210-ft depth). Across this interval (680–1,210-ft depth), gamma ray values are moderate (120–160 API). Sand bodies (right curve deflections in resistivity and neutron curves) are 1–12 ft thick and interbedded with minor silty-clayey sand (left curve deflections).

The composition of the cuttings (mostly Hells Mesa Tuff, relatively higher amounts of quartz grains, and minor intermediate volcanic rocks) is consistent with a westerly source area (i.e., Datil Mountains) and deposition on an alluvial fan, quite possibly the White House Canyon fan. Thus, we interpret that this lower unit reflects a distal western piedmont environment. We label the entire unit QTsupw-bf ('pw' for western piedmont and the hypen indicating interbedding with minor basin floor sediment). Aside from the clayey tongue at 1,093–1,100 ft, most of the interfingering with basin floor sediment probably occurs in the upper part (at 738–865 ft), based on the higher clay fraction values there (Fig. 30) and local leftward deflections in the resistivity and neutron curves (Fig. 28). Overall, the data indicate an initial progradation of an alluvial fan complex with toe(s) that later progressively retrograded (shifted back to the mountains). The apparent lack of intermediate detritus at 750–782 ft (Appendix 4) in inferred basin-floor deposits may reflect sediment input from small drainages derived from a local source in the lower the Datil Mountains, containing abundant Hells Mesa Tuff, immediately north or south of White House Canyon.

Middle Santa Fe Group (1,210 to 2,075 ft depth) — The middle Santa Fe Group contains two subunits. The upper 345 ft (1,210–1,555 ft depths) is pinkish gray to light gray to pinkish white and is composed of sand and clayey-silty sand (unit Tsmbf, Fig. 28, where 'm' stands for middle Santa Fe Group and 'bf' stands for basin floor); it is redder than underlying and overlying deposits. Fines are preserved in the cuttings at 1,210–1,440 ft. A slight rightward shift in the resistivity and neutron curves between 1,210–1,280 ft (relatively lower values) and 1,280–1,465 ft (relatively higher values) suggest a higher clay content in the upper interval (1,210–1,280 ft), consistent with the clay fraction analysis (Fig. 30). A notable washout occurred at 1,465–1,550 ft (Appendix 7). The preserved sand in the cuttings is subangular to subrounded, moderately sorted, as coarse as medium- to very coarse-grained, and composed of felsic grains with 1–20% intermediate volcanic grains; quartz grains are 5–15%. Hells Mesa Tuff detritus appears to dominate in the upper 230 ft (1,210–1,440 ft depth). At 1,440–1,452 ft, the sand in the cuttings is composed of a relatively monolithic, pink, biotite-hornblende dacite(?) (flow or tuff) with 0.1–1.0 mm-size crystals—this is interpreted to be associated with a sand body at 1,435–1,452 that is indicated by a right-deflection spike in resistivity, neutron, and gamma ray curves. Below, at 1,452–1,555 ft depths, the sand contains mainly felsic volcanic fragments, 15–25% feldspar, and 5–10% quartz. The felsic grains are mostly a moderately (15%) porphyritic tuff or rhyolite containing a phenocryst assemblage of quartz, sanidine, and biotite (0.2–2.0 mm in length). At 1,501–1,555 ft, there are subequal quantities of felsic grains and intermediate volcanic rocks.

The resistivity and neutron curves are relatively low-valued in the upper part of the Middle Santa Fe Group (1,210–1,555 ft depths), probably indicating notable clay content and related fine-grained sedimentation consistent with basin floor deposition (Table 3). The clay fraction analyses indicate two particularly clay-rich zones (20–40% clay) at 1,210–1,380 ft and 1,465–1,555 ft (Fig. 30). Higher gamma ray values at 1,465–1,555 ft are consistent with the 38–40% clay indicated by the clay fraction analyses. Lack of separation of resistivity curves (Appendix 7) implies a general low permeability of the formation. We interpret the strata at 1,210–1,555 ft to be a basin floor facies due to the relatively high clay content, mixing of both felsic and intermediate volcanic grains (mostly felsic), and the lack of coarsening-upward sequences. The 30–40% intermediate-volcanic grain content at 1,500–1,555 ft may reflect high sediment input from the White House alluvial fan.

The lower 520 ft of the Middle Santa Fe Group (1,555–2,075 ft depths) consists of a light gray to gray (but having a 5YR hue), medium- to very coarse-grained, angular to subangular, relatively monolithic sand composed of a phenocryst-poor tuff (unit Tsmlp, Fig. 28). There are minor (15–20%)

fragments composed of pink-orange, felsic volcanic rock with phenocrysts that include sanidine, biotite, and quartz. Less clay is inferred due to higher overall values of the resistivity and neutron curves, but the lack of separation of the 32-inch and 64-inch resistivity curves suggests some degree of cementation, consistent with relatively high bulk density values and lack of washouts (as seen in the caliper log). The sand is derived from a phenocryst-poor tuff with a phenocryst composition of: 0.5% biotite (0.2–1 mm), trace-3% sanidine (0.5–2 mm), and trace–3% quartz (up to 2 mm). However, there is 15–20% intermediate volcanic sand and 5–10% quartz grains in the upper ~70 ft (1,555–1,625 ft) and a heterolithic mixture of tuffs at 1,595–1,625 ft; this stratigraphic interval largely corresponds to an upward decreasing-trend of the resistivity and neutron curves, as well as slightly lower values in the gamma-ray curve (compared to immediately underlying strata in the well). At 1,595–2,075 ft, the gamma-ray curve is notably high (170–240 API), in conjunction with a complete lack of intermediate volcanic grains at 1,625–2,075 ft and only 1–3% quartz grains. Both the high gamma-ray signature and the crystal-poor cuttings indicate a source probably derived from the Vicks Peak Tuff. Although this bedrock source could lay to the east-southeast based on provenance arguments for similar sand in the Upper Santa Fe Group (unit QTsupe), another possibility is erosional unroofing of the eastern front of the Datil Mountains and western piedmont deposition by an east- or southeast-flowing drainage. The latter possibility would be consistent with a general unroofing trend in western piedmont deposits, where this concentration of Vicks Peak Tuff detritus (if it is indeed a western piedmont deposit) is followed up-section by a concentration of Hells Mesa Tuff detritus in the Middle Santa Fe Group.

The clay fraction analyses indicates 18–24% clay at 1,830–1,970 ft, but otherwise is ≤5%. The higher clay content at 1,830–1,970 ft is consistent with the left deflections of the resistivity and neutron curves. The gamma-ray curve has a subtle left deflection at 1,830–1,970 ft, even though the clay content is higher, which may be due to dilution of the high-gamma-ray tuff (correlated to the Vicks Peak Tuff) grains by less radiogenic grains, although this was not obvious in the cuttings. This presumed dilution and the higher clay content, along with the lower neutron and resistivity curve values at 1,855–1,925 ft depth, may indicate a widening of the basin floor at this approximate depth interval (Tsmlp-bf; Fig. 28). All three curves (gamma, neutron, resistivity) show an abrupt deflection at 2,075 ft (Fig. 28), suggesting a sharp, possibly unconformable contact.

Lower Santa Fe Group (2,075–3,495 ft depth) — The Lower Santa Fe Group (2,075–3,495 ft in SA-221) consists of a particularly fine-grained, upper subunit and a coarser, lower subunit (Fig. 28).The upper subunit (2,075–2,775 ft, cross section units Tslbf on Fig. 28) is mostly a clayey-silty sand interbedded with minor bodies of clay-poor sand (probably medium- to coarse-grained). Very coarse sand is rare. The sand is mostly subangular, pinkish gray, and composed of felsic tuffs with 5–25% intermediate volcanic grains. The felsic tuff is mostly an orangish-gray rock with 10–20% phenocrysts of quartz, feldspar, and biotite (all three are 0.1–1 mm, very few grains up to 2 mm). The intermediate grains are either aphyric (crystal-lacking) or contain biotite (locally biotite + hornblende) phenocrysts. In the sand fraction are 3–20% grains of vitreous feldspar (sanidine and/or plagioclase), 10–20% opaque feldspar, 1-5% quartz, and trace–3% biotite. Resistivity and gamma ray curves exhibit relatively low values. The upper 249 ft (2,075–2,224 ft depth) of the resistivity and neutron curves exhibit lower values than deeper in the upper unit, probably reflecting a relatively higher clay content. This is consistent with the clay fraction analyses (Fig. 30), which gives ~22% clay for 2,075–2,224 ft and 14–18% at 2,224–2,775 ft (progressively decreasing downhole, consistent with decreasing gamma ray values). Particularly clay-rich intervals are interpreted at 2,075–2,080, 2,104–2,106, 2,248–2,250, 2,456–2,465 ft, and 2,573–2,575 ft by sharp leftward deflections in the resistivity and neutron curves (Appendix 7, Fig. 28). Three relatively clean, symmetrical sand bodies are interpreted from the geophysical curves at 2,227–2,235 ft, 2,242–2,247 ft, and 2,257–2,265 ft (rightward shifts in the resistivity and neutron curves); the resistivity curves are separated in these sands, but the observation that the 64-inch curve is less resistive (Appendix 7) than the shallower curves implies that formation water is more saline than the borehole fluid; enough cementation is present in these sands to prevent washouts (as observed in caliper log). The three sands have relatively high gamma-ray values, and may possibly reflect deposition by a drainage sourced in an area with more radiogenic tuffs (although this is not obvious in cuttings inspection). The relatively higher clay content, the aforementioned distinct, relatively clean sand bodies of possibly unique provenance compared to adjoining strata, and the lack of coarsening-upward (progradational) trends lead us to infer a

basin-floor depositional environment for the upper subunit of the Lower Santa Fe Group.

The sandier, lower subunit (Tsls, 2,775–3,495 ft, with "s" standing for sandy) of the Lower Santa Fe Group consists of clayey-silty to slightly muddy sand interbedded with ~20% light gray, 3–10 ft-thick sand bodies (based on sand in cuttings and patterns of neutron and resistivity curves; Appendices 4 and 7). Clay content is highest at 2,775–2,890 ft (~20% based on Fig. 30), consistent with relatively lower values in the neutron and resistivity curves, but drops to half that value below 2,950 ft. The sand is light gray (5–7.5YR hue) to pinkish gray, subangular to angular, and medium- to coarse-grained (minor fine- and very coarse-grained). Both the resistivity and neutron curves in the lower subunit of the Lower Santa Fe Group show much higher amplitudes (variability) than in the upper subunit of the Lower Santa Fe Group, suggesting that the sand bodies are probably "cleaner" (lack clay) compared to the upper subunit. The two thickest sand bodies above 3,467 ft (at 2,862–2,885 ft and 2,962–3,002 ft) exhibit fining-upward trends suggestive of a laterally migrating river system. Below, sands bodies are mostly 3–15 ft thick and symmetrical. Spreading of the resistivity curves suggests increased permeability, but the rightward deflection of the SP curve and the lower-valued 64-inch resistivity curve compared to the 32-inch resistivity curve suggests that the formation water is more saline than the borehole fluid, with a baseline shift of the SP curve at 3,040 ft indicating a downward increase in salinity of the formation water (Appendix 7). A relatively thick, clay-poor sand at the bottom of the well (3,467–3,495 ft thick) is indicated by the rightward shift of the resistivity and neutron curves. In all of the coarser lower subunit, the sand is composed mostly of an orangish-gray felsic volcanic rock (containing quartz and feldspar phenocrysts with minor biotite and hornblende, similar to the dominate felsic volcanic rock in the upper subunit); there is minor (10–35%) light gray intermediate volcanic rock (containing biotite and minor hornblende phenocrysts), 5–10% vitreous feldspar, 5–10% opaque feldspar, trace–5% quartz, and trace–2% biotite. The proportion of intermediate volcanic grains compared to felsic volcanic grains increases (although irregularly, per Fig. 28) down-section in the lower subunit.

The abundant sand bodies in the lower subunit, with some exhibiting fining-upward trends, may suggest an ephemeral river system that laid down sandy, high-flow energy deposits interbedded with lower-flow energy deposits of slightly clayey-silty sand. This river may have been part of a broad alluvial fan. It drained a paleotopographic high with exposed bedrock that was different from the bedrock source for the middle and upper Santa Fe Groups. This exposed bedrock was predominately an orangish-gray, felsic volcanic rock (probably a tuff) containing quartz, sanidine, biotite, and hornblende phenocrysts; a lesser proportion of the bedrock was intermediate volcanic rocks (biotite±hornblende bearing) that appears different than the intermediate volcanic rock in the uppermost Santa Fe Group. The slight upward-increase in quartz across the entire lower Santa Fe Group (2,075–3,495 ft) corresponds to upward-decreasing amounts of intermediate volcanic detritus. These up-section trends may possibly indicate exhumation of the Datil Mountains and exposure of minor areas of quartz-rich Hells Mesa Tuff, perhaps due to vertical displacement along the western border faults of the North graben.

Although highly uncertain, we speculate that the river that deposited the lower half of the lower Santa Fe Group (Tsls) was sourced in the southern Datil Mountains, which at the time was capped by an orangish-gray felsic rock (tuff?) and a biotite±hornblende-bearing intermediate lava flow (the erosion of which produced the sand in the lower Santa Fe Group cuttings). These rocks were subsequently completely removed by erosion. This river may possibly be considered an ancestral version of White House Canyon.

Stratigraphic Relations and Paleogeography

The cross-sections shown in Figure 19 represent our preliminary attempt to correlate strata encountered in SA-221, SA-222, and the Southland Royalty No. 1 wells across the southern part of the North graben. For illustrative purposes, these units are simplified in Figure 31 for section A-A'. The basin floor facies occupies a central position in the graben, and interfingers westward with the western piedmont facies and eastward with the eastern piedmont facies. In the area of the cross-sections (Fig. 19), the eastern piedmont facies is inferred to consist mainly of the monolithic, light gray, crystal-poor tuff preliminarily correlated with the Vicks Peak Tuff. The unit corresponding to the monolithic sand in the Middle Santa Fe Group (Tsmlp) could be associated with the eastern piedmont facies or perhaps was deposited by western piedmont drainages eroding thick Vicks Peak Tuff in the eastern Datil Mountains (in which case it would extend westward to the basin-bounding

faults in Figures 19, 31 and Plate 1). However, to the north of the eastern part of cross-sections A-A' and B-B', the eastern piedmont facies is expected to have a more diverse composition due to erosion of tuffs and volcaniclastic sediment from the western front of the Gallinas Mountains. In cross-sections A-A' and D-D', note that most Santa Fe Group units, except for the uppermost (Qsuwpc), thicken across the western-bounding faults of the North graben (Figs. 19 and 31).

The uppermost, gravel-bearing unit (Qsupwc) is distinctive in two aspects. First, it does not change thickness appreciably across the western, basin-margin faults of the North graben (340 ft thick in SA-222 and 320 ft thick in SA-221). Second, compared to older units, the uppermost, gravel-bearing unit (Qsupwc) extended much further eastward across the entire North graben (Figs. 19 and 31). Prior to the uppermost, gravel-bearing unit (Qsupwc), the paleogeography of the northern part of the East San Agustin basin (excluding the White Lake and C-N grabens) consisted of a basin floor centered over the deepest part of the North graben (Fig. 29a). The clayey sand, sand, and clay-silt beds associated with this basin floor interfingered with sands of the western and eastern piedmonts. The toes of these piedmonts shifted back and forth with time during most of Santa Fe Group deposition. However, in the early to middle Pleistocene Epoch (i.e., early to middle Quaternary Period), unit Qsupwc extended eastward across the entire North graben (Fig. 29b). The basin floor environment also shifted eastward, so that later in the Quaternary it lay centered near the northern White Lake graben and east of the North graben.

The reason for this dramatic shift in depositional environment may have been climate-related, driven by a stronger amplification of glacial-interglacial cycles that ocurred during the Pleistocene (Zachos et al., 2001). Stream systems across New Mexico carried coarser gravel at the start of the Pleistocene and piedmonts extended basinward [e.g., Ancha Formation (Koning et al., 2002); uppermost basin fill in the eastern Tularosa Basin (Koning and Kelley, 2008); uppermost Palomas Formation (Koning et al., 2015, 2018; Jochems and Koning, 2016; Jochems, 2015); eastern piedmont of the Albuquerque Basin (Connell, 2008)]. Likewise, deposits from ephemeral streams draining the eastern Datil Mountains appear to have coarsened and the streams had higher sediment flux (carried more sediment), extending the piedmont toe to the east. As noted above, the streams also carried more clay that was mixed in with the gravelly sediment. The fact that unit Qsupwc does not change thickness across the western border faults of the North graben indicates that these faults were not notably active during most of the Pleistocene compared to earlier in geologic time (note that these faults did not completely shut down, because there is a minor fault scarp observed on the land surface today). We argue that the slow-down of activity of these faults in the Pleistocene contributed to the eastward expansion of the western piedmont, since sediment was no longer being trapped in a rapidly subsiding North graben, but paleoclimatic factors may have played an equally important role.

Implications for Groundwater Management

Higher clay content can be expected to correlate with decreased permeability. In general, clay content decreases with depth in the southern part of the North graben (Fig. 30) and is highest where we designated basin floor depositional environments in the cross-sections and well interpretations (Figs. 19, 28, 30, 31). Sandy intervals that might correspond to higher-permeability zones appear to largely correspond to the eastern or western piedmont depositional environments (cross section units QTsupe, QTsupw-bf, Tsmlp). These sandy intervals occur at the following depths in Well SA-221: 376–440 ft; 680–1,210 ft; 1,595–1,830 ft; 1,970–2,075 ft; and 2,950–3,495 ft.

Ground subsidence due to large-scale groundwater extraction is a concern. Santa Fe Group sediment in the East San Agustin basin is known to have variable, but locally relatively high (~30-50%), clay content in the middle of the North graben (Fig. 30) and also near C-N playa (Fig. 26). Moreover, the shallower part of the basin fill aquifer sediment has not been deeply buried (i.e., it is currently at its maximum depth-of-burial) and could be further compacted. Similar under-compacted, clay-bearing sediment exists in the Mimbres basin near Deming, where lowering of the water table by large-scale pumping has resulted in ground subsidence and fissuring. By analogy, we caution that a similar subsidence potential exists in the East San Agustin basin.

Hydrostratigraphic Units

Hydrostratigraphic units are based on inferred or demonstrated hydrologic properties of a rock or sediment. These units may or may not correspond to stratigraphic units recognized by lithologic

criteria. Similar to lithologic units, the designation of hydrostratigraphic units depends not only on the hydrologic properties of the unit, but also on the necessity of grouping units based on the scale and extent of a study. For example, in our study the plethora of rhyolitic-dacitic tuffs in the Mogollon and Datil Groups are grouped into one hydrostratigraphic unit, rather than treating each tuff as a unit. We recognize four hydrostratigraphic units in the volcanic bedrock (listed below), some of which are further subdivided into subunits. A single hydrostratigraphic unit corresponds to basin fill of the Santa Fe Group and another is designated for relatively coarse-grained valley fill inset into the Santa Fe Group (primarily found in the Alamosa Creek drainage). Within the Santa Fe Group, potential hydrostratigraphic subunits include proximal-medial piedmont deposits, distal piedmont deposits, and playa deposits. These subunits can be mapped out in the upper Alamosa basin. However, in the East San Agustin basin their relative extents are poorly known, so it is not practical nor accurate to further subdivide the Santa Fe Group there. Table 4 summarizes these hydrostratigraphic units and associated subunits.

Hydrostratigraphic Units in the Volcanic Bedrock

The thick and extensive late Eocene-Oligocene volcanic package in the study area is of particular interest because it underlies mountainous recharge areas. These volcanic rocks also underlie the topographic divide between the East San Agustin basin and upper Alamosa basin plus the topographic divide (McLure hills) between the East and West San Agustin basins. The volcanic package can be differentiated into four hydrostratigraphic units: volcaniclastic sediment of the Spears Group, ignimbrites, lava flows, and upper Rincon Windmill Formation eolianites (sandstone deposited by wind).

As detailed below, we conclude that groundwater travels via fracture flow more so than matrix flow. Moreover, the connectivity of fractures is likely higher in ignimbrites and caldera-fill tuffs than in other volcanic rock types. First, these tuffs are regional in extent, particularly when compared to lava flows, so the fractured medium extends long distances (10s of miles). Second, the felsic nature of these tuffs corresponds to lower material toughness and lower fracture toughness, both of which enhance fracture development (Gudmundsson, 2012).

An example of the importance of fractured igimbrites and lava flows is illustrated in a temperature profile of the Sun No. 1 well (Fig. 32). There, perturbations to the temperature gradient, presumably reflecting influx of groundwater from the adjoining formation, correspond to three tuffs (Hells Mesa, tuff of Lebya Well? and Kneeling Nun Tuff?) and a latite or an andesite flow. Unpublished documents relating to this well indicate that groundwater was encountered at 290–350 ft depths, which would correspond to the lower Vicks Peak Tuff. Volcaniclastic sediment intervals do not appear to transmit notable groundwater flow in the Sun No. 1 well.

Spears Group

All volcaniclastic sediment in the volcanic package is assigned to the Spears Group (Tsp, Table 4). This unit typically consists of well-cemented, poorly fractured sandstones, gravelly sandstones, conglomerates (cemented gravels), and clayey-silty sandstones. Two subunits are differentiated: the lower Spears Group and the middle–upper Spears Group. We also recognized a subunit where the Spears Group interfingers with Datil-Mogollon Group lavas and another subunit where it interfingers with Datil Group lavas and ignimbrites (Table 4).

The lower Spears Group subunit (Tspl, Table 4) corresponds with the Dog Springs Formation in the Datil Mountains and is commonly exposed in the northern part of the study area (Figs. 6, 21). The predominance of tuffaceous debris flows, clay in the sandstone matrix, high degree of cementation, and general lack of well-defined bedding planes make this a relatively impermeable unit corresponding to an aquitard (Chamberlin et al., 1994b). Geophysical logs from the Hunt Oil Company No. 1-16 well, located southwest of Datil, indicate high resistivity and low permeability for the 1,370 ft of the lower Spears Group penetrated by this well (Broadhead and Chamberlin, 1994). East of Quemado, water from this low-yielding aquifer contains anomalously high concentrations of arsenic and selenium (Newcomer, 1994). The lower Spears Group is approximately 1,500–2,000 ft thick in the study area.

The middle–upper Spears Group subunit (Tspmu, Table 4) includes thick volcaniclastic strata that lie above the lower Spears Group (Fig. 20). Subunits Tspmu-Tdml or Tdsp are used where the middle–upper Spears Group intertongue with

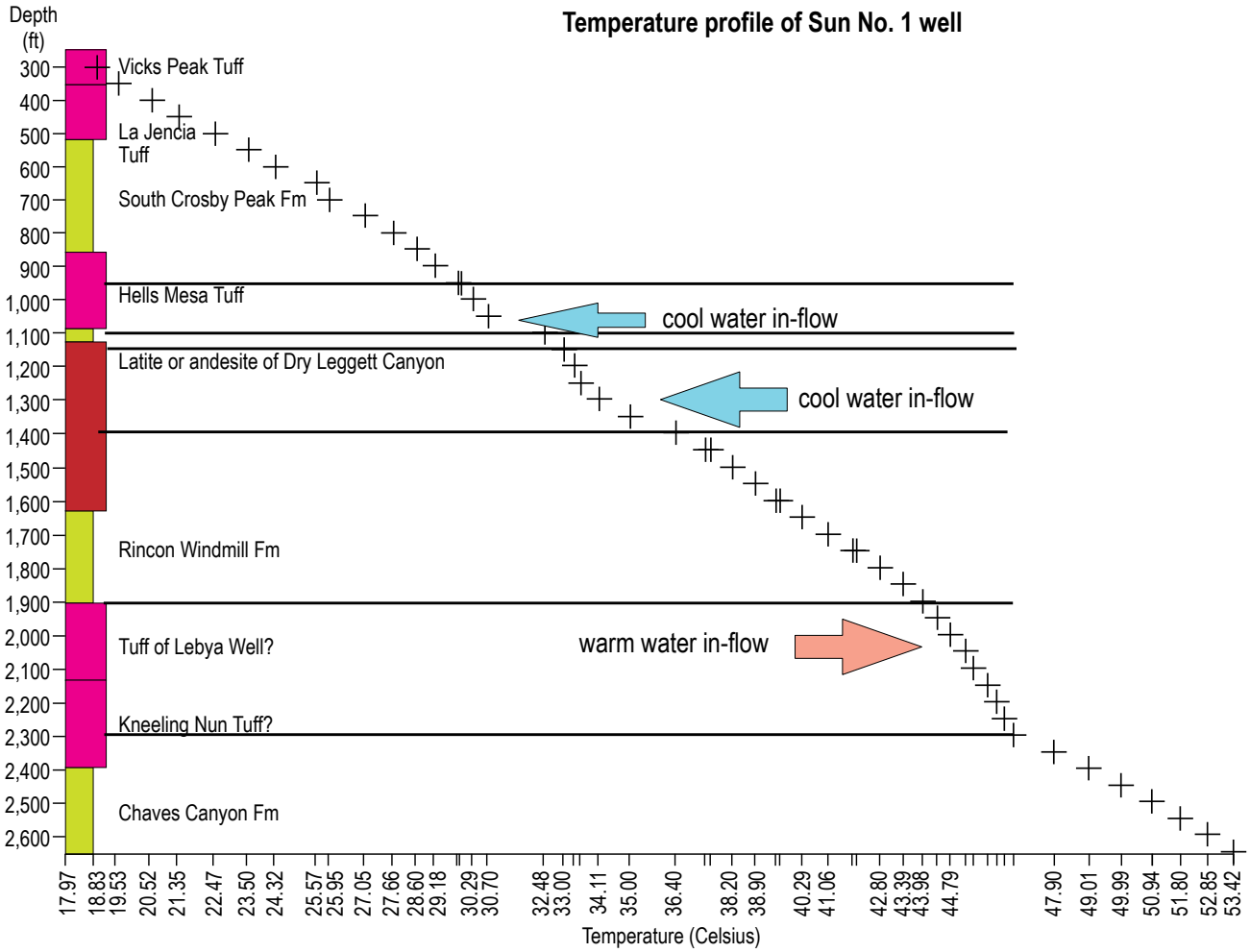

Figure 32. Digitized copy of a temperature profile for the Sun No. 1 well, showing depth (y axis) and temperature (x axis). Temperature measurements were taken between August 13 and 15 of 1970 and are published in Reiter et al. (1976).

lavas or ignimbrites (Table 4). The thickness of the volcanclastic tongues are highly variable, but typically range from 200 to 800 ft. In the Datil Mountains, this unit consists of the Chaves Canyon, lower Rincon Windmill, and South Crosby Peak formations (Figs. 18, 21; Harrison, 1980; Osburn and Chapin, 1983). In the Datil Mountains and northern Gallinas Mountains, the lower part of the Chavez Canyon Formation contains 175–300 ft-thick interval(s) of medium- to coarse-grained, feldspathic sandstone (70% feldspar, 30% ferromagnesium grains; Fig. 18; Harrison, 1980; Coffin, 1981). Otherwise, the sediment typically consists of sandy conglomerate, gravelly sandstone, and minor sandstone that is planar-bedded or locally cross-stratified (Harrison, 1980). Local debris-flow breccias are also present (Harrison, 1980; Coffin, 1981). Volcaniclastic strata above the Hells Mesa Tuff (e.g., South Crosby Peak Formation) include several ash-fall tuffs, tuffaceous sandstones, and minor ash-flow tuffs.

The middle–upper Spears Group is a relatively poor aquifer. Field observations indicate that the Middle–Upper Spears Group tends to be well-cemented (but not as strongly as the Lower Spears Group) and lacks well-developed fracture sets, although weak to moderate fracturing is observed in the Chaves Canyon Formation (Harrison, 1980, p. 45). Practically no springs are associated with the unit in the study area. There are some exceptions to the generally poor quality of the aquifer. One, fracture development is expected to be enhanced along fault lines, where sliding of crustal blocks occurs. Two, thin, unmapped ash-fall tuffs in volcaniclastic sediment in the upper Alamosa basin are inferred to be relatively permeable (C. Ferguson, pers. commun., 2014); pyroclastic rocks, including tuffs, are particularly common in the Beartrap Canyon Formation

Unit\Subunit	**Description**	**Inferred permeability**
Qva 050QUAL	**Coarse Quaternary valley fill related to modern valleys.** Mostly uncemented, weakly consolidated sand and variable gravel; subordinate silt and clay.	Very high; intergranular flow.
QTbf 112QTBF	**Basin fill, undivided.** Includes piedmont, playa, and lacustrine facies as well as coarse Quaternary valley fill related to modern valleys (QTbflac, QTbfpd, QTbfppm, QTbfpm, QTbfpp, Qva on Plate 1).	Low to high
QTbfppm 112QTBFppm	Basin-fill, medial and proximal-piedmont facies, undivided. >35% channel-fills comprised of medium- to very coarse-grained sand. Remainder of sediment is very fine- to medium-grained or silty-clayey fine sand.	High to medium; inter-granular flow.
QTbfpd 112QTBFpd	Basin-fill, distal-piedmont facies; <35% channel-fills comprised of medium- to very coarse-grained sand. Most of the sediment is silty-clayey fine sand or very fine- to medium-grained sand.	Low to medium; intergranular flow.
QTbflac 112QTBFlac	Lacustrine or playa facies: Sediment dominated by clay, silt, and very fine- to fine-grained sand (the sand is concentrated along the edges).	Low to very low; intergranular flow
Tdm_ignimb 123DTMGign	**Ignimbrites of the Datil-Mogollon Groups.** Rhyolitic-dacitic tuffs and welded tuffs that are variably jointed or fractured. Phenocrysts commonly include sanidine with variable amounts of quartz, plagioclase, and biotite. Includes the following regional tuffs: Datil Well (Tddw), Kneeling Nun (Tknt), Rockhouse Canyon (Trhct), Blue Canyon (Tbct), Hells Mesa (Thmt), La Jencia (Tljt), Vicks Peak (Tvpt), South Canyon (Tsct), and Turkey Springs (Ttst).	Mostly low, possibly medium locally if sufficiently fractured. Field studies and drill logs indicate that Trhct, Tvpt, and Thmt locally are water-bearing.
Tdm_ignimbcald	**Thick ignimbrites filling calderas.** Rhyolitic-dacitic tuffs and welded tuffs that fill their source caldera. These are hypothesized to have well-developed joint sets and to be very thick (2,000–7,000 ft, 500–2,000 m).	High
Tdm_lava 123DTMGlava	**Lava flows of the Datil-Mogollon Groups**	
Tdm_rhydac 123DTMGrhydac	Rhyolite and dacite flows of the Datil-Mogollon Group	Low, depending on connectivity of fractures.
Tdm_ablava 123DTMGlava	Andesite, basaltic andesite, and basalt flows of the Datil-Mogollon Group.	Very low, depending on connectivity of fractures.
Tspeol **123SPRSeolinites**	**Eolianites in the Spears Group.** Fine-grained, well-sorted, subrounded sand composed predominately of feldspar, lithic fragments, biotite, and minor quartz. In cross-stratified or planar-bedded intervals. Intertongues with Tspmu to the east and southeast.	Medium; inter-granular, fracture, and bedding-plane flow. Springs noted in the upper Rincon Windmill Fm. in the Datil Mtns.
Tsp 123SPRS	**Volcaniclastic sedimentary rocks of the Spears Group**	
Tspmu 123SPRSmid_upper	Middle-Upper Spears Group volcaniclastic strata. The sediment consists of conglomerate, gravelly sandstone, and sandstone. Unit includes the Chavez Canyon Formation and the Rincon Windmill Formation north of Datil.	Low, locally medium depending on connectivity of fractures and degree of cementation. Bedding-plane flow possible.
Tspl 123SPRSlower	Lower Spears Group. Tuffaceous and conglomeratic debris flows. Massive and very poorly sorted. Well-cemented by zeolites, clay, calcite, or silica.	Very low and likely serves as an aquitard. Degree of fracturing and jointing is very low.
Tdsp 123DTILSPRS	Datil-Spears Group, interbedded. Assigned to interfingering volcaniclastic sediments (Spears Group) and Datil Group lavas+ignimbrites.	Low, depending on connectivity of fractures.
Tspmu-Tdml 123SPRSDTMGlav	Interbedded volcaniclastic sediment and Datil-Mogollon Group lavas (the latter is mostly andesite, basaltic andesite, or basalt). The sediment consists of conglomerate, gravelly sandstone, and sandstone.	Mostly low.

Table 4. Hydrostratigraphic units (bold text) and subunits (non-bold text) for the eastern San Agustin Plains-Alamosa Creek. The code following the hydrostratigraphic unit/subunit (e.g., 112QTBF) is used by the Aquifer Mapping Program (NM Bureau of Geology and Mineral Resources) in their groundwater database. These codes are slightly modified from the primary codes the USGS uses in their Groundwater Site Inventory database.

(Osburn and Ferguson, 2007, 2010). In summary, we infer that in the middle-upper Spears Group hydrostratigraphic unit, relatively limited groundwater flow occurs in fractures and along bedding planes. In addition, there locally may be minor inter-granular flow in conglomeratic sandstones or local ash-fall tuffs.

Volcanic Flows

The lava-flow hydrostratigraphic unit (Tdm_lava, Table 4) could be subdivided into two subunits based on rhyolite-dacite compositions (Tdm_rhydac) or andesite-basalt compositions (Tdm_ablava). Groundwater flow in these flows would primarily be through fractures, with the overall hydraulic conductivity largely determined by the width and connectivity of the fractures. Basaltic andesite flows are more common in the upper part of the volcanic package, and were encountered in the SA-222 well at 724–742 and 940–969 ft depths. These basaltic flows are also common in the Luera Mountains and at the topographic divide between the C-N embayment and Alamosa Creek (cross-section C-C' in Plate 1). A thick rhyolite flow was mapped in the southern Gallinas Mountains (rhyolite of Piñon Well, unit Trpw of cross-section B-B' on Plate 1) and could extend westward under the East San Agustin basin. Due to their lower material toughness and fracture toughness values, rhyolitic-dacitic flow rocks will likely develop better joint/fracture sets than andesite-basalt volcanic flows (Gudmundsson, 2012). However, rhyolite-dacite flows are not as laterally extensive as the basaltic andesites (although often thicker), so the associated aquifer might be more localized.

Ignimbrites

All ignimbrites outside of calderas were lumped together into a single hydrostratigraphic unit (Tdm_ignimb, Table 4). Like lava flows, groundwater flow in ignimbrites would be primarily through fractures, with the overall hydraulic conductivity largely determined by the width and connectivity of the fractures. However, non-welded, fall-out tephra at the base of regional ignimbrites could transmit groundwater via intergranular flow. Two examples of the latter would be the base of the Turkey Springs and South Canyon tuffs, which are inferred to be relatively permeable (C. Ferguson, pers. commun., 2014). Two ignimbrites that are relatively thick (commonly >100 ft thick), widespread, and distinctive are the Rockhouse Canyon and Hells Mesa tuffs.

An important subunit is thick ignimbrites filling the parent caldera (Tdm_ignimbcald on Table 4). Caldera-fill tuffs may potentially be important for groundwater investigations because their cumulative thicknesses and slower cooling times may allow development of well-connected and relatively extensive joint sets. An example of a caldera-fill tuff is the South Canyon Tuff within the Mount Withington caldera. Within the caldera, the South Canyon Tuff is 2,000–7,000 ft thick (cross-section C-C' in Plate 1) and is inferred to have been emplaced in the matter of hours or days (William McIntosh, pers. commun., 2015). This tuff would very likely have cooled more or less as one unit, presumably allowing development of extensive joints, which have been observed on the surface in reconnaissance field outings (Fig. 22e,f). Beneath these caldera-fill tuffs, bedrock of the caldera floor is likely to be complexly faulted or fractured because of the caldera subsidence. The permeability of these inferred fractures, however, depends on the degree of cementation by post-eruption hydrothermal fluids. It is difficult, if not impossible, to generalize the geohydraulic nature of sub-caldera bedrock floors due to complications caused by this cementation and the fact that bedrock floors are typically not exposed.

Eolianite Hydrostratigraphic Unit

Eolianites (sandstones deposited by winds) form local tongues in the middle Spears Group beneath the Hells Mesa Tuff. They are particularly abundant in the upper part of the Rincon Windmill Formation in the Datil Mountains (Harrison, 1980), where they are 30–165 ft thick (Fig. 18; Cather et al., 2008). Here, the sands are well-sorted, subrounded, fine-grained, and composed predominately of feldspar, lithic fragments, biotite, and minor quartz (Harrison, 1980). The sands may exhibit steeply dipping cross-stratification, or they may be in thick, planar-bedded intervals (Fig. 21e,f). This hydrostratigraphic unit interfingers eastward with volcaniclastic sediment of the middle Spears Group, and thickens west of the Datil Mountains (Cather et al., 2008). The planar-bedded part of the unit predominates to the southeast near this interfingering contact, whereas the cross-stratified part becomes more common to the west and north (Harrison, 1980).

Several springs emanate from the eolianite sandstones in the Rincon Windmill Formation in the Datil Mountains (Harrison, 1980), indicating it is

locally a permeable unit. Because the sand is relatively clean (lacks a fine-grained matrix), intergranular flow is likely more voluminous than in the volcaniclastic sediment of the Spears Group. Flow may also occur along bedding planes or fractures (Fig. 21f). Because of the aforementioned interfingering relations with volcaniclastic sediment, these eolianites are expected to be thinner and fewer in the subsurface beneath the East San Agustin basin.

Santa Fe Group Basin Fill Hydrostratigraphic Unit

Basin fill (QTbf, Table 4) was treated similarly for both the East San Agustin and upper Alamosa basins. However, exposure is better in the upper Alamosa basin and hydrostratigraphic subunits could be mapped there. These same subunits would be present under the East San Agustin basin, but away from the three deep wells (e.g., SA-221, SA-222, Southland Royalty SA No. 1), there is a lack of data to constrain the extent and thickness of the units. Overall, the Santa Fe Group hydrostratigraphic unit is commonly 1,000–4,000 ft thick.

The least permeable basin-fill hydrostratigraphic subunit corresponds to lacustrine or playa facies (QTbflac, Table 4). This unit is dominated by clay, silt, and very fine- to fine-grained sand (the sand is concentrated along the edges of a playa). Although its near-surface location and existence is relatively well constrained in the upper Alamosa basin (Koning, 2012), the distribution of this subunit is poorly constrained in the East San Agustin basin. Available data suggests that the relatively thick playa sediment may only be found beneath the modern-day C-N playa (Fig. 26). In the North graben, playa deposits possibly exist north or south of Well SA-221, probably in stratigraphic intervals preliminarily assigned as basin fill facies (Fig. 28), but that possibility remains to be confirmed.

Two of the hydrostratigraphic basin fill subunits (proximal-medial piedmont facies (QTbfppm) and distal piedmont facies (QTbfpd)) are delineated in the upper Alamosa basin based on the proportions of coarse sand and gravel versus sediment composed of very fine- to medium-grained sand and clayey-silty very fine- to medium-grained sand (Table 4). The proximal-medial piedmont facies contains greater than 35–50% coarse sediment, whereas coarse sediment is less than 35–50% in the distal piedmont facies. In the distal piedmont facies subunit, most of the sediment is composed of very fine- to medium-grained sand or clayey-silty sand. Groundwater flow is inferred to be concentrated in the subordinate coarse sediment tongues, unless these are strongly cemented, and the overall hydraulic conductivities of these coarse tongues would depend, in a large part, on their connectivity in the subsurface. Because coarse deposits are more abundant in the proximal piedmont, coarse sediment tongues can be expected to have greater connectivity. To a lesser extent, groundwater may also flow in the finer-grained sediment as intergranular flow. Fracture flow in basin-fill may possibly be significant in areas of strong cementation, but the locations of these cemented areas are poorly constrained.

Coarse Valley Fill Hydrostratigraphic Unit

Late Quaternary coarse valley-fills (Qva in Plate 1, Table 4), are large-scale (>300 ft wide), elongated features inset into bedrock or older, and typically less permeable, sediment. They are composed of weakly consolidated and non-cemented sand and variable gravel. These fills likely have very high permeability via intergranular flow. Accordingly, this unit may have the highest hydraulic conductivities of all our hydrostratigraphic units, but pump test data are not available to adequately support that contention. Subordinate silt and clay may be present and possibly concentrated in the upper parts of the unit (likely above the water table). Coarse valley-fills are particularly important in mountainous terrain (e.g., White House Canyon near Datil) and in the upper Alamosa basin; in the latter, falling geomorphic base level over the middle-late Quaternary has enhanced the development of valley-fills within the older Santa Fe Group basin-fill. The coarse valley-fill underlying Alamosa Creek attains thicknesses up to 100 ft, but it probably averages 30–70 ft in thickness, based on available well data (Fig. 19, cross-section D-D').

III. CONCLUSIONS

Synthesizing previous studies, geophysical data, and well data allows us to construct a conceptual geologic framework model for the East San Agustin basin and the Upper Alamosa basin. The Paleogene bedrock surrounding these basins, and extending beneath Neogene basin fill consists of volcanic and volcaniclastic rocks of the Mogollon-Datil volcanic field. These volcanic rocks overlie 755–1,900 ft of sandstones and mudstones of the Eocene-age Baca Formation. The lower Spears Group (Dog Springs Formation in the Datil Mountains), composed mainly of tuffaceous debris flows and mud flows, comprises the lower 1,500–2,000 ft of the Mogollon-Datil field volcanic package. Above lies 1,300–5,900 ft of interbedded ignimbrites, lava flows (commonly rhyolites, andesites, and basaltic andesites), and volcaniclastic sediment.

Basin-fill strata of the Santa Fe Group can be subdivided into the following facies: proximal to medial piedmont, distal piedmont, basin floor (or alluvial flat), and playa. Exposure in the upper Alamosa basin allows these facies to be mapped with confidence in the Santa Fe Group near the surface. Detailed well analyses, combined with comparison to basin-fill outcrops in the upper Alamosa basin, allow a preliminary stratigraphic assessment of the basin fill in southern part of the North graben, located between the VLA headquarters and the Datil area. Here, we interpret a western piedmont facies interfingering eastward with a finer-grained basin-floor facies, which in turn interfingers eastward with an eastern piedmont facies. The basin-floor facies in the southern North graben lacks evidence for an ancient playa, although clayey playa sediment could possibly be located farther to the north or south in that graben (where it would likely be relatively limited in extent). The relatively coarse, uppermost western piedmont unit prograded eastward in the Pleistocene. This progradation could be related to slow-down of faulting or paleoclimatic changes. This unit has a high clay content, where clay may be occurring in the gravel matrix based on analogy to outcrops in the Palomas Basin. Clay fraction analyses indicate a progressive decrease in clay with depth, but much variability is present. Below the uppermost piedmont unit, basin-floor deposits typically contain a higher clay fraction than piedmont deposits.

Grabens are an important component of the geologic framework; crustal subsidence associated with these features allow basin fill (which compared to bedrock is less-cemented and is more permeable) to be thicker than outside of the grabens. The upper Alamosa basin corresponds to a single half graben called the Winston graben. This graben is tilted to the west, so the basin fill correspondingly thickens westward to an estimated ~4,000 ft. Under the East San Agustin basin, three grabens are interpreted (Fig. 4): the North graben (northwest of the VLA headquarters), the C-N graben (southwest of the headquarters extending into the C-N embayment), and the White Lake graben (a few miles east-northeast of the headquarters). In the southern North graben, basin fill is at least 3,500 ft thick, and basin fill in the C-N graben is inferred to be ~4,000 ft. The White Lake graben is probably shallower than these other two grabens.

Several hydrogeologic inferences are made. The lower Spears Group is interpreted to act as a regional aquitard. Stratigraphically higher volcaniclastic strata of the Spears Group likewise are well consolidated and compacted, lack fractures, and have a relatively strong degree of cementation. Two bedrock units, however, could serve as aquifers: (1) eolianites in the middle Spears Group (via intergranular flow and fracture flow), and (2) regional ignimbrites and some lava flows (via fracture flow). Barring potential cementation effects, hydraulic conductivity in the Santa Fe Group is likely to be higher in the medial-proximal piedmont due to higher proportions of coarse-grained tongues. The high clay content in the coarse, uppermost western piedmont unit of the southern North graben may impede infiltration from the surface to the water table. No evidence of low-permeability playa or lake clay-silt was found in the southern North graben. Such fine-grained sediment is found in the C-N graben near the modern playa, but its vertical extent is not known. The playa sediment in the C-N graben would impede groundwater flow and thus should be incorporated into hydrogeologic analyses.

REFERENCES

Armstrong, R.M., and Chamberlin, R.M., 1994, Preliminary geologic interpretation of the Arma Baca basin seismic reflection profile, northeastern Catron County, New Mexico [minipaper]: New Mexico Geological Society, 45th Annual Field Conference Guidebook, p. 32-33 and Fig. 1.39.

Blakely, R.C., and Gubitosa, R., 1983, Late Triassic paleogeography and depositional history of the Chinle Formation, southern Utah and northern Arizona, *in* Reynolds, M.W., and Dolly, E.D., eds., Mesozoic paleogeography of the west-central United States: Denver, Rocky Mountain Section SEPM, p. 57-76.

Bornhorst, T.J., Jones, D.P., Elston, W.E., Damon, P.E., and Shafiqulla, M., 1982, New radiometric ages on volcanic rocks from the Mogollon-Datil volcanic field, southwestern New Mexico: Isochron/West, no. 35, p. 13-14.

Broadhead, R.F., and Chamberlin, R.M., 1994, Hunt Oil Co. No. 1-16 State well and wireline log responses, Tertiary and Cretaceous sections: New Mexico Geological Society, 45th Annual Field Conference Guidebook, p. 55-56.

Brouillard, L.A., 1984, Geology of the northeastern Gallinas Mountains, Socorro County, New Mexico: New Mexico Bureau of Mines and Mineral Resources, Open File Report 219, 161 p. and 1 plate.

Burke, W.J., Kenny, G.S., Otto, J.B., and Walker, R.D., 1963, Potassium-argon dates, Socorro and Sierra counties, New Mexico: New Mexico Geological Society, 14th Annual Field Conference Guidebook, p. 224.

Cather, S.M., 1980, Petrology, diagenesis, and genetic stratigraphy of the Eocene Baca Formation, Alamo Navajo Reservation and vicinity, Socorro County, New Mexico [M.S. thesis]: Austin, University of Texas, 243 p.

Cather, S.M., 1982, Lacustrine sediments of the Baca Formation (Eocene), western Socorro County, New Mexico: New Mexico Geology, v. 4, p. 1-6.

Cather, S.M., 1983, Lacustrine deposits of the Eocene Baca Formation, western Socorro County, New Mexico: New Mexico Geological Society, 34th Annual Field Conference Guidebook, p. 179-185.

Cather, S.M., 1990, Stress and volcanism in the northern Mogollon-Datil volcanic field, New Mexico: Effects of the post-Laramide tectonic transition: Geological Society of America Bulletin, v. 102, p. 1447-1458.

Cather, S.M., and Johnson, B.D., 1984, Eocene tectonics and depositional setting of west-central New Mexico and eastern Arizona: New Mexico Bureau of Mines and Mineral Resources, Circular 192, 33 p.

Cather, S.M., and Johnson, B.D., 1986, Eocene depositional systems and tectonic framework of west-central New Mexico and eastern Arizona, *in* Peterson, J.A., ed., Paleotectonics and Sedimentation in the Rocky Mountain Region, United States: AAPG Memoir 41, p. 623-652.

Cather, S.M., McIntosh, W.C., and Chapin, C.E., 1987, Stratigraphy, age, and rates of deposition of the Datil Group (Upper Eocene-Lower Oligocene), west-central New Mexico: New Mexico Geology, v. 9, p. 50-54.

Cather, S.M., and Chapin, C.E., 1989, Day 2: Field guide to upper Eocene and lower Oligocene volcaniclastic rocks of the northern Mogollon-Datil volcanic field, *in* Chapin, C.E., and Zidek, J., eds., Field excursions to volcanic terranes in the western United States, Volume I: Southern Rocky Mountain region: New Mexico Bureau of Mines and Mineral Resources, Memoir 46, p. 60-68.

Cather, S.M., Chamberlin, R.M., and Ratté, J.C., 1994, Tertiary stratigraphy and nomenclature for western New Mexico and eastern Arizona: New Mexico Geological Society, 45th Annual Field Conference Guidebook, p. 259-266.

Cather, S.M., Connell, S.D., Chamberlin, R.M., McIntosh, W.C., Jones, G.E., Potochnik, A.R., Lucas, S.G., and Johnson, P.S., 2008, The Chuska erg: Paleogeomorphic and paleoclimatic implications of an Oligocene sand sea on the Colorado Plateau: Geological Society of America Bulletin, vol. 120, no. 1/2, p. 13-33; doi: 10.1130/B26081.

Cepeda, J.C., and Allison, P.S., 1994, Common plants and plant associations of the Mogollon Slope: New Mexico Geological Society Guidebook, 45th Annual Field Conference Guidebook, p. 331-335.

Chamberlin, R.M., 1974, Geology of the Council Rock District, Socorro County, New Mexico: New Mexico Bureau of Mines and Mineral Resources, Open-file Report 40, 134 p. and 1 plate.

Chamberlin, R.M., 1981, Uranium potential of the Datil Mountains-Pie Town area, Catron County, New Mexico: New Mexico Bureau of Geology and Mineral Resources, Open-file Report 138, 51 p.

Chamberlin, R.M, 1989, Criteria for the recognition of a pre-Eocene lateritic weathering profile, west-central New Mexico: New Mexico Geological Society, 40th Annual Field Conference Guidebook, p. 34-35.

Chamberlin, R.M., and Cather, S.M., 1994, Definition of the Mogollon Slope, west-central New Mexico [minipaper]: New Mexico Geological Society, 45th Annual Field Conference Guidebook, p. 5-6.

Chamberlin, R.M., Cather, S.M., McIntosh, W.C., Anderson, O.J., and Ratté, J.C., 1994a, First-day road log from Socorro to Magdalena, Datil, western Crosby Mountains, Sawtooth Mountains, Pie Town, Quemado and Quemado Lake: New Mexico Geological Society Guidebook, 45th Annual Field Conference Guidebook, p. 1-45.

Chamberlin, R.M., Cather, S.M., Anderson, O.J., and Jones, G.E., 1994b, Reconnaissance geologic map of the Quemado 30 x 60' quadrangle, Catron County, New Mexico: New Mexico Bureau of Mines and Mineral Resources, Open-file Report 406, scale 1:100,000.

Chapin, C.E., 1971, The Rio Grande rift, Part I: Modifications and additions: New Mexico Geological Society, 22nd

Annual Field Conference Guidebook, p. 191-201.

Chapin, C.E., 2008, Interplay of oceanographic and paleoclimate events with tectonism during middle to late Miocene sedimentation across the southwestern USA: Geosphere, v. 4, no. 6, p. 976-991.

Chapin, C.E., Jahns, R.H., Chamberlin, R.M., and Osburn, G.R., 1978, First day road log from Socorro to Truth or Consequences via Magdalena and Winston, *in* Chapin, C.E., and Elston, W.E., eds., Field Guide to Selected Cauldrons and Mining Districts of the Datil-Mogollon Volcanic Field, New Mexico: New Mexico Geological Society, Special Publication No. 7, p. 1-31.

Cikoski, C.T., Harrison, R.W., Koning, D.J., and Jahns, R.H., 2012, Geologic map of the Iron Mountain quadrangle, Sierra County, New Mexico: New Mexico Bureau of Geology and Mineral Resources, Open-file Geologic Map 229, scale 1:24,000.

Coffin, G.C., 1981, Geology of the northwestern Gallinas Mountains, Socorro County, New Mexico: New Mexico Bureau of Geology and Mineral Resources, Open-file Report 159, 202 p. and 2 plates.

Cohen, K.M., Finney, S.C., Gibbard, P.L., and Fan, J.-X. (2013; updated) The ICS International Chronostratigraphic Chart: Episodes 36, p. 199-204.

Connell, S.D., 2008, Geologic map of the Albuquerque-Rio Rancho metropolitan area and vicinity, Bernalillo and Sandoval Counties, New Mexico: New Mexico Bureau of Geology and Mineral Resources, Geologic Map 78, scale 1:50,000.

Connell, S.D., Hawley, J.W., and Love, D.W., 2005, Late Cenozoic drainage development in the southeastern Basin and Range of New Mexico, southeastern Arizona, and western Texas, *in* Lucas, S.G., Morgan, G.S., and Zeigler, K.E., eds., New Mexico's Ice Ages, New Mexico Museum of Natural History and Science Bulletin No. 28, p. 125-149.

Crain, E.R., 2019, Crain's petrophysical handbook <<http://spec2000.net>>, last accessed September 15, 2020.

Deal, E.G., 1973, Geology of the northern part of the San Mateo Mountains, Socorro County, New Mexico: a study of a rhyolite ash-flow tuff cauldron and the role of laminar flow in ash-flow tuffs [Ph.D. dissertation]: Albuquerque, University of New Mexico, 268 p.

Deal, E.G., and Rhodes, R.C., 1976, Volcano-tectonic structures in the San Mateo Mountains, Socorro County, New Mexico: New Mexico Geological Society, Special Publication 5, p. 51-56.

Ferguson, C.A., 1986a, Geology of the east-central San Mateo Mountains, Socorro County, New Mexico: New Mexico Bureau of Mines and Mineral Resources, Open-file Report 252, 124 p.

Ferguson, C.A., 1986b, Oligocene eolianites and ichnofossils in the central San Mateo Mountains: New Mexico Geology, v. 8, no. 1, p. 12-13.

Ferguson, C.A., 1991, Stratigraphic and structural studies in the Mt. Withington caldera, Grassy Lookout quadrangle, Socorro County, New Mexico: New Mexico Geology, v. 13, p. 50-54, 59.

Ferguson, C.A., and Osburn, G.R., 1994, Geologic map of the Mount Withington 7.5-minute quadrangle, Socorro County, New Mexico: New Mexico Bureau of Geology and Mineral Resources, Open-file Report 403, scale 1:24000.

Ferguson, C.A., and Osburn, G.R., 2007, Geology of the Welty Hill quadrangle, Socorro County, New Mexico: New Mexico Bureau of Geology and Mineral Resources, Open-file Digital Geologic Map 148, scale 1:24,000.

Ferguson, C.A., and Osburn, G.R., 2011, Geologic map of the C-N Lake 7.5-minute quadrangle, Catron County, New Mexico: New Mexico Bureau of Geology and Mineral Resources, Open-file Digital Geologic Map 218, scale 1:24000.

Ferguson, C.A., and Osburn, G.R., 2012, Geologic map of the Luera Mountains East 7.5-minute quadrangle, Catron County, New Mexico: New Mexico Bureau of Geology and Mineral Resources, Open-file Digital Geologic Map 222, scale 1:24000.

Ferguson, C.A., and Osburn, G.R, 2014, Geology of the Dusty quadrangle, Socorro and Catron Counties, New Mexico: New Mexico Bureau of Geology and Mineral Resources, Open-file Digital Geologic Map 66, scale 1:24,000.

Ferguson, C.A., Osburn, G.R., and McIntosh, W.C., 2012, Oligocene calderas in the San Mateo Mountains, Mogollon-Datil volcanic field, New Mexico [minipaper]: New Mexico Geological Society, 63rd Annual Field Conference Guidebook, p. 74-77.

Finnell, T.L., and Ratté, J.C., 2006, Geologic map of the Luna quadrangle, Catron County, New Mexico: New Mexico Bureau of Geology and Mineral Resources, Open-file Geologic Map 129, scale 1:24,000.

Foreman, F., Clisby, K.H., and Sears, P.B., 1959, Plio-Pleistocene sediments and climates of the San Augustin Plains, New Mexico, with a discussion by Charles E. Stearns: New Mexico Geological Society, 10th Annual Field Conference Guidebook, p. 117-120.

Fossilworks, Gateway to the Paleobiology database <<http://fossilworks.org>>, last accessed December 10, 2014.

Gawthorpe, R.L., and Leeder, M.R., 2000, Tectono-sedimentary evolution of active extensional basins: Basin Research, v. 12, p. 195-218.

Gilbert, G.K., 1875, Report upon the geology of portions of Nevada, Utah, California, and Arizona, examined in the years 1871 and 1872, *in* Report on the geographical and geological explorations and surveys west of the One Hundredth Meridian (Wheeler): U.S. Geological and Geographical Survey, Publication of the Wheeler Survey, v. 3, pt. 1, p. 17-187.

Gile, L.H., Hawley, J.W., and Grossman, R.B., 1981, Soils and geomorphology in the Basin and Range area of southern New Mexico—Guidebook to the Desert Project: New Mexico Bureau of Mines and Mineral Resources, Memoir 39, 222 p.

Gilmer, A.L., Mauldin, R.A., and Keller, G.R., 1986, A gravity study of the Jornado del Muerto and Palomas Basins: New Mexico Geological Society, 37th Annual Field Conference Guidebook, p. 131-134.

Givens, D.V., 1957, Geology of Dog Springs Quadrangle, New Mexico: New Mexico Bureau of Geology and Mineral Resources, Bulletin 58, 37 p. and 1 plate.

Gradstein, F.M., Ogg, J.G., Schmitz, M., and Ogg, G., 2012, The Geologic Time Scale 2012: Boston, USA, Elsevier, https://doi.org/10.1016/B978-0-444-59425-9.00004-4

Gudmundsson, A., 2012, Rock fractures in geological processes: Cambridge, Cambridge University Press, 578 p.

Harrison, R.W., 1980, Geology of the northeastern Datil Mountains, Socorro and Catron Counties, New Mexico: New Mexico Bureau of Mines and Mineral Resources, Open File Report 136, 137 p. and 3 plates.

Harrison, R.W., 1992, Cenozoic stratigraphy, structure, and epithermal mineralization of north-central Black Range, New Mexico, in the regional stratigraphic framework of south-central New Mexico [Ph.D. dissertation]: Socorro, New Mexico Institute of Mining and Technology, 436 p.

Harrison, R.W., 1994, Winston graben: Stratigraphy, structure, and tectonic setting, *in* Keller, G.R., and Cather, S.M., eds., Basins of the Rio Grande Rift: Structure, Stratigraphy, and Tectonic Setting: Boulder, Colorado, Geological Society of America, Special Paper 291, p. 227-240.

Heckert, A.B., and Lucas, S.G., 2003, Triassic stratigraphy in the Zuni Mountains, west-central New Mexico: New Mexico Geological Society Guidebook, 54th Annual Field Conference Guidebook, p. 245-262.

Hook, S.C., Molenaar, C.M., and Cobban, W.A., 1983, Stratigraphy and revision of nomenclature of upper Cenomanian to Turonian (Upper Cretaceous) rocks of west-central New Mexico: New Mexico Bureau of Mines and Mineral Resources, Circular 185, p. 7-28.

Ingram, R.L., 1954, Terminology for the thickness of stratification and parting units in sedimentary rocks: Geological Society of America Bulletin, v. 65, p. 937-938, table 2.

Jahns, R.H., 1955, Geology of the Sierra Cuchillo, New Mexico: New Mexico Geological Society, 6th Annual Field Conference Guidebook, p. 159-174.

Jahns, R.H., McMillan, D.K., O'Brient, J.D., and Fisher, D.L., 1978, Geologic section in the Sierra Cuchillo and flanking areas, Sierra and Socorro Counties New Mexico, *in* Chapin, C.E., and Elston, W.E., eds., Field Guide to Selected Cauldrons and Mining Districts of the Datil-Mogollon Volcanic Field, New Mexico: New Mexico Geological Society, Special Publication No. 7, p. 131-138

Jochems, A.P., 2015, Geologic map of the Williamsburg NW 7.5-minute quadrangle, Sierra County, New Mexico: New Mexico Bureau of Geology and Mineral Resources, Open-File Geologic Map 251, scale 1:24,000.

Jochems, A.P., and Koning, D.J., 2015, Holocene stratigraphy and a preliminary geomorphic history for the Palomas Basin, south-central New Mexico: New Mexico Geology, v. 37, no. 4, p. 77-88.

Jochems, A.P., and Koning, D.J., 2016, Geologic map of the Saladone Tank 7.5-minute quadrangle, Sierra County, New Mexico: New Mexico Bureau of Geology and Mineral Resources, Open-File Geologic Map 259, scale 1:24,000.

Jochems, A.P., and Koning, D.J., 2019, Geologic map of the Black Hill 7.5-minute quadrangle, Socorro County, New Mexico: New Mexico Bureau of Geology and Mineral Resources, Open-File Geologic Map 274, scale 1:24,000.

Johnson, B.D., 1978, Genetic stratigraphy and provenence of the Baca Formation, New Mexico, and the Eager Formation, Arizona [M.S. thesis]: Austin, University of Texas, 150 p.

Kelley, V.C., 1955, Regional tectonics of south-central New Mexico: New Mexico Geological Society, 6th Annual Field Conference Guidebook, p. 96-104.

Koning, D.J., 2012, The Santa Fe Group in the northern Winston graben, southwest New Mexico, and how changing Rio Grande rift tectonism may have influenced its deposition and erosion: New Mexico Geological Society, 63rd Annual Field Conference Guidebook, p. 457-474.

Koning, D.J., and Kelley, S.A., 2008, Geologic map of the Tularosa NE quadrangle, Otero County, New Mexico: New Mexico Bureau of Geology and Mineral Resources, Open-file Geologic Map 185, scale 1:24,000.

Koning, D.J., Connell, S.D., Pazzaglia, F.J., and McIntosh, W.C., 2002, Redefinition of the Ancha Formation and Pliocene-Pleistocene deposition in the Santa Fe embayment, norht-central New Mexico: New Mexico Geology, v. 24, no. 3, p. 75-87.

Koning, D.J., Jochems, A.P., Kelley, S.A., and McLemore, V.T., 2014, Geologic map of the Monticello 7.5-minute quadrangle, Sierra and Socorro Counties, New Mexico: New Mexico Bureau of Geology and Mineral Resources, Open-file Geologic Map 245, scale 1:24,000.

Koning, D.J., Jochems, A.P., and Cikoski, C., 2015, Geologic map of the Skute Stone Arroyo 7.5-Minute quadrangle, Sierra County, New Mexico: New Mexico Bureau of Geology and Mineral Resources, Open-file Geologic Map 252, scale 1:24,000.

Koning, D.J., Jochems, A.P., Foster, R., Cox, B., Lucas, S., Mack, G.H., and Zeigler, K.E., 2018, Geologic map of the Cuchillo 7.5-minute quadrangle, Sierra County, New Mexico: New Mexico: NewMexico Bureau of Geology and Mineral Resources Open-file Geologic Map 271, scale 1:24,000.

Kues, B.S., and Giles, K.A., 2004, The Late Paleozoic Ancestral Rocky Mountains system in New Mexico, *in* Mack, G.H., and Giles, K.A., eds., The Geology of New Mexico, A Geologic History: New Mexico Geological Society, p. 95-136.

Landon, S.M., 1994, Summary, *in* Landon, S.M., Interior Rift Basins: American Association of Petroleum Geologists, Memoir 58, p. 259-269.

Leeder, M.R., and Gawthorpe, R.L., 1987, Sedimentary models for extensional tilt-block/half-graben basins, *in* Coward, M.P., Dewey, J.F., and Hancock, P.L., eds. Continental Extensional Tectonics: Geological Society, London, Special Publication 28, p. 139-152.

Lopez, D.A., and Bornhorst, T.J., 1979, Geologic map of the Datil area, Catron County, New Mexico: U.S. Geological Survey, I-1098, scale 1:50,000.

Love, D.W., and Connell, S.D., 2005, Late Neogene drainage developments of the southeastern Colorado Plateau, New Mexico, *in* Lucas, S.G., Morgan, G.S., and Zeigler, K.E., eds., New Mexico's Ice Ages: New Mexico Museum of Natural History and Science, Bulletin 28, p. 151-169.

Lucas, S.G., 1983, The Baca Formation and the Eocene-Oligocene boundary in New Mexico: New Mexico Geological Society, 34th Annual Field Conference Guidebook, p. 187-192.

Lucas, S.G., 2015, Eocene vertebrate fossils in New Mexico, *in* Lucas, S.G., and Sullivan, R.M., eds., Fossil Vertebrates in New Mexico: New Mexico Museum of Natural History and Science, Bulletin 68, p. 149-157.

Lucas, S.G., 2020, Triassic stratigraphy of the southeastern Colorado Plateau, west-central New Mexico: New Mexico Geological Society, Special Publication 14, Geology of the Mount Taylor area, p. 123-133

Lucas, S.G., and Hayden, S.N., 1989, Triassic stratigraphy of west-central New Mexico: New Mexico Geological Society, 40th Annual Field Conference Guidebook, p. 191-211.

Lucas, S.G., and Kues, B.S., 1994, Permian strata at Horse Mountain [minipaper]: New Mexico Geological Society, 45th Annual Field Conference Guidebook, p. 106-108.

Lucas, S.G., and Williamson, T.E., 1993, Eocene vertebrates and late Laramide stratigraphy of New Mexico: New Mexico Museum of Natural History and Science, Bulletin 2, p. 145-158.

Lucas, S.G., and Heckert, A.B., 1994, Triassic stratigraphy in the Lucero Uplift, Cibola, Valencia, and Socorro Counties, New Mexico: New Mexico Geological Society, 45th Annual Field Conference Guidebook, p. 241-254.

Lucas, S.G., Krainer, K., and Colpitts, R.M., Jr., 2005, Abo-Yeso (Lower Permian) stratigraphy in central New Mexico: New Mexico Museum of Natural History and Science, Bulletin 31, p. 101–117.

Lucas, S.G., Krainer, K., McLemore, V.T., Spielmann, J.A., and Lueth, V.W., 2012a, Mud Springs Mountains, Third-day road log from Truth or Consequences to Mud Mountain and Whiskey Canyon: New Mexico Geological Society, 63rd Annual Field Conference Guidebook, p. 97-121.

Lucas, S.G., Krainer, K., and Spielmann, J.A., 2012b, Pennsylvanian stratigraphy in the Fra Cristobal and Caballo Mountains, Sierra County, New Mexico: New Mexico Geological Society, 63rd Annual Field Conference Guidebook, p. 327-344.

Lucas, S.G., Nelson, W.J., Krainer, K., Elrick, S.D., 2019, The Cretaceous system in central Sierra County, New Mexico: New Mexico Geology, v. 41, no. 1, p. 3-39.

Machette, M.N., compiler, 1978, Preliminary geologic map of the Socorro 1° x 2° quadrangle, central New Mexico: U.S. Geological Survey Open-File Report 78-607, 1 sheet, scale 1:250,000.

Machette, M.N., and McGimsey, R.G., 1983, Map of Quaternary and Pliocene faults in the Socorro and western part of the Fort Sumner 1° x 2° quadrangles, central New Mexico: U.S. Geological Survey Miscellaneous Field Studies Map MF-1465-A, 12 p. pamphlet, 1 sheet, scale 1:250,000.

Machette, M.N., Personius, S.F., Kelson, K.I. Haller, K.M., and Dart, R.L., 1998, Map and data for Quaternary faults and folds in New Mexico: U.S. Geological Survey, Open-file Report 98-521, 443 p.

Mack, G.H., Salyards, S.L., and James, W.C., 1993, Magnetostratigraphy of the Plio-Pleistocene Camp Rice and Palomas Formations in the Rio Grande rift of southern New Mexico: American Journal of Science: v. 293, p. 49-77.

Mack, G.H., Salyards, S.L., McIntosh, W.C., and Leeder, M.R., 1998, Reversal magnetostratigraphy and radioisotopic geochronology of the Plio-Pleistocene Camp Rice and Palomas Formations, southern Rio Grande rift: New Mexico Geological Society, 49th Annual Field Conference Guidebook, p. 229–236.

Mack, G.H., Leeder, M., and Salyards, S.L., 2002, Temporal and spatial variability of alluvial-fan and axial-fluvial sedimentation in the Plio-Pleistocene Palomas half graben, southern Rio Grande rift, New Mexico, USA, *in* Renaut, R.W. and Ashley, G.M. eds., Sedimentation in Continental Rifts: Society of Economic Paleontologists and Mineralogists, Special Publication, p. 165–177.

Maldonado, F., 2012, Summary of the geology of the northern part of the Sierra Cuchillo, Socorro, and Sierra Counties, southwestern New Mexico: New Mexico Geological Society, 63rd Annual Field Conference Guidebook, p. 211-218.

Markgraf, V., Bradbury, J.P., Forester, R.M., McCoy, W., Singh, G., and Sterngberg, R., 1983, Peleoenvironmental reassessment of the 1.6 million-year old record from San Agustin Basin, New Mexico: New Mexico Geological Society, 34th Field Conference Guidebook, p. 291-297.

Markgraf, V., Bradbury, J.P., Forester, R.M., Singh, G., and Sternberg, R.S., 1984, San Agustin Plains, New Mexico: Age and paleoenvironmental potential reassessed: Quaternary Research, v. 22, p. 336-343.

McCraw, D.J., and Williams, S.F., 2012, Terrace stratigraphy and soil chronosequence of Cañada Alamosa, Sierra and Socorro Counties, New Mexico: New Mexico Geological Society, 63rd Annual Field Conference Guidebook, p. 475-490.

McFadden, L.D., Lozinsky, R.P., Menges, C.M., Miller, J.R., and Ritter, J., 1994, Soil, tectonic, and climatic geomorphological investigations in the San Agustin Plains area, NM: New Mexico Geological Society, 45th Annual Field Conference Guidebook, p. 12-14.

McIntosh, W.C., and Chamberlin, R.M., 1994, $^{40}Ar/^{39}Ar$ geochronology of middle to late Cenozoic ignimbrites, mafic lavas, and volcaniclastic rocks in the Quemado region, New Mexico: New Mexico Geological Society, 45th Field Conference Guidebook, p. 165-185.

McIntosh, W.C., Sutter, J.F., Chapin, C.E., and Kedzie, L.L., 1990, High-precision $^{40}Ar/^{39}Ar$ sanidine geochronology of ignimbrites in the Mogollon-Datil volcanic field, southwestern New Mexico: Bulletin of Volcanology, v. 52, p. 584-601.

McIntosh, W.C., Kedzie, L.L., and Sutter, J.F., 1991, Paleomagnetism and $^{40}Ar/^{39}Ar$ ages of ignimbrites, Mogollon-Datil field, southwestern New Mexico: New Mexico Bureau of Geology and Mineral Resources, Bulletin 135, 79 p.

McIntosh, W.C., Chapin, C.E., Ratté, J.C., and Sutter, J.F., 1992, Time-stratigraphic framework for the Eocene-Oligocene Mogollon-Datil volcanic field, southwest New Mexico: Geological Society of America Bulletin, v. 104, p. 851-871.

McIntosh, W.C., and Chamberlin, R.M., 1994, $^{40}Ar/^{39}Ar$ geochronology of middle to late Cenozoic ignimbrites, mafic lavas, and volcaniclastic rocks in the Quemado region, New Mexico: New Mexico Geological Society, 45th Field Conference Guidebook, p. 165-185.

McLemore, V.T., 2014, Geologic map of the Montoya Butte 7.5-minute quadrangle, Socorro County, New Mexico: New Mexico Bureau of Geology and Mineral Resources, Open-file Geologic Map 69, scale 1:24,000.

McLemore, V.T., Heizler, M., Love, D.W., Cikoski, C.T., and Koning, D.J., 2012, $^{40}Ar/^{39}Ar$ ages of selected basalts in the Sierra Cuchillo and Mud Springs Mountains, Sierra and Socorro Counties, New Mexico: New Mexico Geological Society, 63rd Field Conference Guidebook, p. 285-292.

Menges, C.M., Kawaguchi, G.H., Lozinsky, R.P., and McFadden., L.D., 1984, Rates and amounts of Quaternary faulting on the VLA fault scarp, northeastern San Agustin Plains, New Mexico: Geological Society of America Abstracts with Programs, v. 16, p. 248.

Molenaar, C.M., 1983, Principal reference section and correlation of Gallup Sandstone, northwestern New Mexico: New Mexico Bureau of Mines and Mineral Resources, Circular 185, p. 29-40.

Myers, R.G., Everheart, J.T., and Wilson, C.A., 1994, Geohydrology of the San Agustin Basin, Alamosa Creek Basin upstream from Monticello Box, and upper Gila Basin in parts of Catron, Socorro, and Sierra Counties, New Mexico: U.S. Geological Survey, Water-Resources Investigations Report 94-4125, 70 p.

Nagtegaal, P.J.C., 1978, Sandstone-framework instability as a function of burial diagenesis: Journal of the Geological Society of London, v. 135, p. 101-105.

Newcomer, R.W., Jr., 1994, Hydrogeology and ground-water quality, Largo Creek Basin, Catron County, New Mexico: New Mexico Geological Society, 45th Annual Field Conference Guidebook, p. 58-60.

NMBGMR [New Mexico Bureau of Geology and Mineral Resources], 2003, Geologic Map of New Mexico: New Mexico Bureau of Geology and Mineral Resources, scale 1:500,000.

Osburn, G.R., and Chapin, C.E., 1983, Nomenclature for Cenozoic rocks of northeast Mogollon-Datil volcanic field, New Mexico: New Mexico Bureau of Mines and Mineral Resources, Stratigraphic Chart 1, 2 sheets.

Osburn, G.R, Laroche, T.M., and Weber, R. H., 1993, Geology of Lion Mountain

and northern Arrowhead Well quadrangles, Socorro County, New Mexico: New Mexico Bureau of Geology and Mineral Resources, Geologic Map 68, 1:24,000 scale.

Osburn, G.R., and Ferguson, C., 2007, Geologic map of the Bay Buck Peaks quadrangle, Socorro County, New Mexico: New Mexico Bureau of Geology and Mineral Resources, Open-file Geologic Map 147, scale 1:24,000.

Osburn, G.R., and Ferguson, C.A., 2010, Geologic map of the Oak Peak 7.5-minute quadrangle, Catron and Socorro Counties, New Mexico: New Mexico Bureau of Geology and Mineral Resources, Open-File Geologic Map 65, scale 1:24,000.

Osburn, G.R., and Ferguson, C.A., 2011, Geologic map of the Monica Saddle 7.5-minute quadrangle, Socorro County, New Mexico: Open-file Digital Geologic Map GM 217, scale 1:24,000.

Osburn, G.R., and Ferguson, C.A., 2014, Geologic map of the Wahoo Ranch 7.5-minute quadrangle, Socorro and Catron Counties, New Mexico: Open-file Digital Geologic Map 68, scale 1:24000.

Owen, D.E., and Sparks, D.K., 1989, Surface to subsurface correlation of the intertongued Dakota Sandstone-Mancos Shale (Upper Cretaceous) in the Zuni emabayment, New Mexico: New Mexico Geological Society, 40th Field Conference Guidebook, p. 265-267.

Owen, D.E., and Owen, D.E., Jr., 2003, Stratigraphy of the Dakota Sandstone and intertongued Mancos Shale along the southern flank of the San Juan Basin, west-central New Mexico: New Mexico Geological Society, 54th Field Conference Guidebook, p. 325-330.

PACES gravity database, 2014, Pan American Center for Earth and Environmental Studies, gravity database: University of Texas at El Paso <<https://research.utep.edu/default.aspx?tabid=37229>>, last accessed April 2, 2019.

Phillips, F.M., and Campbell, A.R., co-principal investigators, and Kruger, C., Johnson, P., Roberts, R., and Keyes, E., 1992, A reconstruction of the response of the water balance in western United States lake basins to climatic change, volume 1: New Mexico Water Resources Research Institute, Technical Completion Report on Project Numbers 1345662, 1423687, WRRI Report No. 269, 167 p.

Pike, W.S., Jr., 1947, Intertonguing marine and nonmarine Upper Cretaceous deposits of New Mexico, Arizona, and southwestern Colorado: Geological Society of America Memoir, v. 24, 103 p.

Potter, S.C., 1970, Geology of Baca Canyon, Socorro County, New Mexico [M.S. thesis]: Tucson, University of Arizona. p. 54

Prothero, D.R., Ludtke, J.A., and Lucas, S.G., 2004, Magnetic stratigraphy of the Middle Eocene (Duchesnean) Baca Formation, west-central New Mexico, *in* Lucas, S.G., Zeigler, K.E., and Knodrashov, P.E., eds., Paleogene Mammals: New Mexico Museum of Natural History and Science, Bulletin 26, p. 55-58.

Ratté, J.C., McIntosh, W.C., Houser, B.B., 1990, Geologic map of the Horse Mountain West Quadrangle, Catron County, New Mexico: New Mexico Bureau of Mines and Mineral Resources, Geologic Quadrangle Map GQ-1685, scale 1:24,000.

Reiter, M.R., Simmons, G., Chessman, M., England, T., Hartman, H., and Weidman, C., 1976, Terrestrial heat flow near Datil, New Mexico, *in* Kottlowski, F.E., and Staff, Annual Report for the Fiscal Year July 1, 1975 to June 30, 1976: New Mexico Bureau of Mines and Mineral Resources, p. 33-37.

Riggs, N.R., Lehman, T.M., Gehreis, G.E., and Dickinson, W.R., 1996, Detrital zircon link between headwaters and terminus of the Upper Triassic Chinle-Dockum paleoriver system: Science, v. 273, issue number 5271, p. 97-100.

Schiebout, J.A., and Schrodt, A.K., 1981, Vertebrate paleontology of the lower Tertiary Baca Formation of western New Mexico: Geologtical Society of America Bulletin, Part I, v. 92, p. 976-979.

Schrodt, A.K., 1980, Depositional environments, provenance, and vertebrate paleontology of the Eocene-Oligocene Baca Formation, Catron County, New Mexico [M.S. thesis]: Baton Rouge, Louisiana State University, 174 p.

Snyder, D.O., 1970, Fossil evidence of the Eocene age of the Baca Formation: New Mexico Geological Society, 21st Annual Field Conference Guidebook, p. 65-67.

Snyder, D.O., 1971, Stratigraphic analysis of the Baca Formation, west-central New Mexico [Ph.D. dissertation]: Albuquerque, University of New Mexico, 158 p.

Stewert. J.H., Poole, F.G., and Wilson, R.F., 1972, Stratigraphy and origin of the Chinle Formation and related upper Triassic strata in the Colorado Plateau region: U.S. Geological Survey, Geological Survey Professional Paper 690, 336 p.

Weber, R.H., 1994, Pluvial lakes of the Plains of San Agustin [minipaper]: New Mexico Geological Society Guidebook, 45th Annual Field Conference Guidebook, p. 9-11.

Weissmann, G.S., Hartley, A.J., Nichols, G.J., Scuderi, L.A., Olson, M.E., Buehler, H.A., and Massengill, L.C., 2011, Alluvial facies distributions in continental sedimentary basins – distributive fluvial systems, *in* North, C., Davidson, S.K., and Leleu, S., eds., From River to Rock Record: The Preservation of Fluvial Sediments and Their Subsequent Interpretation: Society of Economic Paleontologists and Mineralogists Special Publication 97, p. 327-355.

Wentworth, C.K., 1922, A scale of grade and class terms for clastic sediments: The Journal of Geology, v. 30, no. 5, p. 377-392.

Western Regional Climate Center, 2014, Datil, New Mexico (292367), period of record monthly climate summary, for 9/1/1905 to 8/31/1951 << http://www.wrcc.dri.edu/cgi-bin/cliMAIN.pl?nm2367>>, last accessed November 14, 2014.

Wilkinson, 1976, Geology of the Tres Montosas-Cat Mountain area, Socorro County, New Mexico: New Mexico Bureau of Mines and Mineral Resources, Open-file Report 39, 158 p. and 3 plates.

Willard, M.E., 1957, Reconnaissance geologic map of Luera Spring 30-minute quadrangle: Socorro, New Mexico Bureau of Mines and Mineral Resources Geologic Map 2, scale 1:126,720.

Wipolt, R.H., MacAlpin, A.J., Bates, R.L., and Vorbe, G., 1946, Geologic map and stratigraphic sections of the Paleozoic rocks of Joyita Hills, Los Pinos Mountains, and northern Chupadera Mesa, Valencia, Torrance, and Socorro Counties, New Mexico: U.S. Geological Survey Oil and Gas Investigations, Preliminary Map 61.

Zachos, J., Pagani, M., Sloan, L., Thomas, E., Billups, K., 2001, Trends, rhythms, and aberrations in global climate 65 Ma to present: Science, v. 202, p. 686-693.

ACKNOWLEDGMENTS

We thank the landowners along Upper Alamosa Creek, including the Muncy, Welty, and Henderson families, for allowing access for fieldwork in the late-2000s. Ron Broadhead and Bruce Allen provided helpful reviews of a draft of the manuscript, with Ron focusing on aspects pertaining to wireline logs. Spencer Lucas kindly reviewed Appendix 2. We are particularly grateful for Augustin Plains Ranch LLC and John Shomaker, and Associates, Inc, for allowing access to cuttings and wireline logs for the two deep boreholes drilled on the San Augustin Plains Ranch land in the mid-2000s.

New Mexico Bureau of Geology and Mineral Resources

A Research Division of New Mexico Institute of Mining and Technology

Socorro, NM 87801
(575) 835 5490
Fax (575) 835 6333
www.geoinfo.nmt.edu